2013

Characterization of the Ribosomal Protein L22e Family in Drosophila melanogaster: Evidence for Functional Diversification of Duplicated Ribosomal Protein Genes

Michael G. Kearse
Lehigh University

Characterization of the Ribosomal Protein L22e Family in *Drosophila melanogaster*: Evidence for Functional Diversification of Duplicated Ribosomal Protein Genes

by

Michael G. Kearse

A Dissertation

Presented to the Graduate and Research Committee

of Lehigh University

in Candidacy for the Degree of

Doctor of Philosophy

in

Cell and Molecular Biology

Department of Biological Sciences

Lehigh University

May 2013

Approved and recommended for acceptance as a dissertation in partial fulfillment of the requirements for the degree of Doctor of Philosophy

Michael G. Kearse
Characterization of the Ribosomal Protein L22e Family in *Drosophila melanogaster:* Evidence for Functional Diversification of Duplicated Ribosomal Protein Genes

April 12, 2013

Defense Date

Vassie C. Ware, Ph.D.
Dissertation Director

April 21, 2013

Approved Date

Committee Members:

M. Kathryn Iovine, Ph.D.

Michael R. Kuchka, Ph.D.

Thoru Pederson, Ph.D.

ACKNOWLEDGMENTS

I would first like to extend my deepest and most profound gratitude to my advisor and mentor Dr. Vassie Ware for allowing me to complete my Ph.D. research in her laboratory and under her guidance. She has been an instrumental factor to my graduate education and has constantly given her time, ideas, late hours, and continuous focus to progress our shared research interests. This dissertation represents approximately five years of study that has only been possible with her constant encouragement, guidance, and infectious excitement for research. Her inherent nature to inspire and captivate, to fall in love with the science, has allowed me to overcome the hardships of research, pushing through roadblocks of various projects, and become a better scientist. Her commitment to her job, daughter, husband, family, and morals, is beyond admirable. For this and so many other things, thank you, Vassie.

I would also like to thank Dr. Mike Kuchka, Dr. Kathy Iovine, and Dr. Thoru Pederson for serving as excellent and helpful committee members. Beyond his helpful comments and critiques during this process, Dr. Kuchka always been an approachable faculty member for issues in and outside of the lab. I will surely miss our daily non-science talks in the hallways. His level of professionalism mixed with his approachable personality, critical scientific approach, and precise teaching abilities make him a model of what an educator should be. Much appreciation is given to Dr. Iovine for her time thus far as graduate coordinator, providing a very professional and approachable link between graduate students, department faculty, and the Ph.D. program. Dr. Thoru Pederson has been so very supportive over the years and has always been able to challenge me in ways that have made me a better scientist. His steadfast dedication to the scientific community—advising graduate students and postdocs, serving on committees,

contributing to his field, being a key member of societies, and serving on journal editorial boards (and I'm sure so much more)—is beyond admirable and so very much aspiring.

I would also like to thank Dr. Tami Mysliwiec, Dr. Maureen Dunbar, Dr. Dave Dunbar, Dr. Shun Por Li, Dr. Der-Yang Lee, and Dr. Doug Johns for their support during my undergraduate education and have been key influences in my young career.

Much appreciation is given the Department of Biological Sciences and faculty members of the Cell and Molecular Biology Ph.D. program for providing a stimulating and challenging atmosphere. My sincerest gratitude is given to the hardworking, steadfast, and committed faculty members of the Department of Biological Sciences for their dedication to research and graduate education, as without them, a graduate program would not be possible. Vicki Ruggiero, Heather Sohara, and Maria Brace are also acknowledged for daily contributions to the department and the graduate student life. Much gratitude is extended to Maria Brace for always having an open door for both department and personal matters. I would also like to extend my gratitude to Lee Graham for his friendship over the years and for making the department's equipment operational on a daily basis.

The graduate student body as a whole is a group of talented and hardworking young scientists, who all contribute to a very supportive and collaborative learning environment. Dr. Tina Sie and Dr. Jeff Vassallo have been especially supportive in and outside of the lab and have always offered input and advice. I would like to sincerely thank Dr. Joe Leese for his friendship over the years and his pragmatic opinions. A special thank you is given to Dr. Anna Gumpert as she had welcomed me from day one and has been an

everlasting source of friendship. I would like also to thank Dr. Dylan Dupuis, Dr. Bruce Carney, Josh Slee, Matthew Fischl, Andrew Black, Sonia Weimann, Soumya Rudra, and Victoria Caruso-Silva for their friendship and the support. I would like to also thank Jayalakshmi Govindan for her friendship, diffusible excitement for science, scientific input, and our many shared coffee breaks. I wish all the members of the graduate program (past, present, and future) the best of luck with their future endeavors.

Without a communal working environment, success in any program would not be possible. For this and her friendship over the years, I would like to extend my deepest gratitude to Kandiss Schrader. She has always offered her time to listen and discuss issues related science and life. She is a mother, friend, teacher, scientist, and ever so committed to her children. I would like to also extend my gratitude to the other members of the Ware lab over the years for their input, help, and addition to the communal working environment: Catherine Mageeney, Brett Gershman, Jennifer Colquhoun, Alex Chen, Jill Ireland, Sukhdip "Kammy" Kaur, Smrithi Prem, Elliot Swartz, Brandon Bensel, Casey Hofstaedter, Elizabeth Brown, Christa Buckheit, and Emily Cooper. I would like to extend a special thank you to Alex Chen for his commitment and help in the lab.

I have made many friends in the Lehigh Valley over the years outside of Lehigh and they have been an integral piece in this part of my life. My sincerest thank you to Mr. Charles T. Glass, for being the person he is: a great friend and mentor to many, a committed father to his children, and a true martial artist. I would also like to thank Harry Paul, Owen Finnegan, Ryan Fries, Brian Miller, Dan Bokencamp, Troy Minarovic, Aldo Campos, Andrew Glass, Sean Manni, Paul Morton, Chris Simeone, and Kirk Alexander.

Without their friendship, Lehigh would have not felt like home. I would also like to thank Ryan Ross, Tony Pacenski, Anthony Colantuono, and Walter ‘Cascao’ Vital for their support and friendship.

I would also like to thank my parents, Frank and Christine, for their constant support and instilling in me the personal values and morals that have allowed me become a friend to many and husband. My mother has always been a loving and supportive mother to her eight children and has always provided a warm and loving family environment. My father has always been a role model, as he has always been a caring and loving father to all of his children, an everlasting source of support, instilling the values of hard work in me, and being a defining example of what a father should be. I would like to also thank my brothers, Frankie, Will, Andrew, Matthew, and Thomas, and my sisters, Elizabeth and Katie, for their support and their influence in making me the person that I am. I would also like to thank my in-laws, Mike, Jean, Angie, and Dan Eakin, for their support and welcoming me with open arms to their family.

Lastly and most importantly, I would like to thank my loving, beautiful, and caring wife, Cindy for her everlasting support. You are truly the best person I have ever met. You are a wonderful wife, friend, life partner and you bring out the best in me. Living on opposite sides of the country for four years has been an added challenge for both of us, but now we are together, until the end. I look forward to what the future brings us, knowing that we will be side-by-side, ready to take on any challenge together. I love you. And thank you.

TABLE OF CONTENTS

LIST OF FIGURES

LIST OF TABLES

LIST OF ABBREVIATIONS

aa	Amino acid
Ab	Antibody
bam	*bag-of-marbles*
βME	Beta- mercaptoethanol (2- mercaptoethanol)
bp	Base pair
BSA	Bovine serum albumin
cDNA	Complementary deoxyribonucleic acid
ChIP	Chromatin immunoprecipitation
co-IP	co-immunoprecipitation
$CuSO_4$	Copper(II) sulfate
DBA	Diamond-Blackfan anemia
dsRNA	double stranded RNA
EDTA	Ethylenediaminetetraacetic acid
ELM	Eukaryotic linear motif
EM	Electron microscopy
GFP	Green fluorescent protein
HEPES	4-(2-hydroxyethyl)-1-piperazineethanesulfonic acid
HRP	Horseradish peroxidase
IgG	Immunoglobulin G
IHC	Immunohistochemistry
IP	Immunoprecipitation
kb	Kilobase

kD	Kilodalton
mRNA	messenger ribonucleic acid
MALDI-TOF	matrix-assisted laser desorption/ionization time-of-flight
miRNA	microRNA
µm	Micrometer
µM	Micromolar
mM	Millimolar
MOPS	3-(N-morpholino)propanesulfonic acid
MW	Molecular weight
ng	Nanogram
nM	Nanomolar
ncRNA	non-coding RNA
NEM	N-ethylmaleimide
NLS	Nuclear localization signal
NFDM	Non-fat dry milk
NF-κB	Nuclear factor kappa-light-chain-enhancer of activated B cells
NMD	Nonsense-mediated mRNA decay
nos	*nanos*
nt	Nucleotide
NTC	No template control
pAb	Polyclonal antibody
PBS	Phosphate-buffered saline
PBT	PBS with 0.1% Triton X-100

PBTB	PBT with 3% BSA
PCR	Polymerase chain reaction
PolyA+	Polyadenylated
PTB	Phosphate-buffered saline with
PTM	Post-translational modification
PVDF	Polyvinylidene difluoride
qRT-PCR	quantitative real time polymerase chain reaction
RIPA	Radio-immunoprecipitation assay
RNA	Ribonucleic acid
Rp	Ribosomal protein
RS	Recombinant standard
RT	Room temperature
RT-PCR	Reverse-transcriptase polymerase chain reaction
SDS	Sodium dodecyl sulfate
SDS-PAGE	Sodium dodecyl sulfate polyacrylamide gel electrophoresis
shRNA	Small hairpin RNA
snoRNA	small nucleolar RNA
SUMO	Small ubiquitin-like modifier
TNF	Tumor necrosis factor
tRNA	Transfer RNA
UAS	Upstream activation sequence
UTR	Untranslated region
WB	Western blot

ABSTRACT

Gene duplication is a contributing factor to genome evolution in eukaryotes. With an additional copy, selective pressure is relieved, allowing for accumulation of genetic variation and possible development of new or altered functions. Ribosomal protein (Rp) genes are a common class of duplicated genes found throughout eukaryotes. Typically encoding highly similar or identical proteins at separate loci, duplicated Rps were originally thought to be redundant and to relieve the high demand for translation. However, recent reports in yeast have shown phenotypic differences between Rp paralogue knockouts, suggesting functional non-redundancy.

Little effort has been devoted toward elucidating the function of Rp paralogues in eukaryotes other than in yeast. Furthermore, in yeast, paralogous Rps are typically highly identical, making studying gene function difficult without protein tagging. To explore whether duplicated Rp genes have redundant roles, we focused on the eukaryotic-specific RpL22e family in *Drosophila melanogaster*. The *Drosophila* RpL22e family consists of two members, the ancestral *rpL22e* and its duplicate *rpL22e-like,* which are 37% identical. Divergence is evident in the genomic sequence, codon usage, and protein sequence, but whether this results in novel functions has not been previously addressed and is the focus of this dissertation.

It is widely known that the ancestral RpL22e is ubiquitous, but our data show that RpL22e-like expression is primarily restricted to the male germline and is a true

ribosomal component. Further investigation shows that in testis tissue, RpL22e is primarily SUMOylated and phosphorylated. Only unmodified RpL22e co-sediments with the translation machinery in *Drosophila* S2 cells, leading to the interpretation that the majority of testis RpL22e is not part of the translation machinery and that paralogue functions are non-redundant. Immunohistochemical analysis further supports non-redundant paralogue roles, as RpL22e is primarily restricted to the nucleoplasm in the maturing meiotic germline; RpL22e-like is cytoplasmic in these cells. Additionally, there is an unequal requirement for RpL22e members *in vivo*, as only *rpL22e* is essential in the fly.

Taking the data in this dissertation together, it is evident that the *Drosophila* RpL22e paralogues have diverged in function within the male germline. RpL22e assumes an additional and unique role compared to RpL22e-like.

Chapter 1:

Introduction

1.1 Ribosome Composition and Heterogeneity

The ribosome is a highly abundant and essential cellular complex that provides a platform for translation in all life forms. As ribonucleoprotein particles, ribosomes are assemblies of multiple RNA molecules (rRNA) and numerous ribosomal proteins (Rp) involving over 150 assembly factors, including rRNA processing and modification enzymes (Kressler *et al*., 2010) (Figure 1.1). Although differences are noted between ribosome structure between *and* within kingdoms, the general structure and assembly process is conserved. Ribosomes are the only organelle in eukaryotes that require all three RNA polymerases. RNA polymerase I (Pol I) is solely responsible for the transcription of the 47S pre-rRNA transcript in the nucleolus. The 47S pre-rRNA is subsequently processed into three of the four rRNA molecules that make up the ribosome: 18S, 5.8S, and 28S. Pol III transcribes the fourth rRNA molecule, 5S, from an independent locus outside of the nucleolus. Rp genes are transcribed by Pol II and are translated in the cytoplasm. Rps are then imported into the nucleus and bind rRNA co-transcriptionally. The 28S, 5.8S, and 5S rRNA along with ~ 47 large subunit Rps (designated as L1, L2, L3…) form the 60S large subunit. The 40S small subunit is composed of the 18S rRNA and ~ 32 small subunit Rps (designated as S1, S2, S3…). Together, the 60S large and 40S small subunit form the translationally active 80S monosome.

While the peptidyl transferase activity of the ribosome is solely catalyzed by the 28S rRNA, Rps have key roles in ribosome assembly and structure, and they modulate the functional activity of the ribosome as well. Protein interactions between ribosome components and other members of the translation machinery are necessary for translation. RNA-RNA interactions are required for translation as well, demonstrated by many examples including direct RNA hybridization between the mRNA and 16S rRNA (at the Shine-Dalgarno sequence) for proper translation initiation in prokaryotes. Aside from their role in ribosome biogenesis, Rps are found to have other roles in translation. For example, the ribosomal protein L23a has a role in binding the signal recognition particle (Gu *et al*., 2003) and Sec61 (Beckman *et al*., 2001) during co-translational translocation of ER-directed proteins. Rps also contribute other important enzymatic activities for ribosome function, such as the mRNA helicase activity of bacterial ribosomes (Takyar *et al*., 2005).

Ribosome composition (aside from assembly) has classically been viewed as static; however, recent evidence has shown that ribosome composition varies with multiple factors. Evidence supporting ribosome heterogeneity clearly exists, but its functional significance is not widely understood. *Plasmodium* spp. has separate rRNA genes expressed at different life stages (van Spaendonk *et al*., 2001); yet, the impact of incorporation of different rRNAs into ribosomes is unclear. Numerous prokaryotic species also have multiple, yet diverse copies of rRNA genes that produce rRNAs with

minimal secondary and tertiary structural differences (Pei *et al*., 2009). Furthermore, phosphorylation of Rps is developmentally regulated in maize (Szick-Miranda and Bailey-Serres, 2001). Differential phosphorylation is also seen in exponentially growing yeast compared to cells in stationary phase (Saenz-Robles *et al*., 1990).

Even more provocative evidence for ribosome heterogeneity is noted in rapeseed where the expression of 966 Rp genes, which only encode 79 Rps, is developmental- and tissue-specific (Whittle and Krochko, 2009). The social amoebae *Dictyostelium discoideum* also provides an example where Rps are developmentally-regulated. RpS19 is phosphorylated and RpL2 is methylated when *D. discoideum* is a single cell amoeba, but are lost (de-modified) when developing into a multicellular fruiting body. Conversely, RpL20 is phosphorylated during this transition. Additionally, RpL18 is only found in ribosomes of spores and not in the single cell amoeba (Ramagopa and Ennis, 1981; Ramagopa, 1990). Mutational analysis to determine the developmental impact of ribosome heterogeneity has yet to be explored.

While differential post-translational modification of Rps is evident and most likely important in the development of higher eukaryotes, exploration of the widespread abundance is difficult without laborious biochemical analyses, even with current analytical advances. However, recent advances in genomics and bioinformatics have been key in finding that duplicated Rps (separate loci typically encoding highly similar or identical proteins) are abundant in eukaryotic genomes, including yeast, invertebrates,

and mammals. Overall, duplicated Rps could be the leading contributor to ribosome heterogeneity.

1.2 Duplicated Ribosomal Proteins and Redundancy

Gene duplication is a contributing factor to genome evolution and can be found in all kingdoms of life. Gene duplications can arise from multiple mechanisms, including whole genome duplication, retrotransposition, and unequal crossing over during meiosis. With two (or more) copies of a gene, selective pressure is relieved, allowing for the accumulation of genetic variation. Consequently, if one copy evolves faster and acquires more genetic variation, new or altered functions may develop. However, not all gene duplications results in functionally diverse gene products. Whether gene divergence alters expression profiles, regulation, or impacts the gene product's function must be determined empirically.

The eukaryotic ribosome consists of 4 rRNAs and ~ 80 Rps, some of which are non-essential and some of which are encoded by duplicated genes. Duplicated Rps are most evident in yeast (Deutschbauer *et al*., 2005; Komili *et al*., 2007; Kim *et al*., 2009) and plants (Whittle and Krochko, 2009; Hummel *et al*., 2012), but are still found to a lesser extent in flies (Marygold *et al*., 2007), mice (Sugihara *et al*., 2010) and humans (Lopes *et al*., 2010). Additionally, the human genome also contains >2,000 Rp pseudogenes (Zhang *et al*., 2002; Balasubramanian *et al*., 2009; Tonner *et al*., 2012).

In *Saccharomyces cerevisiae*, 59 of the 78 Rps are encoded by two genes (138 Rp genes total), typically encoding highly similar or identical proteins (Kim *et al*., 2009). Only five (5) of the 118 duplicated Rp genes are essential, compared to 16 essential genes among the 19 *single* copy Rps (Deutschbauer *et* al., 2005). In most cases, abundance of duplicated Rps decreases in higher eukaryotes. For example, *Drosophila* contains 93 genes encoding 79 Rps (Marygold *et al*., 2007). However, exceptions to this general trend do exist. An extreme example of Rp duplication is seen in rapeseed (*Brassica napus*), for which multiple whole genome duplication events have been described. Of the 79 Rps found in the plant ribosome, each is encoded by at least two highly similar paralogous genes, with a total of 966 Rp genes (Whittle and Krochko, 2009).

The concept that paralogous Rps are functionally redundant has had widespread acceptance until most recently. Early studies showed that overexpression of one Rp rescues the growth defect resulting from genetic or biochemical depletion of its paralogue, supporting the notion of functionally redundancy (Rotenberg *et al*., 1988). Deutschbauer *et al*. (2005) reported that duplicated Rp genes have less severe haploinsufficiency defects than their non-duplicated partners, suggesting that duplication provides fitness to the organism. Many of the 14 duplicated Rps in *Drosophila* are not equally associated with the haploinsufficiency-related *Minute* phenotype (Marygold *et al*., 2007), suggesting non-redundancy.

Recent studies are challenging the view that duplicated Rps are functionally equivalent. Baudin-Bailieu *et al*. (1997) studied the RpS27 paralogues and showed that a yeast RpS27a knockout strain with wild-type growth rates has alterations and defects in ribosomal assembly and rRNA processing. Furthermore, localization of some paralogous Rps in yeast does not overlap, suggesting separate functions (Komili *et al*., 2007; Kim *et al*., 2009). However, this is not a widespread observation. Only five Rp pairs include paralogues with unique, separate localization patterns, suggesting possible non-redundant roles (Kim *et al*., 2009).

If paralogues are functionally redundant, one would expect to see identical phenotypes upon deletion or alteration. As noted above for yeast RpS27a knockout studies, defects in ribosomal maturation were prevalent even though growth rates were comparable to wild-type. Komili *et al*. (2007) has provided very compelling evidence for non-redundancy as they reported Rp deletions in yeast that exhibit paralogue-specific effects on transcription profiles and cause unique phenotypes. For example, the RpL7 paralogues (RpL7A and RpL7B) are 97.5% identical, 99.6% similar, and have similar localization patterns in wildtype yeast. However, single RpL7 paralogue knockout strains show unequal drug sensitivity, different requirements for cellular localization factors, and different effects on cell size (Komili *et al*., 2007). Moreover, this differential phenotype pattern between paralogue knockout strains is clearly evident in large and small subunit Rp paralogues (Komili *et al*., 2007). Whether the differential effects seen between paralogues are due to aberrations to the translation machinery (and ultimately

which mRNAs are translated) or are the result of a secondary effect from extra-ribosomal functions of Rps (discussed further in Chapter 1.4) remains to be investigated.

1.3 Proposal of 'Specialized Ribosomes' and 'Ribosome Code'

The widespread observation of Rp paralogues displaying different phenotypes taken together with differential localization of paralogues has led Komili *et al*. (2007) to propose a 'ribosome code'. Analogous to the histone code hypothesis, different combinations and post-translational modifications of Rps, along with modifications to the rRNA would allow for translation of specific mRNAs, and create new complexity in gene regulation. Xue and Barna (2012) have recently expanded this view and proposed 'specialized ribosomes' based on recent reports of ribosome heterogeneity, notably with effects associated with (but not limited to) tissue- or developmental-specific Rps.

The idea of selective translation as a mode of gene regulation has been previously described as the 'ribosome filter hypothesis' (Mauro and Edelman, 2002; Mauro and Edelman, 2007). According to this hypothesis, differences in ribosomal composition could affect translation initiation. The most compelling evidence to support this hypothesis includes 18S rRNA interactions in translation initiation (see references within Mauro and Edelman, 2002). Relatively little evidence supporting a role for Rps in this proposal has been forthcoming despite recognition of Rp heterogeneity in eukaryotes (see references within Mauro and Edelman, 2002).

In recent years, multiple reports have shown tissue-specific phenotypes associated with aberrations to Rp expression (see greater discussion and references below and within chapters 1.4-1.5). This raises the interesting possibility that Rps (and ribosome heterogeneity) may contribute to a higher order of gene regulation that is essential in higher eukaryotes.

Kondrashov *et al*. (2011) has recently provided the most compelling evidence that Rps can contribute to translation-specificity of particular mRNAs. Deletion of *rpL38* in mice leads to tissue-specific phenotypes, most notably axial skeletal patterning defects. While protein synthesis overall was unchanged in affected tissues, translation of a subset of Homeobox (Hox) genes was affected. Hox genes are the key regulators of morphology along the axial skeleton with spatiotemporal expression in development (Deschamps and van Nes, 2005; Pourquie, 2009; Wellik, 2009). Importantly, it was demonstrated that RpL38 is associated with the active translation machinery (polysomes) in these tissues, providing support that RpL38 confers translation specificity for a subset of Hox genes in these tissues.

Furthermore, Kondrashov *et al*. (2011), as well as others (Bortoluzzi *et al*., 2001; Thorrez *et al*., 2008; Whittle and Krochko, 2009), have shown that expression of individual Rps dramatically differs between tissues. Together, these data provide a foundation for future studies of how Rps may regulate translation of specific mRNAs in a developmental- and tissue-specific manner.

Other reports showing tissue-specific phenotypes of Rps support the possibility that Rps may regulate translation. *rpL29* knockout mice are smaller in size and have increased bone fragility (Oristian *et al*., 2009). Dominate mutations in murine *rpL24* are associated with a white ventral midline spot, white hind feet, a kinked tail, decrease in ganglion cells, and extra digits in the limbs (Oliver *et al*., 2011). When *Drosophila rpL14* is depleted by RNAi, fly development halts at pupation, where further investigations found that flies began metamorphosis but were headless (Enerly *et al*., 2003). In zebrafish and mice, knockdown of *rpL22e* only affects the T-cell lineage (Anderson *et al*., 2007; Zhang *et al*., 2013).

Few reports have focused on expression patterns of duplicated Rps and any associated phenotypes. Tissue-specific expression of duplicated Rps in mammals has been recently reported and the paralogues were confirmed to be ribosomal components, as is the case for mouse L10-like, L22-like 1, and L39-like (Sugihara *et al*., 2010). *Arabidopsis* RpL23a paralogues (RpL23aA and RpL23aB) are 94.6% identical and are expressed asymmetrically with RpL23aB having tissue-specific expression (McIntosh and Bonham-Smith *et al*., 2005). Depletion of RpL23aA severely disrupted development; however, knockdown of RpL23aB produced no phenotype (Degenhardt and Bonham-Smith, 2008). Additionally, Degenhardt and Bonham-Smith (2008) show differential requirement for nucleolar localization between the *Arabidopsis* RpL23a paralogues. In general, reports

investigating the function and associated phenotypes of duplicated Rps in metazoans are lacking.

Overall, the prevalence of tissue-specific phenotypes associated with Rps, as well as the distinct phenotypes displayed between highly homologous duplicated Rps shown in yeast, sets a precedent that Rps (as part of the translation machinery) may provide a new layer of gene regulation complexity.

1.4 Extra-Ribosomal Functions of Ribosomal Proteins

Rps in prokaryotes and eukaryotes, acting as multifunctional proteins with extra-ribosomal functions has recently gained traction (reviewed by Wool [1996], Lindstrom, [2009], and Warner and McIntosh [2009]). Various examples exist for both small and large subunit Rps in multiple prokaryotic and eukaryotic models, with functions ranging from ribosome-related functions to novel functions foreign to translation.

Proper ribosomal biogenesis and Rp expression is essential and some extra-ribosomal functions have evolved to ensure homeostasis. For example, as a form of autoregulation, yeast RpL30 (Eng and Warner, 1991), yeast RpS14 (Fewell and Woolford, 1999), and human RpS13 (Malygin *et al*., 2007) all inhibit splicing of their own mRNA when overepxressed. Additionally, ribosome stress is often monitored by the cell by excess Rps, which signals and stimulates p53-dependent apoptosis. Under normal conditions, the ubiquitin E3 ligase MDM2 (human orthologue HDM2) interacts with and modifies p53,

leading to rapid degradation of p53. However, excess RpL5, RpL11, RpL23, and RpS9 can bind MDM2/HDM2, resulting in the stabilization and accumulation of p53, thereby activating apoptosis (Marechal *et al*., 1994; Lohrum *et al*., 2003; Dai *et al*., 2004; Zhang *et al*., 2003; Jin *et al*., 2004; Chen *et al*., 2007).

Other extra-ribosomal functions found are truly extra-ribosomal and have no association with ribosome biogenesis or translation. For example, *Drosophila* and mammalian RpS3 can nick DNA at abasic sites and can interact with and increase the activity of the DNA repair enzyme uracil-DNA glycosylase (Wilson *et al*., 1994; Kim *et al*., 1995; Ko *et al*., 2008). Uniquely, RpS3 has also been found to respond to TNF stimulation and interact and stabilize the transcription factor complex KFκB (Wan *et al*., 2007). In zebra finch, the *rpL7* gene encodes a 44kD polypeptide that can be differentially processed/cleaved, resulting on one hand in the 27kD Rp or in the other case, the 31kD estrogen receptor coactivator in the avian brain (Duncan and Carruth, 2007; Duncan *et al*., 2009).

It is clear that a diverse array of functions beyond binding to rRNA and serving as a ribosomal component have been ascribed for multiple Rps. Unfortunately, few studies have focused on whether Rp paralogues have developed extra-ribosomal functions (due to sequence divergence and reduced selective pressure). Nevertheless, if Rps have multiple cellular roles, false interpretation of mutational analyses may be prevalent as phenotypes (e.g. tissue-specific effects) may be a result of aberration of the ribosomal and/or the extra-ribosomal function.

1.5 Ribosomes and Disease: Ribosomopathies

Rp deficiencies and haploinsufficiency have been linked to diseases and, more recently, tumorigenesis. Overall, ribosome-related diseases, including rRNA processing-associated diseases, have been termed 'ribosomopathies' and uniquely, manifest with tissue-specificity (reviewed by Narla and Ebert, 2010) (Table 1.1 and Figure 1.2). Although protein translation is crucial for all cells in an organism, it is unclear why Rp and rRNA processing mutations cause effects in specific tissues.

In recent years, the human bone marrow failure syndrome Diamond-Blackfan anemia (DBA) has gained clinical attention and has been linked to defects in ribosome synthesis and with heterozygous mutations in many Rps genes (Narla and Ebert, 2010). In 1999, Draptchinskaia *et al*. discovered that RpS19 is commonly mutated in DBA patients. Subsequent investigations have associated DBA with nine other Rps: RpS26, RpS24, RpS17, RpS10, RpS7, RpL35a, RpL26, RpL11, and RpL5 (Gazda *et al*., 2006; Gazda *et al*. 2008; Farrar *et al*., 2008; Doherty *et al*., 2010; Gazda *et al*., 2012; Cmejla *et al*., 2007). A direct mechanism of DBA has not been fully elucidated, but may include cell-lineage specific sensitivities to altered translation capabilities due to mutated Rps. Not mutually exclusive with this hypothesis, an alternate explanation has been proposed based on the cell cycle regulatory and non-ribosomal role of the nucleolus (Pederson, 2007 and references within). It is plausible that mutated Rps have pleiotropic effects, causing aberrations in ribosome assembly and subsequently in other nucleolar processes,

leading to pathogenesis (Pederson, 2007). Nevertheless, Rps are closely linked to DBA and other pathology.

In *Drosophila*, the *Minute* phenotype—characterized by prolonged development, low fertility and viability, altered body size and abnormally short, thin bristles on the adult body—has been linked to the haploinsufficiency of 68 Rps (Marygold *et al*., 2007). Recently, Casad *et al*. (2011) have showed that Rp mutations associated with the *Minute* phenotype have distinct and varying degrees of cardiomyopathy, suggesting that while generally having the same phenotype, individual Rp mutations can have distinct impacts on tissues.

Other developmental and tumorigenic defects have been mapped to Rps as well (reviewed in Montanaro *et al*., 2008; Amsterdam *et al*., 2004; Uechi *et al*., 2006; MacInnes *et al*., 2008; Lai *et al*., 2009). Ribosomopathies due to rRNA and Rp aberrations have been noted to contribute to the risk of cancer (Luft 2010; Narla and Ebert, 2010; Fumagalli and Thomas, 2011). While a complete mechanism is not clear, Rps have been shown to affect the stability of the key tumor suppressor p53 (see references within Chapter 1.4), which is the most commonly mutated gene in human cancers (Lane, 1992; Levine *et al*., 2009).

Notably, mutations in Rps and altered rRNA modification can lead to decreased translation fidelity, thus leading to the accumulation of altered proteins that may affect

genomic stability and homeostasis of the cell and may contribute to cancer progression. For example, mutations in RpS5 (Kirthi *et al*., 206), RpL3 (Peltz *et al*., 1999), RpL13a (Chaudhuri *et al*., 2007), and RpS12 (Agarwal *et al*., 2011) cause significant effects on translation fidelity. Similar effects are seen with alterations to rRNA (Baudin-Baillieu *et al*., 2009), leading to the conclusion that structure and/or interactions mediated by specific ribosomal components are essential for proper translation. Belin *et al*. (2009) has shown that while the Rp content of ribosomes in aggressive human breast cancer cell lines did not change, the rRNA methylation pattern was significantly altered. As a result, cap-independent translation initiation and overall translation fidelity, but not global translation rates, were significantly reduced in this cancer cell line.

A change in translation fidelity is not associated with all Rps and therefore the impact of individual Rps on translation fidelity must be determined empirically. For example, deletion of yeast RpL26 had no effect on multiple translation properties, including −1 and +1 frameshifting, read-through of nonsense codons, and the stringency of start codon selection (Babiano *et al*., 2012).

Overall, it is clearly evident that altered ribosome composition as a consequence of both Rp mutation and altered rRNA processing, results in distinct, clinically relevant diseases, often with tissue-specificity. While extra-ribosomal functions cannot be completely disregarded as contributors to such manifestations, data largely support the link between disease and translation defects. How tissue-specific phenotypes result from mutations in

ubiquitously-expressed genes remains enigmatic, but may be due to differential tissue sensitivity or lack of compensatory mechanisms present in other tissues.

1.6 RpL22e Family

To explore whether duplicated Rps are redundant or have developed novel functions, we have focused on the RpL22e family in *Drosophila melanogaster*, which consists of two members—the ancestral *rpL22e* and the duplicated *rpL22e-like*. This Rp family is 37% identical in protein sequence (Marygold *et al*., 2007) and divergence in the mRNA and amino acid sequences provides ample opportunity for paralogue-specific detection of mRNA and proteins, as well as specific targeting for RNAi knockdown.

RpL22e is a conserved eukaryotic-specific Rp that binds to stem-loop 7 of the 28S rRNA (Michot *et al*., 1984; Dobbelstein and Shenk, 1995). According to the recent 5.5Å cryo-EM map of the 80S ribosome, RpL22e is bound to the exterior surface of the large subunit (Armache *et al*., 2010; Ben-Shem *et al*., 2011) (Figure 1.3). Furthermore, the loop of helix 57, which is an interaction partner for RpL22e, is conserved in eukaryotes, suggesting similar positioning in other eukaryotic ribosomes (Armache *et al*., 2010). Additionally, mutational analysis of human RpL22e has identified multiple domains responsible for nucleolar localization (residues 65-69) and rRNA binding (residues 80-84 and 88-93), which are conserved in other eukaryotes, including *Drosophila*.

RpL22e is a non-essential protein in several eukaryotic systems (*in vitro* studies in rat [Lavergne *et al*., 1987], *in vivo* mouse knockout studies [Anderson *et al*., 2007]). Both RpL22e paralogues in yeast (RpL22eA and RpL22eB) are also non-essential (Komili *et al*., 2007). However, paralogue-distinct phenotypes were seen in yeast (*rpL22eA* with bud site selection; *rpL22eB* with cell size; Komili et al., 2007). Although non-essential in mice, Anderson *et al*. (2007) have shown, despite ubiquitous expression, that deletion of RpL22e causes a developmental p53-dependent arrest in T lymphocytes. Whether or not the mouse paralogue RpL22e-like1 compensates was not addressed.

rpL22e has recently been linked to multiple cancers. Genomic analysis has identified *rpL22e* mutations in microsatellite instability (MSI)-high endometrioid endometrial cancer (Novetsky *et al*., 2013), MSI-positive gastric cancer (Nagarajan *et al*., 2012) and T-acute lymphoblastic leukemia (Rao *et al*., 2012). MSI-high endometrioid endometrial cancers and MSI-positive cancers were typically heterozygous for a single nucleotide deletion within the *rpL22e* coding sequence, resulting in a frameshift. Whether *rpL22e* has an active role in cancer progression in these cancers has not been investigated; however, Rao *et al*. (2012) has identified that monoallelic *rpL22e* inactivation enhances development of thymic lymphoma through activation of the stemness factor, Lin28B.

P-element gene disruption in *Drosophila* at the *rpL22e* locus (Crosby *et al*., 2007), as well as RNAi knockdown in cultured S2 cells (Boutros *et al*., 2004) is lethal, demonstrating an essential role for RpL22e within the fly. Considering that conserved

regions exist between RpL22e orthologues, an explanation for the varied phenotype upon gene disruption in different organisms is unclear. However, *Drosophila* RpL22e is structurally distinct from other orthologues (Figure 1.4) and this may provide an explanation.

Koyama *et al*. (1999) reported that RpL22e contains an N-terminal extension with homology to the C-terminal portion of histone H1. While the role of this extension remains unknown, the resulting polypeptide is approximately twice as long as its orthologues (Koyama *et al*., 1999; Figure 1.4). Aside from its role in translation, human and insect RpL22e have been shown to interact with several other molecules, including: Poly(ADP-ribose) polymerase (Koyama *et al*., 1999), Epstein-Barr virus small RNA (Toczyski *et al*., 1994; Fok *et al*., 2006; Houmani *et al*., 2009), casein kinase II (Zhao *et al*., 2002), human telomerase RNA (Le *et al*., 2000), and the herpes simplex virus 1 major regulatory protein ICP4 (Leopardi and Roizman, 1996; Leopardi *et al*., 1997). Additionally, *Drosophila* RpL22e has also been associated with regulation of gene expression via interactions with chromatin. Ni *et al*. (2006) showed that, when overexpressed in cultured Kc cells, RpL22e binds chromatin and suppresses gene expression globally. Notably, the authors neither defined a DNA binding domain within RpL22e itself in their studies nor did they make reference to the N-terminal domain homology with histone H1 as previously described by Koyama *et al*. (1999). Whether or not this domain accounts for the chromatin interaction has not been addressed, but could, at least in part, provide an explanation.

In *D. melanogaster*, nine (9) of 79 Rps have paralogues, along with five (5) less conserved ribosomal protein '-like' genes (Marygold *et al*., 2007). Recent reports in *D. melanogaster* have identified an *rpL22e* paralogue encoded by *rpL22e-like*, due to its similarity in amino acid sequence (Kai *et al*., 2005; Shigenobu *et al*., 2006). Expression profiles of adult ovary germline stem cells show that *rpL22e-like* mRNA levels are 6.6% of *rpL22e* levels (Kai *et al*., 2005). Interestingly, *in situ* hybridization shows that *rpL22e-like* expression is tissue-specific, primarily localized to the gonads during embryogenesis (Shigenobu *et al*. 2006). *rpL22e-like* mRNA localization is ubiquitous in initial stages of *Drosophila* embryogenesis, followed by a sharp decrease in expression shortly thereafter, with localization to the pole cells (precursors to the germline). Later stage expression is primarily found in the gonads, with slight detection in parts of the stomatogastric nervous system. Although a specific role for RpL22e-like in the gonad has not been formally determined, it is thought to be a constituent of ribosomes due to its conservation with RpL22e (Crosby *et al*., 2007). Consistent with the proposal that RpL22e-like functions (at least in part) as an Rp are data from predicted protein interactions. Based on homology, copious interactions are predicted with numerous components of the translation machinery (DroID: the Drosophila Interactions Database: Yu *et al*., 2008). Interestingly, DroID also reports yeast-two hybrid results showing protein interactions not related to translation. Direct biochemical evidence for *Drosophila* RpL22e-like as a ribosomal component, however, is lacking.

Tissue specificity of RpL22e-like has also evolved in vertebrates. Mouse RpL22e-like1 is detected as a minor ribosomal component in liver and mammary gland (Sugihara *et al*., 2010). Zhang *et al*. (2013) has recently shown zebrafish RpL22e and RpL22-like1 (73% sequence identity) are ubiquitously expressed, but have distinct and opposite roles in hematopoietic development. Knockdown of *rpL22e* in embryos selectively blocks the development of T lineage progenitors and knockdown of *rpL22e-like1* impairs the emergence of hematopoietic stem cells in the aorta-gonad-mesonephros. While data support both paralogues as *bona fide* Rps in 24h zebrafish embryos, whether this cell-type effect between paralogues is due to 'specialized ribosomes' or extra-ribosomal functions was not addressed in this report. Nevertheless, these data do suggest that the RpL22e paralogues in zebrafish have developed unique functions (Zhang *et al*., 2013).

The nine (9) Rp paralogues in *Drosophila* (designated as '*a*' and '*b*') have very high amino acid sequence identity, ranging from 65-100%. However, for the five (5) 'Rp-like' genes, sequence identity ranges from 18-38%, with RpL22e and RpL22e-like having only 37% sequence identity (Marygold *et al*., 2007). Based on structural differences between RpL22e and RpL22e-like, it is possible that there are differences in paralogue function within the gonad.

Microarray data show that expression of *rpL22e-like* is primarily expressed in adult testes, suggesting a sex-specific function in translation (Chintapalli *et al*., 2007). Even more compelling is the observation that *rpL22e* is down-regulated, while *rpL22e-like* is

up-regulated in testes. If incorporated into ribosomes, what function, if any, does RpL22e-like provide that is not met by RpL22e? Assuming that RpL22e and RpL22e-like are mutually exclusive within the ribosome, what functional or regulatory differences could distinguish the two types of ribosomes?

In addition to defining functionally-distinct populations of ribosomes, RpL22e and RpL22e-like paralogues may also be implicated in extra-ribosomal functions yet to be discovered. In the case of *Drosophila* RpL22e, many non-ribosomal interactions have been noted. As stated earlier, *D. melanogaster* RpL22e has been shown to interact with casein kinase II (Zhao *et al*., 2002), poly (ADP-ribose) polymerase (Koyama *et al*., 1999), and chromatin (Ni *et al*., 2006). Whether or not similar interactions exist for RpL22e-like is unknown, but is worthy of investigation. Given the relatively low homology between RpL22e and RpL22e-like compared to other Rp paralogues (37% sequence identity; Marygold *et al*., 2007), it is possible that evolutionary constraints on RpL22e-like function have been relieved, allowing novel functions to develop.

1.7 Hypothesis and Research Objectives

Direct evidence that demonstrates differences in ribosome function due to incorporation (or assembly) of duplicated Rps is limited. This dissertation focuses on the *Drosophila melanogaster* RpL22e family to test the hypothesis that these structurally distinct Rp paralogues have distinct, tissue-specific roles which provide paralogue-specific functions (not limited to translation) in selected cells or tissues.

The following research objectives will provide evidence that RpL22e paralogues are either redundant in function or have acquired divergent roles in development:

1. To determine the expression pattern of *rpL22e-like* and to determine if RpL22e-like has maintained a conserved role as a component of the translation machinery.

   This objective is represented as Chapter 2 and is a peer-reviewed, published body of work: Kearse MG, Chen AS, Ware VC. Expression of ribosomal protein L22e family members in *Drosophila melanogaster*: *rpL22-like* is differentially expressed and alternatively spliced. Nucleic Acids Res 2011; 39:2701-2716. (Epub 2010 Dec 7)

2. To characterize the molecular weight shift in immunoreactive RpL22e species in the testis and characterize the localization pattern of the RpL22e paralogues in the testis and male germline.

   This objective is represented as Chapter 3 and is currently in review in the peer-reviewed journal, *Nucleus*: Kearse MG, Ireland JA, Prem SM, Ware VC. Expression of the Ribosomal Protein L22e family: RpL22e, but not RpL22e-like-PA, is SUMOylated and localizes to the nucleoplasm of meiotic spermatocytes in the testis of *Drosophila melanogaster*.

3. To determine if the RpL22e paralogues are equally required *in vivo* and in male germline development using paralogue-specific RNAi knockdown.

   This objective is represented as Chapter 4. It is our plan to submit this body of work (at least in part) after the work represented in Chapter 3 (Kearse *et al*., 2013, in review) has been accepted for publication.

1.8 Figures

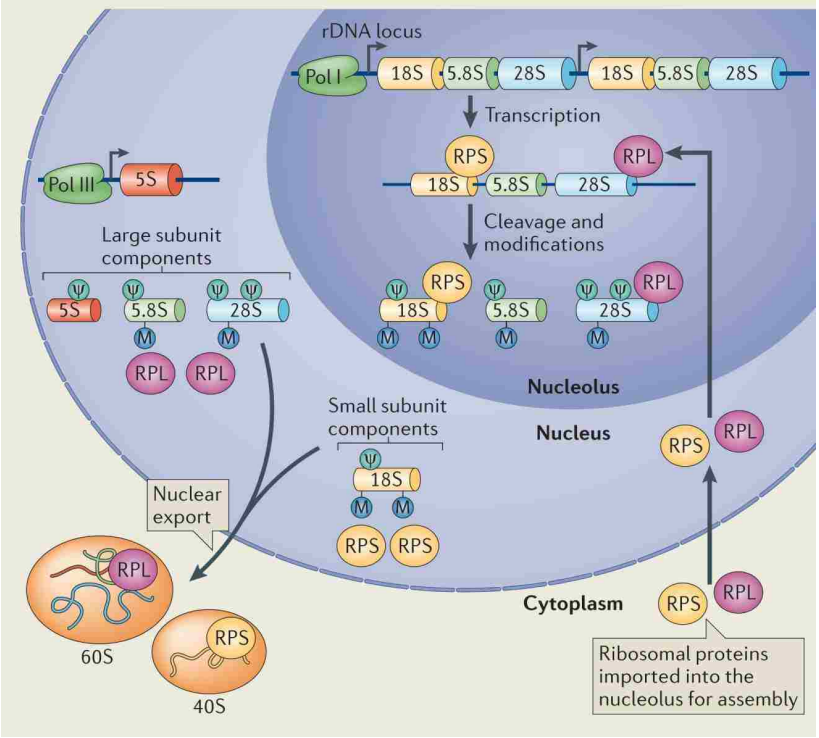

Figure 1.1. Ribosome assembly in eukaryotes. Ribosome assembly is a highly complex and dynamic event that requires the coordination of hundreds of factors, including distinct RNA polymerases, multiple rRNA modification enzymes with associated guide RNAs, ~80 ribosomal proteins, and many assembly factors that associate transiently during biogenesis. Ribosome assembly also primarily occurs within the nucleolus; however, maturation events do occur within the cytoplasm, requiring coordination between nuclear import and export of individual components, assembly factors, Rps, and subunits. Figure adapted from Xue and Barna (2013).

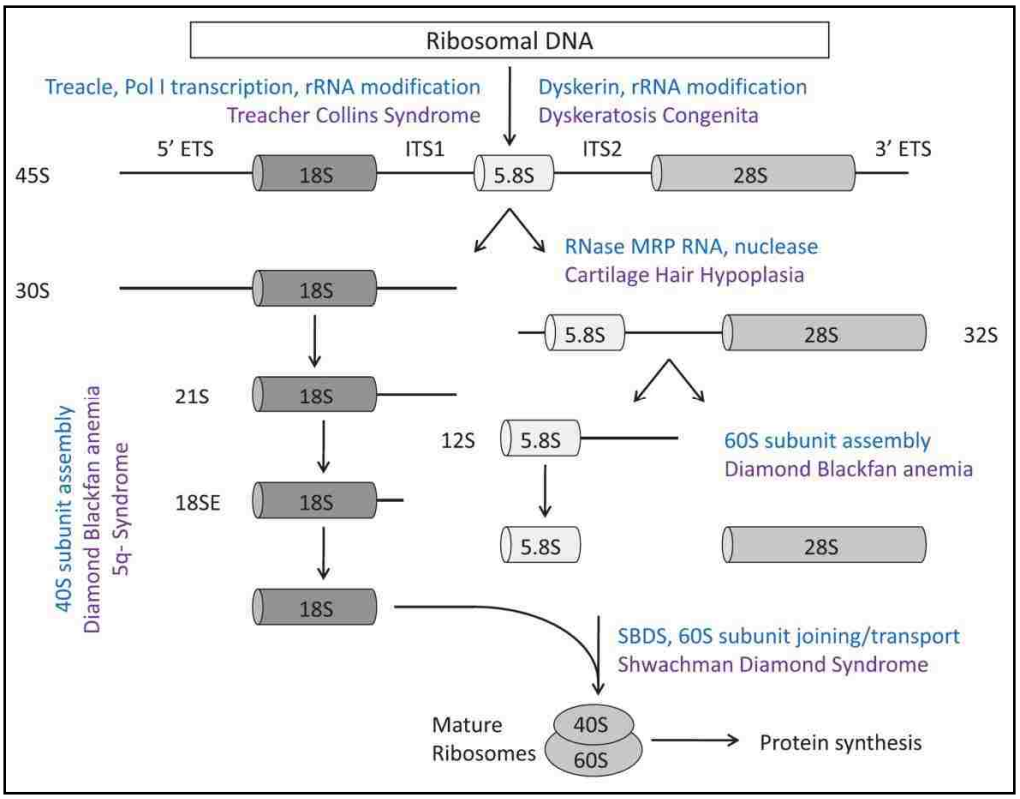

Figure 1.2. Ribosomopathies are associated with aberrations in rRNA processing and Rps. Ribosome biogenesis is a highly coordinated and sensitive process that results in various human diseases when disrupted. Importantly, different diseases are associated with separate steps and factors of ribosome biogenesis, including rRNA modification and processing, as well as defects in Rps of the large and small subunit. Figure adapted from Narla and Ebert (2010) and Liu and Ellis (2006).

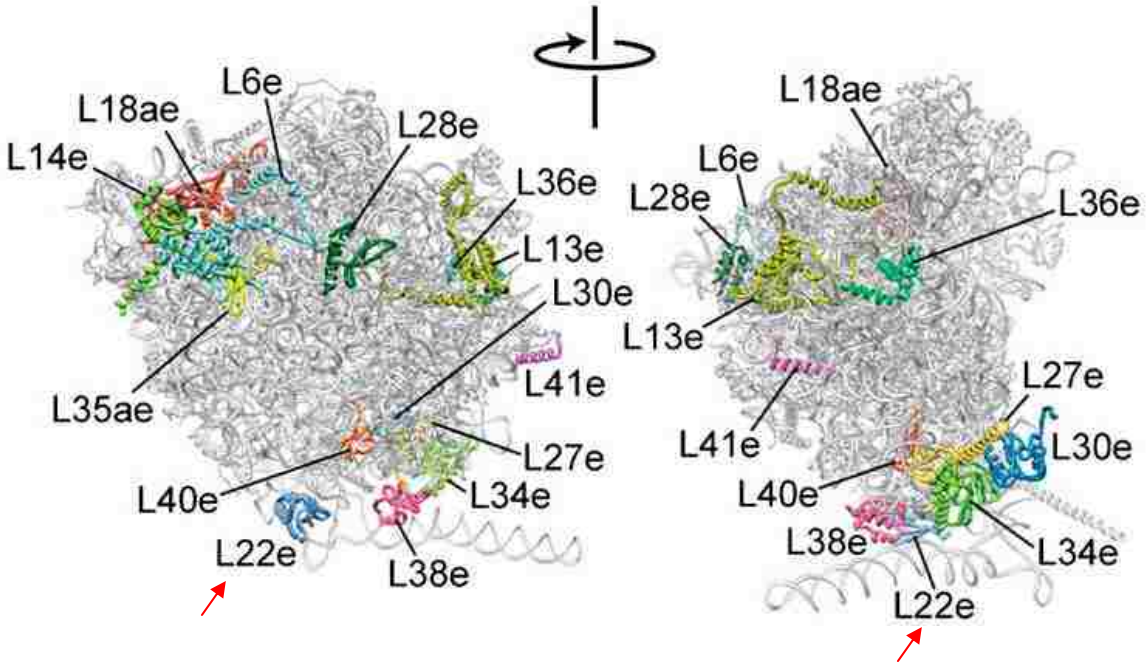

Figure 1.3. RpL22e is bound to the surface of the large subunit. Interface (left) and side (right) view of the 60S large subunit from *T. aestivum* showing the position of the eukaryotic-specific Rps. RpL22e (red arrow) is mapped to the surface of the large subunit, away from the peptidyl transferase center (center of interface view). Figure adapted from Armache *et al*. (2010).

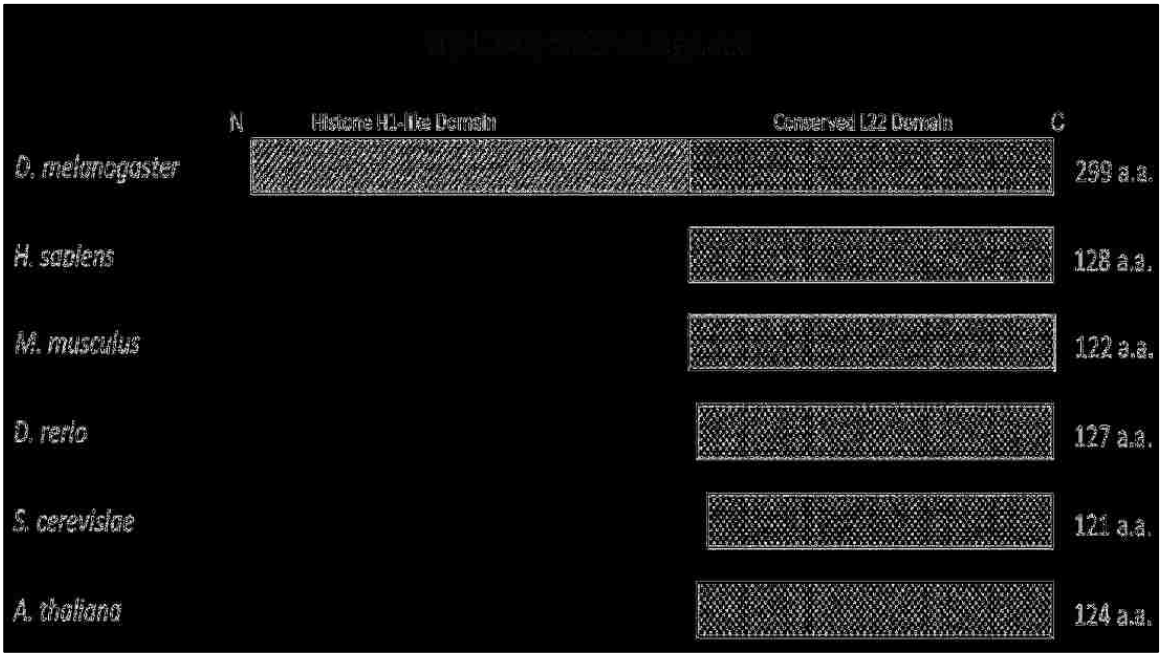

Figure 1.4. *Drosophila* RpL22e is structurally distinct from eukaryotic orthologues. *Drosophila melanogaster* RpL22e contains a fly-specific N-terminal domain that is homologous to the C-terminus of histone H1 (Koyama *et al*., 1999), resulting in a protein of approximately twice the length of other eukaryotic orthologues. The function of this domain remains to be determined. GenBank accession numbers used for comparison: *D. melanogaster*, (NP_477134.1); *H. sapiens* (NP_000974.1); *M. musculus* (NP_033105.1); *D. rerio* (NP_001032766.1); *S. cerevisiae* (NP_013162.1); *A. thaliana* (NP_187207.1).

Disease	Gene Defect	Clinical Features	Cancer Risk	Diagnosis
Diamond Blackfan anemia	RPS19, RPS24, RPS17, RPL35A, RPL5, RPL11, RPS7, RPL36, RPS15, RPS27A	Macrocytic anemia Short stature Craniofacial defects Thumb abnormalities	?osteosarcoma ?MDS	RPS19/RPS24 Sequencing Elevated ADA Elevated Hgb F levels
5q-syndrome	RPS14	Macrocytic anemia Hypolobulated micromegakaryocytes	10% progression to AML	Bone marrow aspiration/biopsy with karyotype
Shwachman-Diamond syndrome	SBDS	Neutropenia/infections Pancreatic insufficiency Short stature	MDS and AML	SBDS gene testing
X-linked dyskeratosis congenita	DKC1	Cytopenias Skin hyperpigmentation Nail dystrophy Oral leukoplakia	AML Head+neck tumors	Telomere length analysis
Cartilage hair hypoplasia	RMRP	Hypoplastic anemia Short limbed dwarfism Hypoplastic hair	Non-Hodgkin lymphoma Basal cell carcinoma	RMRP sequencing
Treacher Collins syndrome	TCOF1	Craniofacial abnormalities	None reported	Physical exam (imaging if needed)

Table 1.1. List of ribosomopathies, associated genes, and clinical features. Adapted from Narla and Ebert (2010).

Chapter 2:

rpL22e-like is differentially expressed and alternatively spliced

---

2.1 Introduction

In several ribosomal protein (Rp) gene families (most notable in certain yeast species and plant systems, reviewed by McIntosh and Bonham-Smith, 2006), paralogous proteins exist, presumably derived from duplication events in the evolutionary history of the gene. Paralogous Rps may have functionally redundant roles within the ribosome, or in some instances, their roles may be specialized in ribosome biogenesis or translation, contributing to heterogeneity within the ribosome cycle (Sugihara *et al*., 2010). Alternatively, specialized roles for paralogous Rps may include extra-ribosomal or extra-translational functions (see review by Warner and McIntosh [2009] for some discussion on this issue). Specialized roles may be indicated particularly if a paralogue is expressed in a cell-, tissue- or developmental stage-specific manner.

Recent studies in *Saccharomyces cerevisiae* have revised the previously held view that many RP paralogues dually expressed in that species are functionally equivalent (Komili *et al*., 2007). Instead, some paralogues are specialized for differential functions or cellular locations (Komili *et al*., 2007; Kim *et al*., 2009), leading Komili *et al*. to propose a ‘ribosome code’ that regulates translation of specific mRNAs in different physiological states. Tissue-specific ribosome heterogeneity due to assembly of Rp variants into

ribosomes has also recently been reported in rodent mammary gland and liver for RpL22e-like1 and in testis for RpL10- and RpL39-like (Sugihara *et al*., 2010).

In *Drosophila melanogaster*, RpL22e and RpL22e-like are members of the conserved RpL22e family specific to eukaryotes. Unlike most fly RP paralogues that display between 65% and 100% amino acid identity (Marygold *et al*, 2007), RpL22e and RpL22e-like are instead only 37% identical (Marygold *et al*, 2007), suggesting considerable 'opportunity' for disparate functions between family members. RpL22e family members in *Drosophila* also exhibit unique structural features at the N-terminus compared to orthologues in other species. Fly RpL22e family members contain an N-terminal extension of unknown function that is homologous to the C-terminal end of histone H1 [previously described only for RpL23a and RpL22e by ref. (Koyama *et al*., 1999)]. Structural divergence between RpL22e and RpL22e-like is most prominent within the N-terminal extension. Over time the novel domain may have specified new functions for these proteins in addition to their functions in the ribosome cycle.

In addition to considerable amino acids divergence between these paralogues in *D. melanogaster*, their expression patterns are also dissimilar. Transcripts for *rpL22e* are ubiquitously expressed. Previous studies have revealed *rpL22e-like* mRNA expression in embryonic gonads, adult ovary and germline stem cells by *in situ* hybridization or RT-PCR (Kai *et al*., 2005; Shigenobu *et al*., 2006a; Shigenobu *et al*., 2006b). Recent microarray analyses showed enrichment of *rpL22e-like* in adult testis, but not in adult

ovary (FlyAtlas; Chintapalli *et al*., 2002). Shotgun mass spectrometric data support the existence of RpL22e-like protein in fly embryos (www.ebi.ac.uk/pride/Q8T3X3), but no protein expression data for other developmental stages and/or specific tissues have been established. Tissue-specificity of *rpL22e-like* expression suggests that RpL22-like may have a distinct role compared to its paralogue RpL22e, at least in the embryonic gonad.

Although its position on the 60S subunit has recently been mapped by cryoEM to the base of the subunit on the most recently published 80S ribosome model (Armache *et al*., 2010), the cellular role for RpL22e has not been completely characterized (Lavergne *et al*., 1987). Interestingly, partially reconstituted ribosomes that lack RpL22e are still translation competent, suggesting that the protein may have a regulatory or non-ribosomal role (Lavergne *et al*., 1987), or alternatively, function under different physiological conditions. In *Drosophila*, additional roles and interactions for RpL22e have been proposed [based on high-throughput yeast two hybrid screens assembled in the Drosophila Interactions Database version 2010_10 (DroID: http://www.droidb.org)], awaiting further characterization. Among these interactions are several putative extra-ribosomal roles for RpL22e, including interactions with a transcriptional repressor complex in Kc cells (Ni *et al*., 2006) and with nuclear enzyme poly-ADP ribose polymerase (mediated through the N-terminal histone H1-like domain [Koyama *et al*., 1999]), for example.

Based on C-terminal homology to RpL22e and its tissue-specific expression pattern, it is reasonable to hypothesize that RpL22e-like has a gonad-specific ribosomal function, although other functions cannot be excluded. In fact, several protein–protein interactions are also catalogued for RpL22e-like in the Drosophila Interactions Database and none overlap with those proposed for RpL22e, including those that are likely to be non-ribosomal in nature. Together, this information suggests that RpL22e and RpL22e-like have distinct functions, either within the ribosomal cycle and/or in non-ribosomal pathways. That one of the functions of RpL22e-like is as a ribosomal component had not been previously investigated prior to this study. Such developmental or tissue-specific regulation of a putative Rp is not widely known in animal systems and is more commonplace in plants (McIntosh and Bonham-Smith, 2006).

To explore the possibility that RpL22e-like functions as a tissue-specific ribosomal component, we first refined its developmental and tissue-specific expression pattern to facilitate its biochemical characterization. By quantitative (q) RT-PCR, we determined that *rpL22e-like* mRNA is highly enriched in adult testes compared to ovaries. Using paralogue-specific antibodies (Abs) in Western blots, we detected a highly abundant protein of the predicted molecular weight (MW) for RpL22e-like in testes. A higher MW immunoreactive species was also detected in fly heads. Immunohistochemical (IHC) analysis of the male reproductive tract shows that RpL22e-like is exclusively found within testes and not within seminal vesicles or accessory glands. We further

demonstrate that RpL22e-like is a ribosomal component (80S and polysomes), suggesting its incorporation into actively translating ribosomes.

These studies also led to a novel finding that *rpL22e-like* is alternatively spliced using non-canonical splice sites to remove an intron that generates a short form designated *rpL22e-like-PB,* found in lower abundance than the full-length mRNA isoform (*rpL22e-like-PA*). Surprisingly, the most abundant *rpL22e-like* mRNA isoform *retains* the previously uncharacterized intron (*rpL22e-like-PA*). *rpL22e-like-PB* mRNA would encode a protein consisting nearly exclusively of amino acid residues in the N-terminal domain of RpL22e-like fused in frame to residues at the very end of the C-terminus, thereby eliminating the majority of the conserved RpL22e ribosomal signature. Detection of *rpL22e-like-PB* mRNA on polysomes and the presence of a low abundant protein of the predicted MW in testis extracts suggest that the spliced variant may be translated. This study provides the first experimental confirmation that RpL22e-like is a ribosomal component that is enriched in testis, and that its gene through alternative splicing may also encode a novel protein (RpL22-like-PB) with a novel non-ribosomal function based on its predicted amino acid structure.

2.2 Results

rpL22-like mRNA transcripts are enriched in the testis.

Gene expression profiling of embryonic germline stem cells (Shigenobu *et al*., 2006a) and adult ovary germline stem cells (Kai *et al*., 2005) previously identified a novel and possible germline stem cell-specific gene known as *rpL22e-like* (due to its similarity to *rpL22e*; Figure 2.1A). An important goal was to refine previously reported *rpL22e-like* mRNA expression profiles (Kai *et al*., 2005; Shigenobu *et al*., 2006a; Shigenobu *et al*., 2006b) in order to initiate studies on RpL22e-like protein expression and function. By RT-PCR analysis, we determined that *rpL22e-like* is expressed not only in embryos, larvae and adults, but also in an embryonic-derived S2 cell line, as well as within gonads and heads of both sexes (Figure 2.2). The expected amplicon of ~939 bp was present in all samples using primers determined by BLAST analysis to target only *rpL22e-like* in the *D. melanogaster* genome. Interestingly, in addition to the expected RT-PCR product for *rpL22e-like* there was a prominent lower MW amplicon of ~392 bp that was reproducibly amplified in multiple experiments for all RNA samples analyzed (Figure 2.2). Molecular characterization (cloning and sequencing) of both amplicons indicated that both are derived from the *rpL22e-like* gene. We refer to this lower MW amplicon as *rpL22e-like-PB* (described in detail below).

Based on RT-PCR data, *rpL22e-like* isoforms were detected in a variety of developmental stages and tissues. To determine isoform abundance in fly gonads, heads and S2 cells, we used qRT-PCR and isoform-specific primers on different RNA samples

(Figure 2.3; Table 2.1), showing that both *rpL22e-like-PA* and *rpL22e-like-PB* mRNAs are enriched in testis compared with other tissues examined. These data corroborate previously published microarray analyses (Chintapalli *et al*., 2002) and high-throughput expression analyses (FlyAtlas: flyatlas.org), showing that *rpL22e-like* mRNA is highly enriched (~4300-fold in this study) in testis compared with ovary (Table 2.2). Using the testis-specific *β2-tubulin* gene (Kemphues *et al*., 1979) and the germline-specific *Vasa* gene (males: Tazuke *et al*., 2002; females: Sano *et al*., 2002) for comparative purposes in the fly gonad, mRNA levels seen for *rpL22e-like-PB* (and for *rpL22e-like-PA*) in tissues other than in testis may be due to basal level transcription (Figure 2.3) as *β2-tubulin* mRNA (widely regarded as a *testis*-specific protein [Kemphues *et al*., 1979; Rudolph *et al*., 1987]) has some level of detection even in ovaries.

While found at ~9800-fold lower levels compared with rp*L22e-like* in testes, all samples showed that *rpL22e-like-PB* is not the prominent isoform, with highest and lowest amounts in testes and in S2 cells, respectively. Steady-state levels of both *rpL22e-like* mRNA isoforms are therefore highest in the testis.

RpL22-like protein is differentially expressed and found in active ribosomes.

Based on the relative abundance of *rpL22e-like* mRNA, we determined that RpL22e-like protein expression would best be analyzed in testes compared with other tissues. Since no RpL22e-like Abs were previously available, paralogue-specific polyclonal Abs targeting C-terminal amino acid residues were designed for recognition of RpL22e or

RpL22e-like (Figure 2.1A). The C-terminal peptide Ab for RpL22e is identical to that used successfully by Ni *et al*. (2006) in IHC experiments and ChIP analysis; therefore, we anticipated that this Ab would be useful in our protein blots and IHC studies to detect RpL22e. The C-terminal Ab for RpL22e-like recognition in protein blots and IHC studies was similarly based on the location of the Ab epitope for paralogue RpL22e.

We first confirmed that our Abs were specific for the proteins of interest by pre-immune sera analysis and detection of recombinant tagged proteins (Figures 2.4 and 2.5). Western blot analysis was used to screen adult gonads, larval salivary glands, S2 cells and fly heads for the presence of RpL22e. As RpL22e is ubiquitously expressed, we expected that RpL22e would be detected in all tissues. Two prominent immunoreactive species, one at the predicted MW (~33 kD) for RpL22e and the other at ~50 kD (the latter seen in all tissues), were identified (Figure 2.6A). The amount of 50 kD species varied in different tissues in multiple experiments and may represent incorporation of RpL22e into an SDS-resistant complex. Interestingly, relatively little, if any RpL22e of the expected size is found in the testis and in heads.

Further, Western analysis confirmed that RpL22e-like expression within the gonad is confined to males, as a protein of the expected MW (~34 kD) is highly enriched in testis tissue and not ovary (Figure 2.6A). We also noted an immunoreactive product (found in lower abundance than in testes) in an insoluble head extract (only a very limited amount of this product is seen in a soluble head fraction in some preparations). Surprisingly in

head tissue, immunodetection is seen at a higher MW (~60 kD). What factors contribute to the electrophoretic shift for both RpL22e and RpL22e-like are unknown, but may include post-translational modifications or assembly into SDS-resistant complexes. In fact, *in silico* analysis for both RpL22e and RpL22e-like predicts several sites for post-translational modifications, particularly for phosphorylation [Eukaryotic Linear Motif resource for functional sites in proteins (ELM; http://elm.eu.org/)]. Unlike the protein expression pattern in the gonad, RpL22e-like is detected in both male and female heads (Figure 2.6B). Detection of RpL22e-like in soluble and insoluble fractions in different tissues, coupled with a difference in some aspect of structural configuration (accounting for the higher MW) may indicate that RpL22e-like has a different function in different tissues. Alternatively, the protein may have the same function in different tissues, but its subcellular distribution may be subject to specific regulation.

The absence of RpL22e-like detection in an extract from heads in which eyes were excised (Figure 2.6A) suggests that RpL22e-like may be expressed in the eye; however, removal of eyes from fly heads sometimes removes underlying brain medulla tissue as well. We were unable to resolve this issue by analyzing extracts from isolated eyes due to eye pigment interference in protein fractionation and Western blot analyses. Instead, we analyzed the amount of RpL22e-like in *eyeless* (*ey*) mutant heads where the amount of eye tissue is significantly reduced compared to wild-type, and determined that there is a significant decrease in the amount of RpL22e-like in quantitatively similar amounts of

head protein (Figure 2.7). Resolution of RpL22e-like expression in the head/eye awaits IHC analyses.

Given that RpL22e-like is enriched in testis, we used IHC to confirm its presence in the testis and to determine its localization relative to RpL22e by using the same paralogue-specific Abs as were used for protein blots. Immunohistochemistry on the adult male reproductive tract confirmed that RpL22e-like expression is confined to testes and is not detected within seminal vesicles, accessory glands or the ejaculatory duct (Figure 2.8). RpL22e-like is present within all stages of sperm cells, contained within testes [see extruded sperm (ES) and testis internal contents]. In contrast, RpL22e is expressed throughout the tract, including sperm cells. A more detailed description of the staining patterns for RpL22e and RpL22e-like within the germline is found in Chapter 3 (Kearse *et al*., 2013, in review).

Comparison of the amino acid sequence of RpL22e-like with that of RpL22e shows conservation of documented functional residues (Houmani and Ruf, 2009; Figure 2.1A) though their functionality within RpL22e-like has not been confirmed. Yet, we might predict that RpL22e-like is an RNA binding Rp competent. In order to resolve this fundamental question about RpL22e-like function, we performed Western analysis on pooled fractions (from whole male flies) containing polysomes and 80S ribosomes isolated on 10–50% sucrose density gradients (Figure 2.9). Both RpL22e and RpL22e-like are detected in 80S ribosome and polysome fractions, indicating that both proteins

are stably associated with ribosomes. As RpL22e-like is highly abundant in testis, we infer that the protein is a component of testis ribosomes. The presence of RpL22e in ribosome fractions from male extracts, however, does not verify that RpL22e functions as an Rp in the testis; this determination will require additional analyses. Interestingly, only RpL22e of the expected MW is detected in ribosome and polysome fractions. The higher MW protein detected in Western blots is not an apparent component of ribosomes, suggesting that this RpL22e-containing component may have a non-ribosomal role (further investigation in Chapter 3).

***rpL2e2-like-PB* is an alternatively spliced mRNA variant.**

Only one annotated transcript has previously been reported in FlyBase for *rpL22e-like*; therefore, the identification of additional amplicons was not anticipated. To rule out non-specific or off-target amplification, the lower MW amplicon was cloned and sequenced. Sequence analysis of 29 different clones (embryo: 2; larvae: 2; testis: 6; ovary: 19) derived from PCR products using different RNA samples and primer sets (Table 2.2) confirmed that the lower MW amplicon was derived from the *rpL22e-like* gene and therefore presumed to be a previously unidentified spliced variant of *rpL22e-like* mRNA (Figure 2.2). We have named this novel mRNA product '*rpL22e-like-PB*' to reflect its truncated structure. Its deduced sequence of 123 amino acid would consist of the fly-specific histone H1-like N-terminal extension fused in frame to the last 10 amino acid in the C-terminus (Figure 2.1B). The proposed protein sequence lacks 189 amino acids that comprises the majority of the conserved RpL22e family signature at the C-terminal end.

Alignment of the coding sequences for *rpL22e-like-PB* (GenBank accession no. HM756190) and *rpL22e-like-PA* (GenBank accession no. HQ190956) revealed a surprising finding that the proposed splice sites surrounding the uncharacterized intron (0.567 kb) were non-canonical in sequence [5′ splice site (SS): CT; 3′ SS: CG] compared to typical sequences found in most introns (5′ SS: GT; 3′ SS: AG), including the annotated intron within the *rpL22e-like* gene (Figure 2.10). Non-canonical splice sites are indeed rare, but have been described in other eukaryotic genes as well (Burset *et al*., 2000). In all 29 *rpL22e-like-PB* sequenced clones, proposed 5′ splice donor and 3′ splice acceptor sites were identical to those shown in Figure 2.10, strongly supporting new intron-exon definitions within *rpL22e-like.*

Template switching artifacts can occur in some cases where RT-PCR is performed on templates that have direct repeats flanking a proposed intron, thereby giving false signals of truncated, alternatively spliced products (Cocquet *et al*., 2006). Although direct repeats do not flank the proposed retained intron in this case, we used additional RT-PCR analyses with primers that specifically hybridize to proposed exon–exon junctions and overlap the junction by 4 nt, expecting that an *rpL22e-like*-PB amplicon would be produced (using stringent conditions) only if the proposed exon–exon junction was present. In all cases, RT-PCR amplicons were consistent with expected product sizes: ~950 bp for *rpL22e-like* and ~392 bp for *rpL22e-like-PB* using an exon1/2 bridge

primer, and ~370 bp derived from *rpL22e-like-PB* using the novel exon2/3 bridge primer (Figure 2.11A).

Additional control RT-PCR experiments to rule out artificial amplification of a shortened transcript were performed using *in vitro* synthesized *rpL22e-like-PA* and *-PB* transcripts derived from cloned cDNA templates and flanking or bridge primer sets (Figure 2.12). With flanking primers and full-length *in vitro* synthesized RNA, a single amplicon of ~939 bp was generated, as expected. Notably low MW amplicons representing *rpL22e-like-PB* cDNAs were not produced. Using *in vitro rpL22e-like-PB* RNA as a template, an expected amplicon of ~392 bp was generated. Only when bridge primer sets (novel exon2/exon3) were used with *rpL22e-like-PB in vitro* RNA templates were amplified products of the expected size generated; no amplicons were produced with bridge primers and full-length *in vitro* RNA. We conclude that the low MW amplicon generated from *in vivo* polyA+ mRNA templates from different developmental stages as well as from various tissues is an *rpL22e-like* mRNA variant and not an artifact of aberrant RT-PCR amplification.

Further evidence for the presence of lower MW *rpL22e-like* mRNA isoforms was shown in Northern blot analyses using embryonic, larval and/or adult polyA+ RNA and 5′ and 3′ flanking *rpL22e-like* oligonucleotide probes that would detect both *rpL22e-like-PA* and *rpL22e-like-PB* mRNAs or an intron-specific probe that would detect full-length mRNA and the ‘retained’ intron (if sufficiently stable). It should be noted that the bridge primer

used in RT-PCR experiments described above would not be expected to detect *rpL22e-like-PB* mRNA exclusively since the majority of sequences in that probe would also hybridize to full-length mRNA under the standard hybridization conditions used.

Using probes that should detect both *rpL22e-like-PA* and *rpL22e-like-PB* mRNAs, we identified in each developmental stage, two prominent hybridization signals at ~0.7 and 0.5 kb (in addition to a signal at ~1.2 kb) that are smaller in size than the length expected for *rpL22e-like-PA* mRNA. The 0.7 kb species falls within the range of the minimum size for an *rpL22e-like-PB* transcript at ~0.625 kb (Figure 2.11B), not accounting for possible variation in polyadenylation. The lower MW RNA species are less abundant than the RNA species at ~1.2 kb (which likely represents *rpL22e-like-PA* mRNA)—an expected quantitative result for *rpL22e-like-PB* mRNA based on qRT-PCR results (Figure 2.3). The identity of the ~0.5 kb species is unknown; however, it is unlikely to represent the excised intron itself since flanking *rpL22e-like* probes would not hybridize exclusively to retained intron sequences.

Interestingly, in northern blot experiments where embryo polyA+ RNA (different sample than used in Figure 2.11B) was initially probed with an intron-specific probe, we detected an RNA of the size expected for *rpL22e-like-PA* mRNA and a lower MW species that may represent the excised intron of 0.57 kb (Figure 2.11C). The putative intron species is less abundant than *rpL22e-like-PA* (expected based on the relative amount of spliced variant compared to full-length mRNA from qRT-PCR data; Figure 2.3) and would only

be detected as such if *rpL22e-like* mRNA is alternatively spliced and the intron is stable. Alternatively, this species may represent a specific degradation product derived from *rpL22e-like* mRNA. In general, detection of introns would be rare, unless the proposed intron encodes a stable, functional small RNA, as has been shown for small nucleolar RNAs (Psi18S-531; Psi28S-2179; FlyBase) encoded by *rpL22e* introns.

When the same embryo RNA blot was stripped and re-probed with flanking probes, the pattern of hybridization differed from the intron-specific hybridization pattern in that the ~0.7 and 0.5 kb species were clearly present as previously noted in the developmental RNA blot. The presumptive intron species was not apparent in this blot using flanking probes. An unidentified RNA species of ~0.9 kb is also prominent, and may be faintly represented in all stages in the developmental blot (Figure 2.11B). Importantly, the Northern blot data demonstrate the presence of smaller RNA species not previously predicted for *rpL22e-like* based on genome annotation in FlyBase and may represent alternatively spliced mRNA variants although we cannot conclusively discount the possibility that smaller RNA species might represent specific *rpL22e-like* mRNA degradation products detected with our probes. When Northern blot data together with RT-PCR amplification data using *in vivo* and *in vitro* RNA templates are considered, we favor the conclusion that *rpL22e-like-PB* mRNA is a *bona fide* transcript produced by alternative splicing of the retained intron found within *rpL22e-like* mRNA.

***rpL22e-like-PB* mRNA is associated with polysomes and may be translated.**

Initial Western analysis of testis extracts (at protein concentrations sufficient to detect RpL22e-like) did not detect a protein product of the expected MW for RpL22e-like-PB (Figure 2.6A). Based on the low abundance of the *rpL22e-like-PB* mRNA within testes, we speculated that a putative RpL22e-like-PB protein product may be equally rare. To determine if the *rpL22e-like-PB* mRNA might be translated, we analyzed RNA isolated from polysomes (from male extracts) by RT-PCR (Figure 2.13A). *rpL22e-like-PB* (and *rpL22e-like-PA*) mRNA was detected in polysomes (Figure 2.13A), suggesting that the *rpL22e-like-PB* mRNA is translated.

Based on our qRT-PCR results that indicated a large quantitative imbalance in the two mRNA isoform levels in the testis with *rpL22e-like-PB* being ~9800-fold less abundant (Figure 2.3), we increased significantly (by nearly an order of magnitude) the amount of protein loaded for Western analysis (100–120 µg compared with 15 µg) in an attempt to detect a protein that putatively might be RpL22e-like-PB. With this protein loading strategy, additional immunodetection is seen at ~25 and ~13 kD (Figure 2.13B and C). Notably, recombinant RpL22e-like-PB migrates at the identical position with the ~13 kD reference band. The ~25 kD (and ~13 kD) protein may be a degradation product, only visualized with protein overloading or alternatively, the ~25 kD protein may be a post-translationally modified outcome of *rpL22e-like-PB* expression. Whether or not these bands represent degradation products derived from RpL22e-like is unclear; however, a computational investigation of proteolytic sites that would be found in the *Drosophila* RpL22e-like amino acid sequence (FlyBase ID: FBgn0034837) does not predict

degradation products of either MW (PeptideCutter, Expasy.org). A definitive resolution of this issue was not addressed in this study, but may be addressed by MALDI-TOF analysis. The relatively low abundance of the ~13 kD protein (estimated based on exposure times required to visualize RpL22e-like-PB compared to RpL22-like-PA; Figure 2.13B and C) is similar to what might be expected if RpL22e-like-PB protein expression (when compared to RpL22e-like-PA expression) is approximately proportional to the amounts of *rpL22e-like-PB* and *rpL22e-like-PA* mRNAs in testis.

2.3 Discussion

RpL22-like is a tissue-specific Rp.

We refined the expression pattern for *rpL22e-like* in several tissues and developmental stages, showing that both *rpL22e-like* mRNA and its protein product are highly enriched in adult testes compared to other tissues as analyzed by qRT-PCR and Western analysis, respectively. Within the male reproductive tract, RpL22e-like expression is limited to testes, as visualized by IHC.

In a microarray study evaluating testis-specific paralogue gene expression in general, Mikhaylova *et al*. (2008) identified RpL22e as one of 12 down-regulated Rp genes. In this study, RpL22-like escaped identification as a paralogue and as an up-regulated gene in testes because its homology to RpL22 fell below the minimum 50% homology threshold. Microarray data from FlyAtlas suggest that the levels of *rpL22e* and *rpL22e-like* mRNAs in testis are comparable. RpL22e-like may augment a function(s) of RpL22e by providing a testis-specific ribosomal role under specific developmental or physiological conditions.

Outside of the reproductive system, RpL22e-like is found within head tissue in possibly the eye (but in lower abundance compared with testes) from both sexes at a MW that is distinct from the testis conformation, suggesting a possible alternative functional role for RpL22e-like in the head. Although *rpL22e-like* mRNA levels in male and female heads are low based on qRT-PCR results (Figure 2.3), higher levels of *rpL22e-like* expression

in the relevant tissue in the head may be masked by the abundance of other tissue types. Interestingly, the quantity of *rpL22e-like* mRNA measured in heads and ovaries is similar (Figure 2.3); yet, protein expression differs considerably with no protein detected in ovaries.

We have confirmed the prediction that RpL22e-like is a ribosomal component based on its co-sedimentation with gradient-purified ribosomes and polysomes from male extracts. Taken together with quantitative expression data from testis, we infer that RpL22e-like is a component of testis ribosomes. The majority of RpL22e-like in male extracts was found in association with ribosomes or polysomes (and little, if any, was detected at the top of gradient profiles), suggesting that RpL22e-like is a more permanent ribosomal component than has been determined for *RACK1* (see review by Warner and McIntosh, 2009). Yet, not necessarily a protein with an exclusively ribosomal function, RpL22e-like may have an alternate role(s) as well. Though it is known that RpL22e is ubiquitously expressed (e.g. shown in the entire male reproductive tract by IHC), it is unclear if RpL22e functions exclusively as an Rp within the testis.

Differences in RpL22e-like structure compared with its paralogue RpL22e are most apparent in the N-terminal domain; however, there are also C-terminal amino acid differences that may contribute to functional differences between RpL22e-like and RpL22e. A small C-terminal extension of nine amino acids is apparent at the very C-terminal end of RpL22e-like. The recently published 5.5 Å model of the eukaryotic 80S

ribosome shows the position of RpL22e on the 60S subunit surface near its base (Armache *et al*., 2010). In this model, the N- and C-terminal segments of RpL22e are positioned near each other, extending from the subunit surface, which may allow for interactions with other components. If paralogue binding is mutually exclusive (though our data do not discount a model in which both RpL22e and RpL22e-like are present within the same ribosome), it is reasonable to position RpL22e-like similarly, yet propose that its interactions may differ.

Alternative splicing of *rpL22e-like* through intron retention.

This study demonstrated that alternative splicing of *rpL22e-like* generates two structurally distinct mRNA isoforms that are enriched within testes. A rare novel mRNA transcript called *rpL22e-like-PB* results from splicing of an intron that is retained within the more abundant, *rpL22e-like-PA*. Basal levels of *rpL22e-like-PB* mRNA are detectable by RT-PCR within heads and ovaries suggesting that the alternative splicing machinery is not limited to testis; however, the process may be subject to specific regulation within the testis where *rpL22e-like-PB* mRNA levels are comparatively more abundant.

It is unknown if alternative splicing of *rpL22e-like* occurs in all stages of spermatogenesis or if splicing is cell-type specific. The low abundance of *rpL22e-like-PB* mRNA relative to *rpL22e-like-PA* may be consistent with a specialized role in a subset of spermatocytes. Stage-specific gene expression during fly spermatogenesis has

been the subject of intense study, showing that some testis-specific genes are activated in primary spermatocytes while others (*comet* and *cup* genes) are transcribed post-meiotically, even within mid-to-late stage elongating spermatids in *Drosophila* (reviewed by White-Cooper, 2010). Although unique splicing phenomena of this type have not been described in this system, stage-specific splicing in spermatogenesis remains an intriguing possibility.

Intron retention is among the rarest forms of splicing in vertebrates and invertebrates; yet, it is the most prevalent type of alternative splicing found in protozoa, fungi and plants (reviewed by Keren *et al*., 2010). This phenomenon has been described in several other *Drosophila* genes (*Suppressor-of-white-apricot* [Zachar *et al*., 1987], *c-cam3* [Cheung *et al*., 1993], *Sxl* [Samuels *et al*., 1991], *erect wing* [Koushika *et al*., 1999], *transformer-2* [Mattox and Baker, 1991], *nuclear export factor 1* [Ivankova *et al*., 2010]) and the consequences of retaining an intron can have profound effects on gene expression leading to an unequal accumulation of mRNA variants. For *rpL22e-like*, the major form retains the intron.

Sakabe and de Souza (2007) identified several features that support a higher incidence of intron retention: weak splice sites, genes with overall short intron lengths and higher expression levels, and specific densities of splicing regulatory elements. Non-canonical splice sites were eliminated from the analysis, although it was apparent that *bona fide*

examples of splicing using non-canonical splice site recognition were present in their human gene data sets.

Other studies have further evaluated non-canonical splice site usage in a number of organisms (Mount *et al*., 1992; Burset *et al*., 2000; Sheth *et al*., 2006). Sheth *et al*. (2006) categorized sub-types of splice sites based on U2- and U12-dependent spliceosomes and described additional rare splice site types. In at least one case in *Drosophila*, an intron within the *rudimentary* gene is defined by a CT donor SS (FlyBase.org). Although originally noted in Mount *et al*. (1992) that the fly *perB* intron E has a 3′SS of CG, the most recent version of FlyBase (2010_08) has revised this proposal to reflect a canonical splice site.

The proposed retained intron is defined by a set of non-canonical splice site signals (5′SS: CT; 3′SS: CG) that may impact not only the mechanism of splicing, but also the kinetics of splicing regulation. It is noted that both 5′ and 3′ splice site sequence motifs are weak (MAXENT scores: −15.93 and −15.67, respectively) compared to the 5′ and 3′ scores for the upstream intron in *rpL22-like* (MAXENT scores: 8.57 and 7.23, respectively) when analyzed using a human splice site model to predict splice site strength (MaxEntScan: (Yeo and Burge, 2004). These data are consistent with an intron retention model (Sakabe and de Souza, 2007) and support the conclusion that the splicing rates for the upstream intron and the retained intron are different.

Intron retention often results in premature stop codon insertion, thereby directing the alternative transcript to the nonsense mediated decay (NMD) pathway (Lareu *et al*., 2004). The absence of premature termination codons in *rpL22e-like-PB* sequence likely eliminates this variant from NMD, and favors the interpretation that *rpL22e-like-PB* has functional significance by generating a novel protein, as proposed in this study.

Using *D. melanogaster* nucleotide and amino acid sequences for *rpL22- like* in a BLAST search for homologous sequences in other sequenced *Drosophila* species, we show that five other species (*D. sechellia*, *D. simulans*, *D. erecta*, *D. ananassae* and *D. yakuba*) contain an orthologous gene (Figures 2.14 and 2.15). The other six species (*D. pseudoobscura, D. persimilis, D. wilistoni, D. mojavensis, D. virilis* and *D. grimshawi*) lack an *rpL22e-like* orthologue. Within species that contain an *rpL22e-like* orthologue, production of an *rpL22e-like-PB* orthologue is also theoretically possible, generated by alternative splicing using conserved non-canonical sequences (5′SS: CT; 3′SS: CG) at the retained intron/exon boundaries (Figures 2.14 and 2.15). Evolutionary conservation of the alternative splicing pattern in the *melanogaster* lineage would lend further support that the alternative transcript encodes a functional product with a structure that is generally conserved in all members of the *melanogaster* group except *D. ananassae* (see sequence alignment Figures 2.15).

Protein structural diversity generated through alternative splicing of *rpL22e-like.*

Alternative splicing contributes to the enormous amount of protein diversity observed within eukaryotic cells. The rarer mRNA isoform (*rpL22e-like-PB*) encodes a protein in which the majority of the C-terminal Rp signature has been eliminated. Most of the structure of RpL22e-like-PB is comprised of the majority of the divergent N-terminal domain. Functional residues previously identified in RpL22e that are required for nuclear and nucleolar localization as well as RNA binding (Houmani and Ruf, 2009) are absent from RpL22e-like-PB, possibly restricting its subcellular compartmentalization and RNA binding ability. Alternatively, other regions of the protein may have redundant functions that would replace missing functional segments. In fact, a computational prediction using ELM (http://elm.eu.org/) highlights a bipartite variant of the classical NLS containing basic residues at RpL22e-like-PB amino acid positions 90–111 (and also predicted for RpL22e-like) that may prove functional for nuclear import and subnuclear compartmentalization.

Collectively, our data support the conclusion that *rpL22e-like* encodes not only an Rp, but a protein with extra-ribosomal function as well. *In silico* analyses may provide clues about a putative extra-ribosomal function for RpL22e-like-PB. Although no specific DNA-binding motifs are apparent (Wilson *et al*., 2008), 51 of 123 amino acid residues have DNA binding capacity, with 18 of those residues clustered within the first 24 amino acid at the very N-terminal end (Hwang *et al*., 2007; Kuznetsov *et al*., 2006). Given this prediction (and its limited structural similarity to histone H1), we speculate that RpL22e-like-PB may interact with testis chromatin and have a role in chromatin repackaging and

condensation during the transition from a nucleosome-based to a protamine-based configuration, as occurs in maturing sperm cells during spermiogenesis (reviewed by Hennig, 2003).

Perspectives on RpL22e paralogue function and evolution.

Paralogous members of the RpL22e family have been described in other animal genomes (*rpL22e-like1* in *Mus musculus* [NP_080793.1], *Danio rerio* N[P_001038800], *Xenopus tropicalis* [Q5I0R6], *Homo sapiens* [AAH62731], *Rattus norvegicus* [NP_001102018.1]) and their tissue-specific expression often varies considerably compared with the fly pattern described here (Bastian *et al*., 2008). Relatively little is known about functional redundancy or specificity of other *rpL22e* paralogues in other species; however, in at least one case, an *rpL22e* knockout mouse only exhibited a mild phenotype in T cell development, but was otherwise viable and fertile (Anderson *et al*., 2007), suggesting that mouse paralogue *rpL22e-like1* could rescue critical functions lost by *rpL22e* disruption.

Proteins of the RpL22e family in *Caenorhabditis elegans* (Kamath *et al*., 2003) and *Drosophila* are essential (Bourbon *et al*., 2002; Boutros *et al*., 2004). However, this is not the case for RpL22e in yeast (Deutschbauer *et al*., 2005) or in mice as discussed above (Anderson *et al*, 2007). FlyBase reports that a P-element chromosomal insertion located 150 nts upstream of *rpL22e-like* is lethal in fly development, suggesting that the *rpL22e-like* gene is also essential. The nature of the essential RpL22e-like function within the fly is intriguing, since one would predict that disruption of Rp function in the

testis would affect male fertility, and not viability. This suggests that *rpL22e-like* has an essential role (ribosomal or non-ribosomal) in another tissue(s) (head or eye) at some stage in fly development. In this case, it appears that RpL22e cannot replace the function lost by RpL22e-like disruption, either because of a lack of co-expression in the appropriate tissue in time and space or because the role of RpL22e-like is unique. Similarly, RpL22e-like is unable to replace functions lost by RpL22e disruption, correspondingly suggesting that essential functions prescribed by each protein are not redundant.

Do the essential roles of these paralogues include non-ribosomal roles? The presence of anti-RpL22e-like and anti-RpL22e immunoreactive products in high-MW complexes within eye tissue and the testis, respectively, raises the possibility that each paralogue may be post-translationally modified or bound within detergent-resistant complexes and function in a role(s) that is distinct from its ribosomal role, since neither high-MW species was found in association with ribosomes.

From an evolutionary perspective, gene duplication is the likely mechanism by which paralogous genes arise and generate tissue- or lineage-specific genes (Copley *et al*., 2003). Several inferences about RpL22e family evolutionary history become apparent from genomic analyses of the *Drosophilidae*. We and others (Shigenobu *et al*., 2006a) propose that *rpL22e* is the ancestral gene that was duplicated in a series of complex events whose extant outcome is the ubiquitous expression of *rpL22e* and cell lineage-

specific expression of *rpL22e-like*. The *rpL22e-like* gene is only found in the *melanogaster* group. One hypothesis addressing why *obscura* lineage genomes lack the *rpL22e-like* gene requires that gene duplication occurred in the *melanogaster* group, allowing for essential functions to be shared between paralogues. Over time gene divergence may have directed changes in paralogue function. The absence of the *rpL22e-like* gene from the *obscura* lineage may indicate that 'essential' functions were retained in the ancestral *rpL22e* gene or are provided by another gene(s). No doubt comparative analyses of paralogue expression and function in different *Drosophila* species will be instrumental in providing further insights into the evolutionary history and functional diversity displayed within the RpL22e family.

2.4 Materials and Methods

Fly stocks

Wild-type Canton S *D. melanogaster* were used for polysome profiling (a kind gift from Todd Laverty, HHMI-JFRC). All other experiments used wild-type Oregon R *D. melanogaster* obtained from Carolina Biological.

Primers

For a list of primers and oligonucleotides (Integrated DNA Technologies) used in this study, see Table 2.2.

Antibodies

The following peptide sequences were obtained from FlyBase (Crosby *et al*., 2007) and used for polyclonal Ab generation from GenScript: RpL22e: FRISSNDDEDDDAE; RpL22e-like: ADDNGGKTFA. Polyclonal Abs were protein A purified from rabbit and mouse, respectively. HRP-conjugated secondary Abs (Promega) were used in Western analysis. Antibody specificity was tested using bacterially expressed recombinant RpL22e and RpL22e-like (Figure 2.4). Pre-immune sera from rabbit and mouse were used to confirm the absence of immunoreactive proteins in fly extracts (Figure 2.4). Anti-mouse Alexa 488 Fluor and anti-rabbit Alexa 568 Fluor secondary Abs (Invitrogen) were used for IHC.

RNA isolation from fly tissue and cultured cells

Tissues were dissected from wild-type adult flies of mixed age (2- to 7-day old) in sterile 1X PBS and immediately frozen on dry ice. S2 cells were cultured under standard conditions in S2 media (Invitrogen) and collected during log phase. RNA isolation was completed using TRIzol reagent (Invitrogen) following manufacturer's guidelines. RNase-free glycogen (10 µg; Invitrogen) was used as a carrier to increase yield. Samples with $A_{260/280}$ and $A_{260/230}$ ratios <1.8 were discarded. Qualitative analysis of ~300 ng total RNA via gel electrophoresis ensured RNA integrity. Only samples that passed both spectrophotometric and qualitative analyses were used for further experiments.

RT-PCR Analysis

Total RNA (500 ng) from adult tissues and cultured S2 cells or 100 ng of embryo, larval and adult polyA+ RNA (Clontech) was used in RT-PCR analyses. SuperScript One-Step RT-PCR System with Platinum Taq DNA Polymerase (Invitrogen) was used following manufacturer's guidelines.

Cloning and Sequencing of *rpL22e-like* cDNAs

Gel-purified RT-PCR products were cloned into pMT/V5-His-TOPO® (Invitrogen), transformed into One Shot TOP10 Chemically Competent *E. coli* (Invitrogen), plated onto selective media (LB, ampicillin 100 µg/ml) and plasmid DNAs purified using the miniPrep system (Qiagen). Multiple clones for *rpL22e-like* cDNAs were sequenced

using an ABI 310 Genetic Analyzer (Applied Biosystems) or by GeneWay Research Laboratories.

Bacterial recombinant protein expression for Western analysis

Gel-purified RT-PCR amplicons were cloned into *E. coli* expression vector pEXP5-CT/TOPO (Invitrogen) following manufacturer's guidelines. Recombinant expression in transformed OneShot BL21 Star (DE3) Chemically Competent *E. coli* (Invitrogen) was induced with 0.5 mM IPTG.

cDNA synthesis and qRT-PCR analysis

Total RNA (1 µg) was used in cDNA synthesis using the SuperScript III First-Strand Synthesis System (Invitrogen) following manufacturer's guidelines and cDNAs stored at −80°C. One microliter of cDNA was used for qRT-PCR using the ABI 7300 real-time PCR system (Applied Biosystems) with SYBR green power master mix reagent (Applied Biosystems). Primers were designed using Primer Express software (Applied Biosystems). Primers (200 nM final concentration) were annealed at 55°C in a three-step amplification stage. Average ΔC_T values obtained for all genes were normalized to *rpL32* (*rpL32*/*rp49*) for comparison to data by Shigenobu *et al*. (2006a). All samples were run in triplicate with an $n = 3$. Standard deviations for each sample were calculated using the average ΔC_T of three runs. $\Delta\Delta C_T$ values were calculated using the average ΔC_T from each sample. Fold differences were calculated using the comparative C_T method ($\Delta\Delta C_T$), using fold difference = $2^{-\Delta\Delta C_T}$, as directed by the ABI 7300 qRT-PCR manual.

Protein extract preparation, SDS–PAGE and Western blotting

Drosophila tissues were dissected in 0.7X PBS supplemented with Mini Complete protease inhibitor cocktail without EDTA (Roche) and immediately frozen on dry ice. S2 cells were cultured as described above. Pelleted S2 cells were homogenized and lysed in RIPA buffer supplemented with Mini Complete protease inhibitor cocktail without EDTA (Roche) and microcentrifuged at maximum speed for 5 min. Soluble fractions were quantitated using the DC protein assay system (BioRad).

Soluble extract (10–15 µg) or insoluble fractions were mixed with reducing SDS-sample buffer and proteins separated by SDS–PAGE (5% stacking gel; 12.5% separating gel) at 200 V and electro-transferred onto 0.2 µm Westran S PVDF membrane (Whatman) at 100 V for 1 h. After blocking with 5% non-fat dry milk (NFDM) in 1× PBS with 0.1% Tween-20 (5% NFDM) for 1 h, membranes were incubated overnight with primary Ab (1:1000 in 3% NFDM) at 4°C. HRP-conjugated secondary Abs (1:50 000) were incubated at 4°C for 2 h. Chemilluminescent detection was achieved using ECL-Plus (GE Healthcare) and BioMax Chemilluminescence film (Kodak).

Northern analysis

Embryonic, larval, and adult poly(A+) mRNAs (15 µg; Clontech) were resolved on a 1.5% formaldehyde agarose gel in MOPS buffer and blotted onto a 0.2 µm Optitran nitrocellulose membrane. Filters were hybridized with ^{32}P-labelled oligonucleotide probes complementary to coding regions within *rpL22e-like* (Table 2.2) according to

hybridization conditions in Sambrook *et al*. (1989). RNAs were visualized by phosphorimaging. Filters were stripped in boiling 0.1% SDS and re-hybridized as above. Size estimates for detected RNAs were determined using RNA markers (Promega or Invitrogen).

Immunohistochemistry

Testis squashes and IHC preparation was performed as previously reported (Hime *et al*., 1996; Tazuke *et al*., 2002) with minor modifications. Testes from mature adult wild-type flies of mixed age (2–7-day old) were dissected in 0.7% saline, squashed and quickly frozen on dry ice. Tissues were fixed and permeablized in ice-cold ethanol for 10 min and in 4% formaldehyde (in 1× PBS) for 7 min at room temperature (RT), followed by 2× 15 min washes in PBS with 0.3% Triton X-100 and 0.3% sodium deoxycholate and a single wash of PBT (PBS with 0.1% Triton X-100). Blocking occurred for 1 h with PBTB (PBT with 3% BSA) at RT. Squashes were incubated overnight at 4°C with primary Ab (1:100 in PBTB) in a humid chamber and washed four times for 15 min in PBTB at RT. Alexa Fluor-conjugated secondary Abs (1:200 in PBTB) were incubated at 4°C in a humid chamber for 1 h and then washed four times for 10 min in PBTB at RT. DAPI staining (0.2 µg/ml in PBS) was performed after final Ab washes for 5 min, washed twice for 1 min in PBS and mounted in Cytoseal 60 (Richard-Allan Scientific). Fluorescent micrographs were taken using Nikon Eclipse TE200U inverted fluorescence microscope coupled to a digital CCD camera.

Polysome analysis

Ribosome extracts were prepared using modified procedures from Qin *et al*. (2007), Houmani and Ruf (2009) and Pelczar and Filipowicz (1998). Adult male Canton S flies (2.37g) were homogenized in lysis buffer (1:5 w/v; Qin *et al*., 2007) and homogenates clarified by centrifugation at 10K rpm for 10 min. Approximately 100 OD_{260} U/µl were loaded onto a 10–50% linear sucrose gradient (prepared by the horizontal method described by Houmani and Run, 2009) and spun at 35K rpm for 160 min in a SW-41 rotor. Gradient fractions (0.5 ml) were collected and read at OD_{260} using a DU-800 spectrophotometer. Fractions were pooled and pelleted with equal volumes of 20 mM Tris–HCl, pH 7.2 and spun at 40K rpm for 12 h in an SW41 rotor. Pellets were resuspended in 20 mM Tris-HCl, pH 7.2 and subjected to SDS–PAGE and Western analysis.

***In vitro* transcription of *rpL22e-like* mRNA isoforms**

Constructs used for recombinant expression (see above) of RpL22e-like-PA and RpL22e-like-PB were also utilized for *in vitro* transcription using the MEGAscript T7 kit (Ambion). These constructs served as PCR templates to amplify the T7 recognition site and coding sequence using Platinum *Taq* High-Fidelity DNA Polymearse (Invitrogen). The resulting amplicons were gel-purified using standard methods and used as templates for *in vitro* transcription following the manufactures recommendations. One picogram of purified *in vitro* transcribed RNA was used in each RT-PCR analysis using the SuperScript One-Step RT-PCR system with Platinum *Taq* DNA Polymearse (Invitrogen).

FLAG-tagged RpL22-like Plasmid Construction and Expression in S2 cells

FLAG-tagged L22-like was constructed using a PCR method, incorporating the sequencing encoding the dodecapeptide (IGRGDYKDDDDK) into the reverse primer (see Table 1). DNA from a previously sequenced pMT/V5-His-TOPO L22-likeFL clone was used as a template. The purified amplicon was cloned into pMT/V5-His-TOPO (Invitrogen).

S2 cells were obtained from Drosophila Genomics Resource Center and cultured at 25^0C in Schneider's Drosophila media (Gibco) supplemented with 10% heat-inactivated fetal bovine serum (Gibco). DNA for S2 cell transfection was purified using the Qiagen plasmid Maxi prep kit. Cells were seeded at $1x10^6$ cells/ml per well (3ml) in a standard six-well plate. Following overnight growth into log-phase, 19µg of DNA was transfected per well, according to manufacturer's instructions (Invitrogen), using the calcium phosphate transfection kit (Invitrogen). Expression constructs were induced at a final concentration of 500µM $CuSO_4$.

For protein extraction, cells were collected via centrifugation and lysed with RIPA buffer (25mM Tris-HCl, pH7.4, 150mM NaCl, 1% Triton X-100, 1% sodium deoxycholate, 0.1% SDS; Pierce) supplemented with Mini Complete protease inhibitor cocktail without EDTA (Roche) for 30 min at room temperature (RT). Cell debris was removed by microcentrifugation at maximum speed for 3 min. Soluble extracts were quantified using

the DC protein assay (Bio-Rad). SDS-PAGE and Western analysis were performed as described above.

2.5 Figures and Tables

A

```
L22             -MAPTAKTNKGDTKTAAAKPAEKKAAPAAAAAKGKVE--KPKAEAAKPAAAAAKNVKKAS 57
L22-like        MSSQTQKKNASKAKSKAGPQPSKKAPAKVTPVETATPSAAPPLSSKKVAKAPAVALKNLD 60
                  : * *.* ..:*: *.  ..***.. .:..:  .    *  .: * * *.*  :*: .

L22             EAAKDVKAAAAAAKPAAAKPAAAKPAAASKDAGKKAPAAAAAPKKDAKAAAAPAPAKAAPA 117
L22-like        LAMKESAKKAAEAADQKLVSKAKKGQNASRKNLMQVPEPVAPEVDNKKKSAPPKRGNAEI 120
                 * *:    ** *      . * *   **:.   :.* ..**: * *  :**.    *

L22             KKAASTPAAAPPAKKAAPAKAAAP-AAAAPAPAAAAPAVAKPAPKPKAKAAPAPSKVVKK 176
L22-like        PTVVPAKKAALVQEKPKEQAAAAPKAENVEVPAAKAKSVKKSLATP---ANPKPKPKRTK 177
                 ....:  **   :*.    **** *  . .*** * :* *. ..*   * * *.   .*

L22             NVLRGKGQKKKKVSLRFTIDCTNIAEDSIMDVADFEKYIKARLKVNGKVNNLGNNVTFER 236
L22-like        NVLRGKRLAKKKAWQRFVIDCACVAEDMILDLADFEQYLKTHIKIKNKLNQLKDQVTFER 237
                ******  ***.  **.***: :*** *:*:****:*:*:::*:::*:*:* ::******
                        1

L22             SK-LKLIVSSDVHFSKAYLKYLTKKYLKKNSLRDWIRVVANEKDSYELRYFRISSN--DD 293
L22-like        TKNFSLIIHSGVHFSKRYFKYLTKRYLKKVSLRDWLRVVSTAKDTFAMTYFKIQDKDFDD 297
                :* :.**: *.***** *:*****:**** *****:***:. **:: : **:*..:  **
                         2          3

L22             EDDDAE--------- 299
L22-like        DDDDVADDNGGKTFA 312
                .***.
```

B

```
L22e-like-PA    MSSQTQKKNASKAKSKAGPQPSKKAPAKVTPVETATPSAAPPLS
L22e-like-PB    MSSQTQKKNASKAKSKAGPQPSKKAPAKVTPVETATPSAAPPLS

SKKVAKAPAVALKNLDLAMKESAKKAAEAADQKLVSKAKKGQNASRKNLMQVPEPVAPEV
SKKVAKAPAVALKNLDLAMKESAKKAAEAADQKLVSKAKKGQNASRKNLMQVPEPVAPEV

DNKKKSAPLKRGNAEIPTVVPAKKAALVQEKPKEQAAAAPKAENVEVPAAKAKSVKKSLA
DNKKKSAPL----------------------------------------------------

TPANPKPKPKRTKNVLRGKRLAKKKAWQRFVIDCACVAEDMILDLADFEQYLKTHIKIKN
------------------------------------------------------------

KLNQLKDQVTFERTKNFSLIIHSGVHFSKRYFKYLTKRYLKKVSLRDWLRVVSTAKDTFA
------------------------------------------------------------

MTYFKIQDKDFDDDDDVADDNGGKTFA   312
------------------ADDNGGKTFA   123 (Δ189aa)
```

Figure 2.1. Alignment of RpL22e paralogues and alternatively spliced products. A) Clustal W alignment of *D. melanogaster* RpL22e and RpL22e-like sequences. Aligned sequences (RpL22e: FBgn0015288; RpL22e-like: FBgn0034837) show conservation at the C-terminus (yellow: 46% sequence identity; 73% sequence similarity), but divergence

at the N-terminus (sequence identity 36%; sequence similarity 47%). Overall amino acid identity is 37% (Marygold *et al*., 2007). Shaded amino acid residues mark conservation within the RpL22e superfamily. Other residues define the N-terminal extension with homology to histone H1 [(Koyama *et al*., 1999) for RpL22e and RpL23a]. Boxes highlight functional residues involved in nuclear localization (box 1), rRNA binding (boxes 2 and 3) and nucleolar localization (boxes 2 and 3) (Houmani and Ruf, 2009). Underlined residues in the C-termini were used to make polyclonal peptide Abs. B) Translation of *rpL22e-like-PB* mRNA (GenBank accession no. HM756190) using Translation Tool (expasy.org) revealed a putative protein of 123 amino acid, consisting primarily of the histone H1-like domain (N-terminus) and not the RpL22e-like domain (C-terminus).

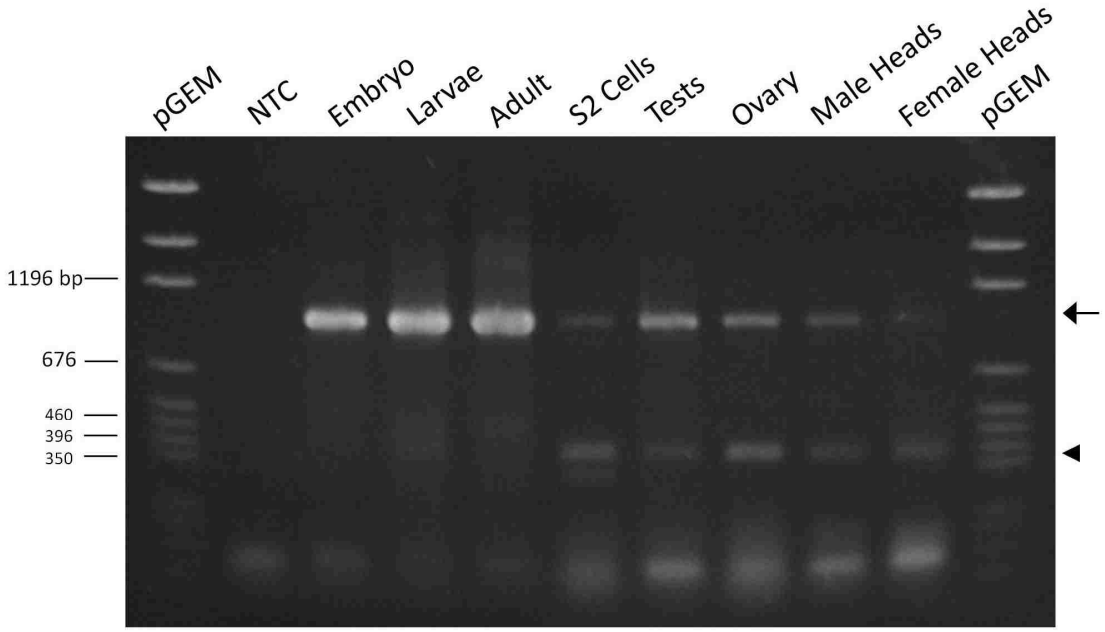

Figure 2.2. RT-PCR analysis of *rpL22e-like* in different developmental stages, tissues, and in S2 cells. RT-PCR using *rpL22e-like* primers to amplify the coding sequence resulted in the expected 939 bp amplicon (*rpL22e-like-PA,* arrow) in all samples. An additional smaller amplicon (*rpL22e-like-PB,* arrowhead) of ~390 bp was present in all samples. Variability in the intensity of *rpL22e-like-PB* was noted in numerous replicates of the RT-PCR for various samples as noted here for embryonic and adult samples. NTC: no template control.

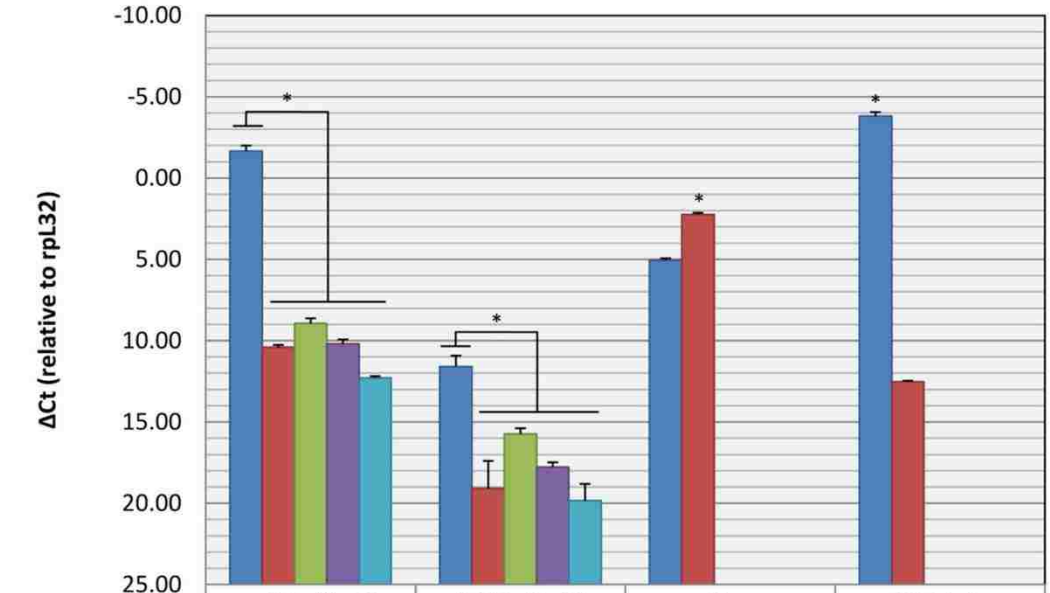

	RpL22e-like-PA	RpL22e-like-PB	Vasa	β2-Tubulin
Testes (n=3)	-1.67	11.59	5.05	-3.81
Ovaries (n=3)	10.40	19.09	2.24	12.52
Male Heads (n=3)	8.93	15.72		
Female Heads (n=3)	10.19	17.77		
S2 (n=3)	12.29	19.84		

Figure 2.3. qRT-PCR reveals *rpL22e-like* mRNA enrichment in testis. Using isoform-specific primers, qRT-PCR shows that both isoforms are more highly expressed in testis compared with other tissues. *Vasa* and *β2-tubulin* serve as germ cell- and testis-specific controls, respectively. Numbers in table represent C_T values. Bars represent standard error, $*p < 0.01$.

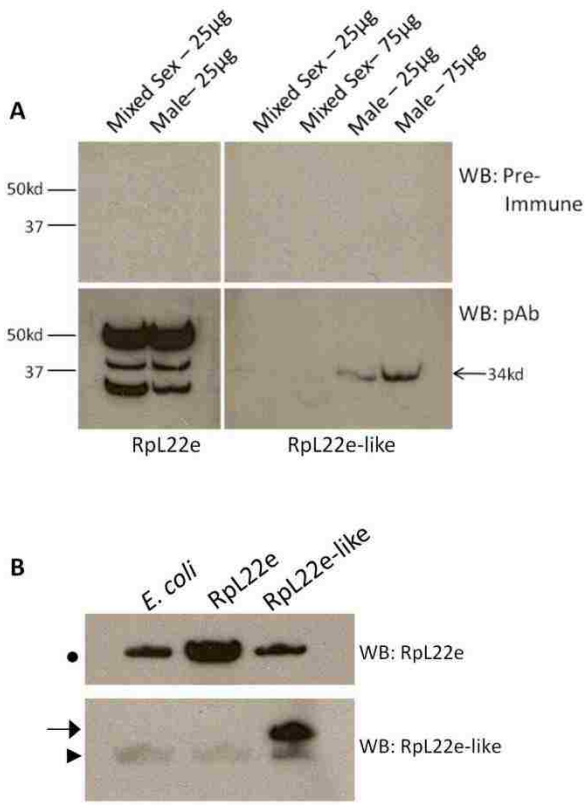

Figure 2.4. Paralogue-specific polyclonal antibodies (pAbs) are specific and do not cross-react. A) Western analysis performed with pre-immune serum and subsequent paralogue-specific pAbs shows each pAb is specific to the designated paralogue. B) Bacterially-expressed recombinant RpL22e and RpL22e-like are not detected when blotted with opposite paralogue-specific Ab. When pre-immune serum from rabbit (for RpL22e) or mouse (for RpL22e-like) were used to detect fly proteins, no immunodetection was seen, indicating that no endogenous Abs within rabbit or mouse sera recognized fly proteins. When the same blots were used for RpL22e or RpL22e-like detection, three prominent bands at ~33kD, 40kD, and ~50kD were visible for RpL22e. The ~33kD band correlates well with the expected MW for RpL22e. Other bands

detected in this blot may represent post-translationally modified RpL22e and/or RpL22e found in highly resistant complexes.

Using the RpL22e-like Ab, only one protein at the expected MW (~34kD) for RpL22e-like was prominent in male extracts. Lack of detection of RpL22e-like-PA within mixed sex extracts is likely due to a lower proportion of males within the extract sample, as we have observed that female representation is about 50% greater than males in random samples of flies on average (unpublished observations). Taken together, these experiments indicate that Abs detect different immunoreactive species of expected sizes for RpL22e and RpL22e-like in extracts and do not cross-react.

Equal amounts of protein (whole cell lysates) for untransformed *E. coli* (strain used in recombinant expression), recombinant RpL22e, and recombinant RpL22e-like were subjected to Western analysis. While some bacterial immunoreactive background (bullet) is seen when blotting for RpL22e, the increase of immunodetection seen in the recombinant RpL22e sample suggests antibody specificity between recombinant paralogues. When blotting for RpL22e-like, a lower MW bacterial immunoreactive background (arrowhead) is also seen in all samples, but immunodetection at the expected MW is only seen in the recombinant RpL22e-like-PA (arrow).

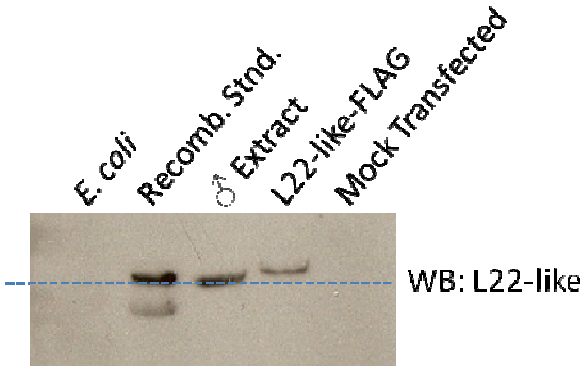

Figure 2.5. Detection of RpL22e-like using anti-RpL22e-like C-terminal peptide polyclonal Ab. In order to determine if our RpL22e-like Ab recognizes RpL22e-like, we designed several recombinant constructs for expression in bacterial cells or in S2 cells. Extracts from bacterial cells transformed with pEXP5/RpL22e and pEXP5/RpL22e-like-PA were used as markers in protein blots and to determine Ab specificity. Extracts from S2 cells transfected with a pMT/RpL22e-like-PA-FLAG served as a specificity control as well. Western analysis using the RpL22e-like Ab shows immunoreactive species in recombinant bacterial and male extracts at ~34kD and in the S2 extract at ~35kD, the latter shift expected based on the addition of the 1.5kD FLAG-tag. These experiments, coupled with specificity data (Figure 2.4) provide compelling evidence that the RpL22e-like Ab recognizes RpL22e-like. This Ab was used in all immunoblots and IHC experiments in this study.

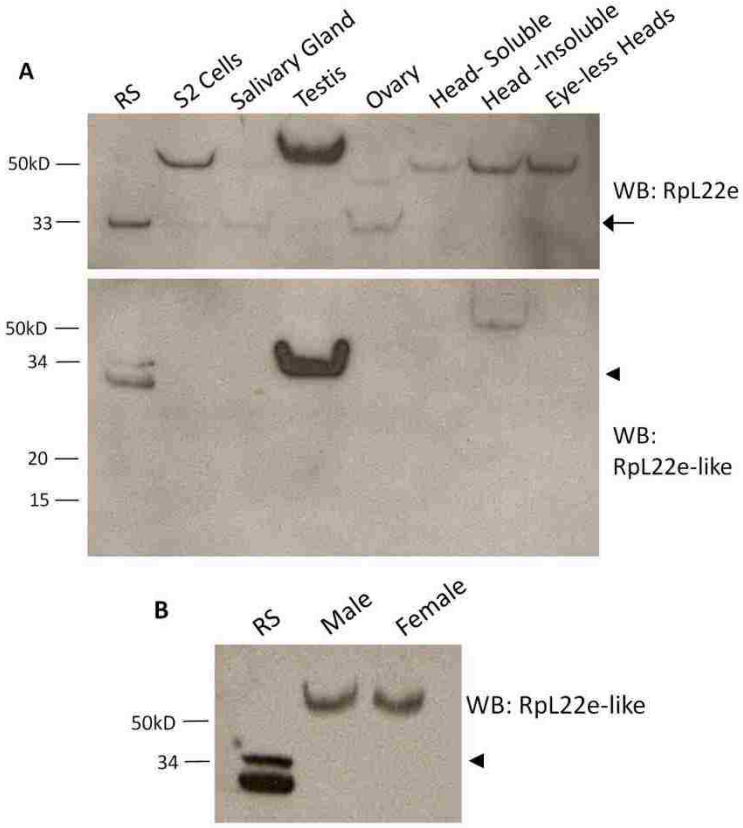

Figure 2.6. Western blot analysis confirms differential expression of RpL22e-like. A) Compared to the recombinant standard (RS), western analysis for RpL22e shows immunodetection at either the expected MW of 32.9 kD (arrow) and/or at a higher MW at ~50 kD in all tissues. Immunodetection of RpL22e-like at the expected MW of 34.3 kD (arrowhead) is solely visible in testes. Insoluble extracts from male and female heads contain a higher MW species of RpL22e-like. No immunoreactive species is seen in eye-less heads (eyes are dissected out) or in a soluble head extract. The additional lower band in the RS sample is endogenous bacterial protein recognized by mouse antisera (see Figure 2.4 for additional explanation). B) The electrophoretic shift in RpL22e-like is not sex specific as seen by Western analysis of whole head tissue from males and females. RS: recombinant standard.

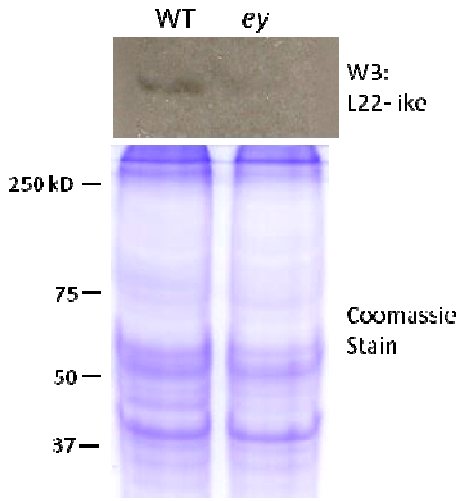

Figure 2.7. RpL22e-like is enriched in *Drosophila melanogaster* eyes. With equal loading shown by Coomassie Stain, immunodetection of RpL22e-like by Western analysis is significantly reduced in *eyeless* (*ey*) mutants compared to wildtype (WT).

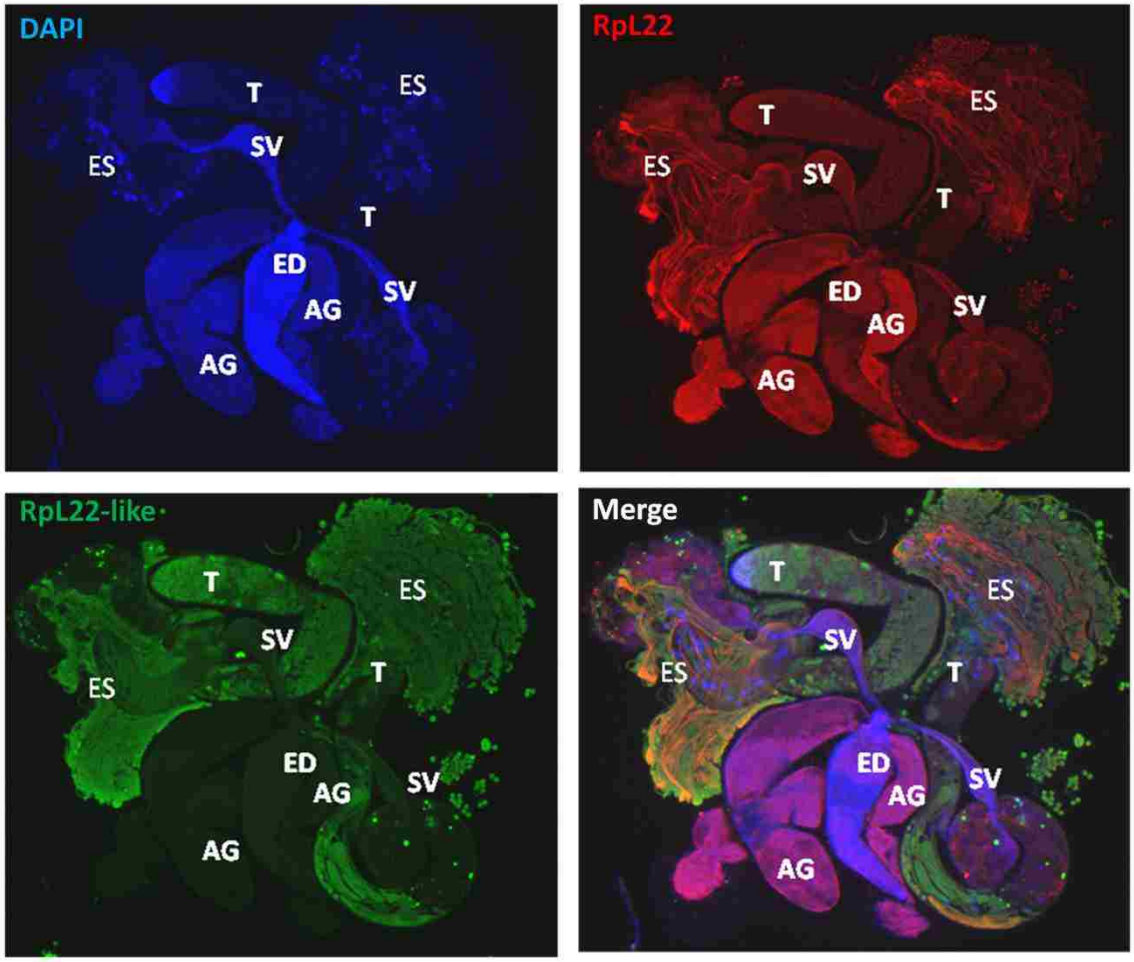

Figure 2.8. Immunofluorescent staining of RpL22e and RpL22e-like in adult male reproductive tract using paralogue-specific Abs. Extruded sperm (ES) were released from the testes during dissection. Spermatogenesis is initiated at the apical tip of the testis (T) and progresses through the testis coils. The most mature sperm are, therefore, located distal to the apical end of the testis. Mature sperm pass from the testis into the seminal vesicle (SV). Seminal fluid is added to sperm from the accessory gland (AG), and sperm are released through the ejaculatory duct (ED). RpL22e (red) is ubiquitously expressed in the reproductive system. RpL22e-like (green) is expressed exclusively within the testis and within sperm cells. DNA is visualized by DAPI staining (blue).

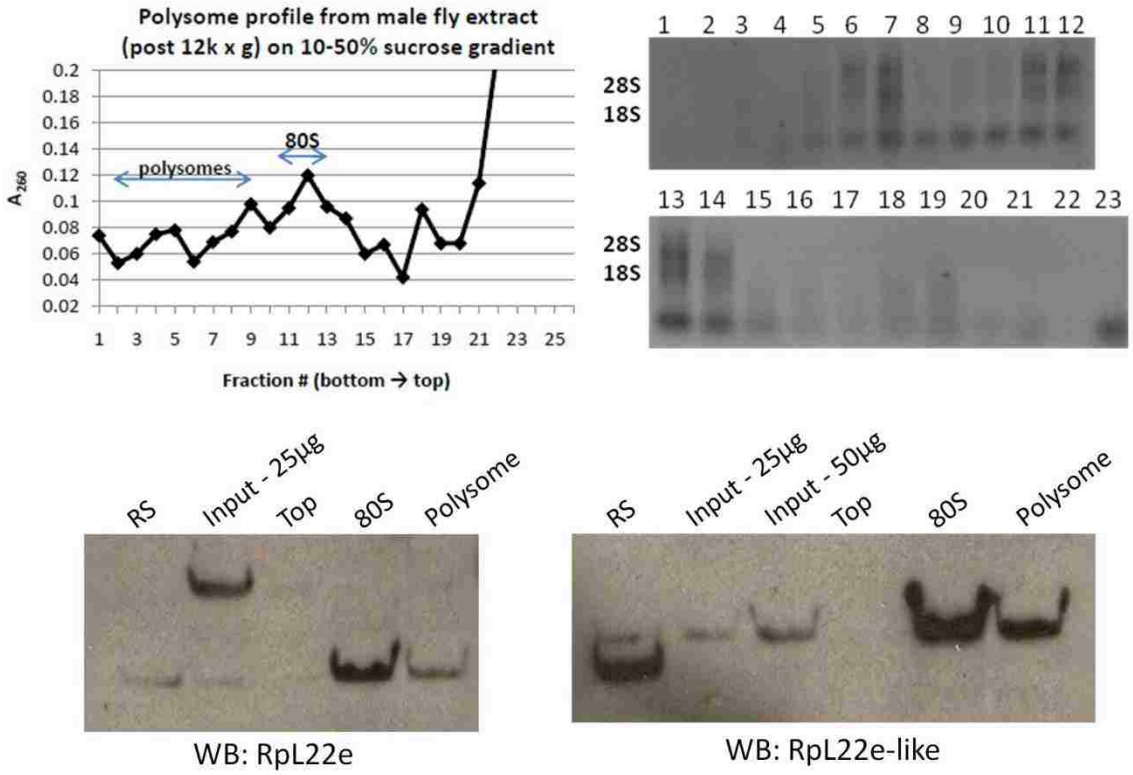

Figure 2.9. Density gradient ultra-centrifugation showing RpL22e-like-PA association with active translational machinery. Soluble extracts from adult male flies were fractionated on 10–50% sucrose gradients. The top left panel shows the absorbance profile of the sucrose gradient. Extracted RNAs from fractions are shown on the top right. Fractions containing polysomes (poly) and 80S ribosomes were pooled, pelleted separately and subjected to western analysis (bottom panels). Both paralogues were detected at the expected MW in fractions containing 80S ribosomes and polysomes, indicating that both are stable components of translating ribosomes. No sizeable amount of either protein was detected at the top (T) of the gradient. Input: 25 µg and/or 50 µg whole male extract.

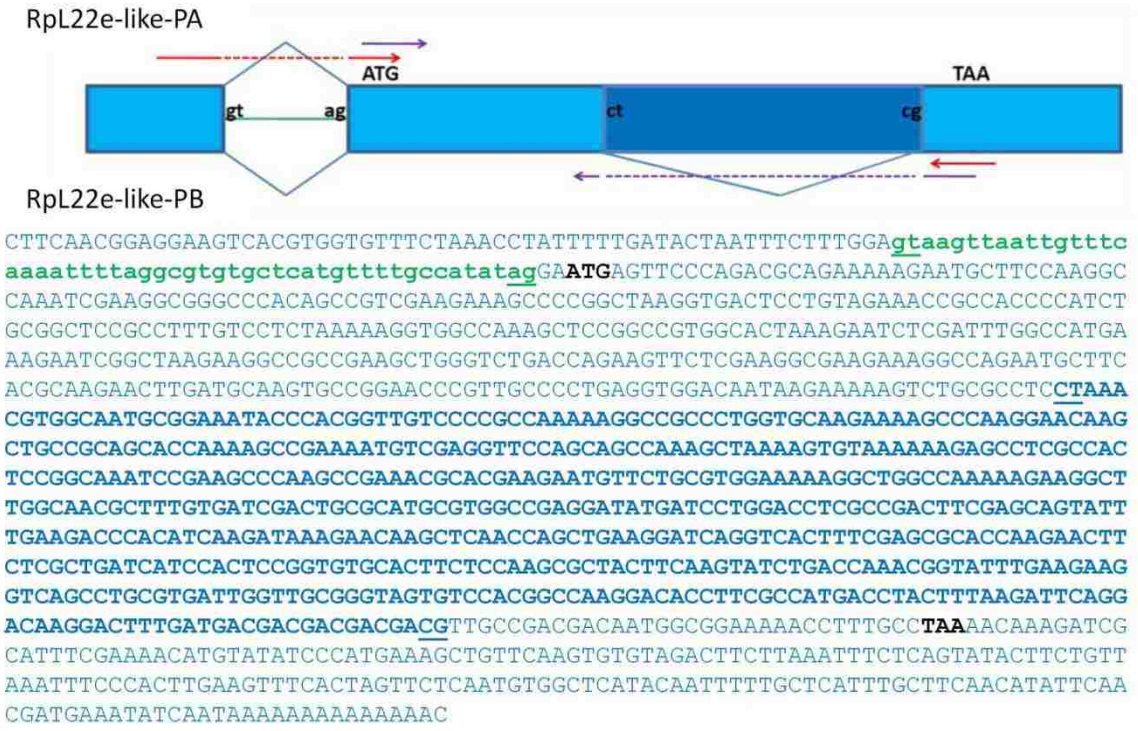

Figure 2.10. ***rpL22e-like*** **coding region showing novel splice site junctions for** ***rpL22e like-PB*****.** Exon sequences (capitalized) and intronic sequences (lowercase) were derived from FlyBase (FBgn0034837). The coding region of *rpL22e-like-PA* is shown in blue caps. The previously annotated intron (FlyBase FB2010_06) is shown in green lowercase. The novel intron is represented in bold with non-canonical splice sites underlined (5′SS: CT, 3′SS: CG). The *rpL22-like-PB* sequence (GenBank accession no. HM756190) was derived from sequencing multiple (29 total) cloned cDNAs from RT-PCR analyses (Figure 2.2). Red and purple arrows in the splicing diagram represent primer pairs used in RT-PCR analyses in Figure 2.11A and Figure 2.12.

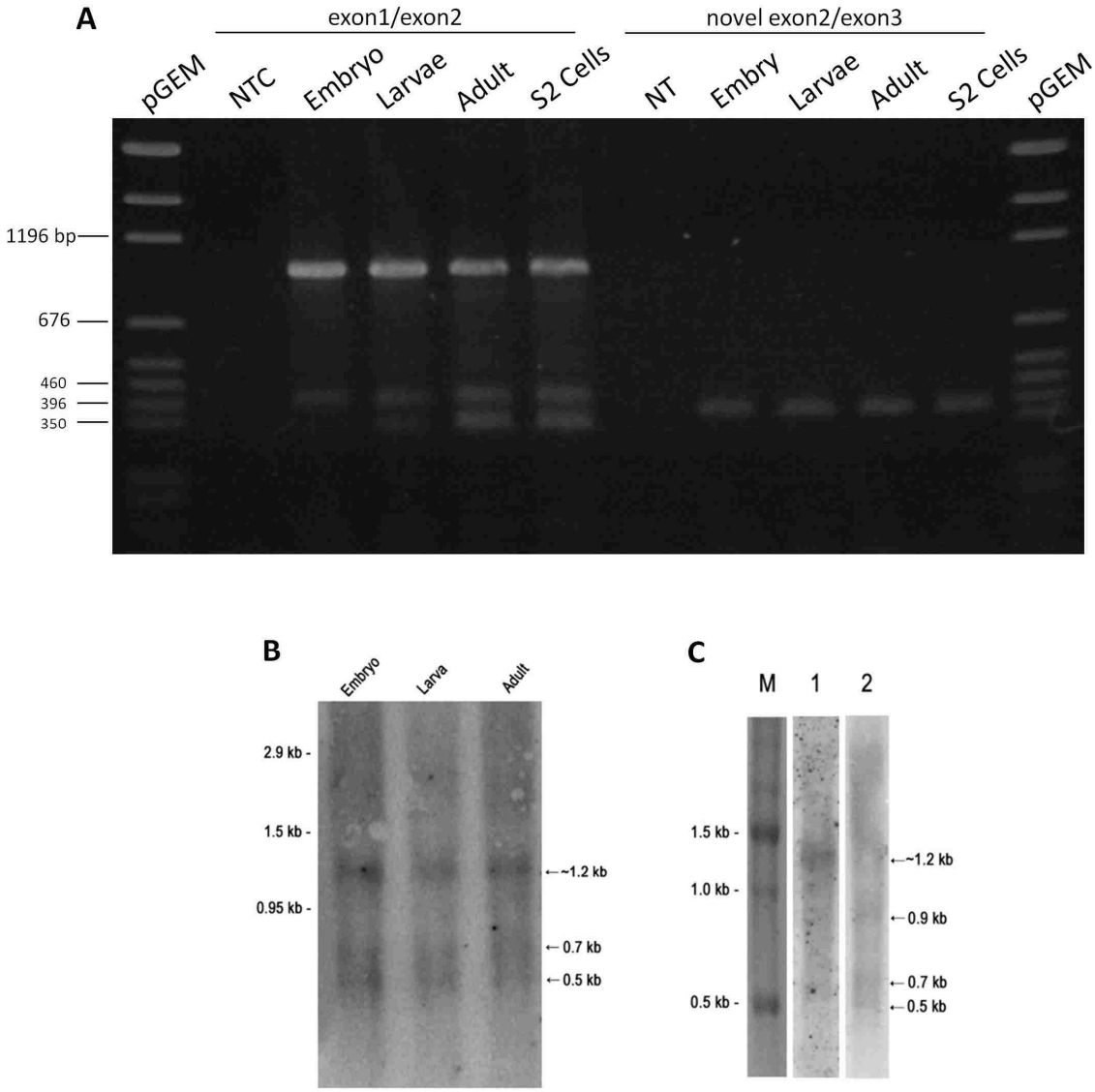

Figure 2.11. RT-PCR and Northern analysis novel smaller *rpL22e-like* mRNAs. *A*) RT-PCR analysis of *rpL22e-like* transcripts using primers that bridge exons in *rpL22e-like-PA* and *rpL22e-like-PB*. RT-PCR products using the exon1/2 bridge primer should hybridize to *rpL22e-like-PA* and *rpL22e-like-PB*, producing bands of ~950 bp (arrow) and 392 bp (closed arrowhead), respectively (red primer set in Figure 2.10). All samples show such products in multiple experiments. Other amplicons (<350 bp) were cloned and

sequenced and determined to be the result of non-specific amplification. The novel *rpL22e-like-PB* exon2/3 bridge primer should specifically hybridize only to *rpL22e-like-PB* (purple primer set in Figure 2.10). The expected amplicon of ~370 bp (open arrowhead) is seen in all samples, confirming the presence of *rpL22e-like-PB*. B) Northern blot analysis of *rpL22e-like* mRNAs from different developmental stages. PolyA+ RNA from embryonic, larval and adult fly stages was probed with ^{32}P-labelled *rpL22e-like*-specific cDNA oligomers. Estimated transcript sizes based on RNA markers are shown in kilobases (kb). *rpL22e-like-PA* mRNA is predicted to be 1.194 kb (FlyBase). *rpL22e-like-PB* mRNA is predicted to be a minimum size of ~0.625 kb. Arrows highlight prominent transcripts detected in all stages. C) Embryonic PolyA+ RNA was probed with ^{32}P-labelled *rpL22e-like*-specific cDNA oligomers [(PA-specific—lane1) or (flanking—lane 2)]. RNA sizes were determined relative to an RNA marker.

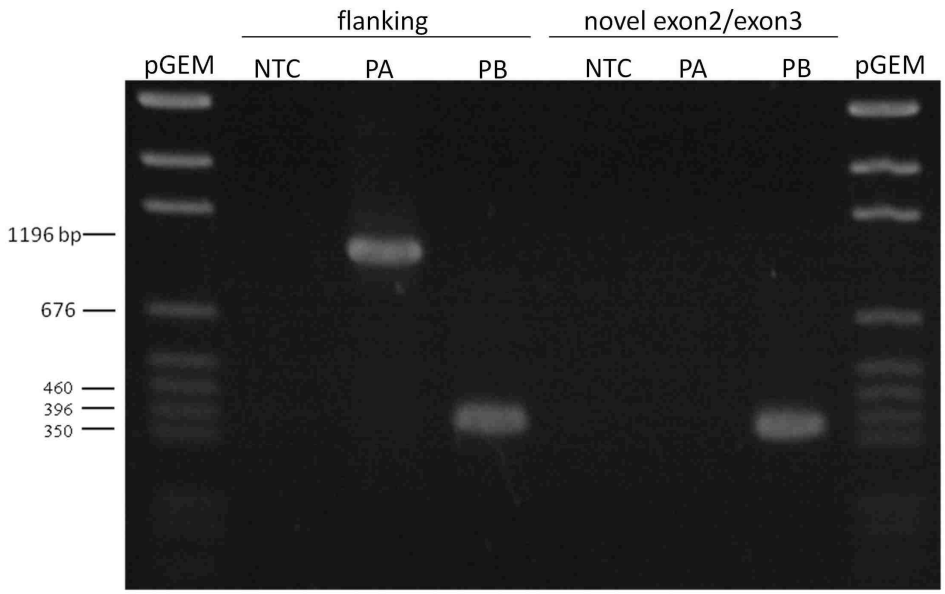

Figure 2.12. Amplification of *rpL22e-like-PB* is not an artifact of RT-PCR. Purified *in vitro* transcribed *rpL22e-like-PA* and *rpL22e-like-PB* RNA were used as templates in RT-PCR reactions with primer sets described in this manuscript. Flanking primers designed to hybridize to the 5' and 3' ends of both coding sequences (as used in Figure 2.2) produce distinct amplicons. Furthermore, the novel exon2/exon3 bridge primer designed to hybridize only to the novel junction specifically amplifies only *rpL22e-like-PB* (as seen in Figures 2.10 & 2.11A). NTC: no template control; PA: *rpL22e-like-PA*; PB: *rpL22e-like-PB*.

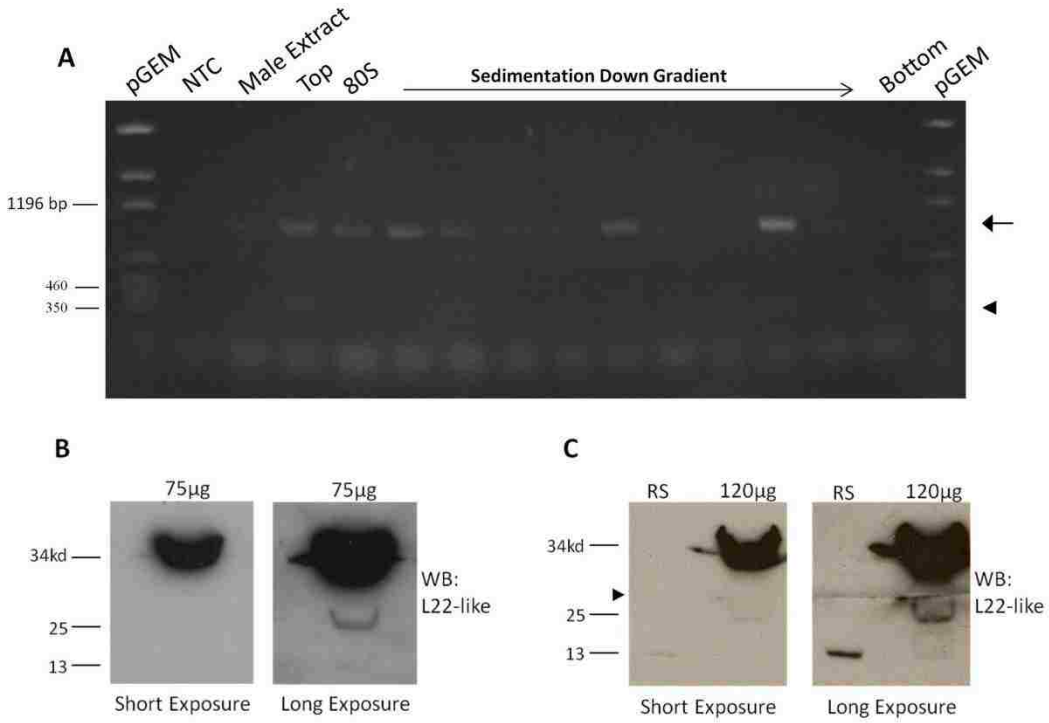

Figure 2.13. *rpL22e-like-PB* mRNA may be translated. A) Whole male extract was subjected to 10–50% linear sucrose gradient ultra-centrifugation. RT-PCR analysis of gradient fractions representing 80S subunits and polysomes shows association of *rpL22e-like-PA* (arrow) and *rpL22e-like-PB* arrowhead) mRNAs with active translating ribosomes, suggesting *rpL22e-like-PB* is translated. B) An initial Western analysis of 75µg of testis extract shows immunodetection at the expected MW of ~34 kD and lower at ~25 and ~13 kD (faint band; arrow). 'Short exposure' was for 3 s and 'long exposure' was for 30 min. C) Increased protein loading to 120µg of testis extract enhanced immunodetection of the ~13 kD band (arrow) with a longer exposure (30 min compared to 4 s for short exposure). Given the abundance of RpL22e-like-PA as a 'sink' for anti-RpL22e-like Ab, the membrane was cut to maximize immunodetection of smaller MW

proteins (arrowhead). The ~13 kD band (arrow) aligns with the recombinant RpL22e-like short protein standard. NTC: no template control; RS: recombinant standard.

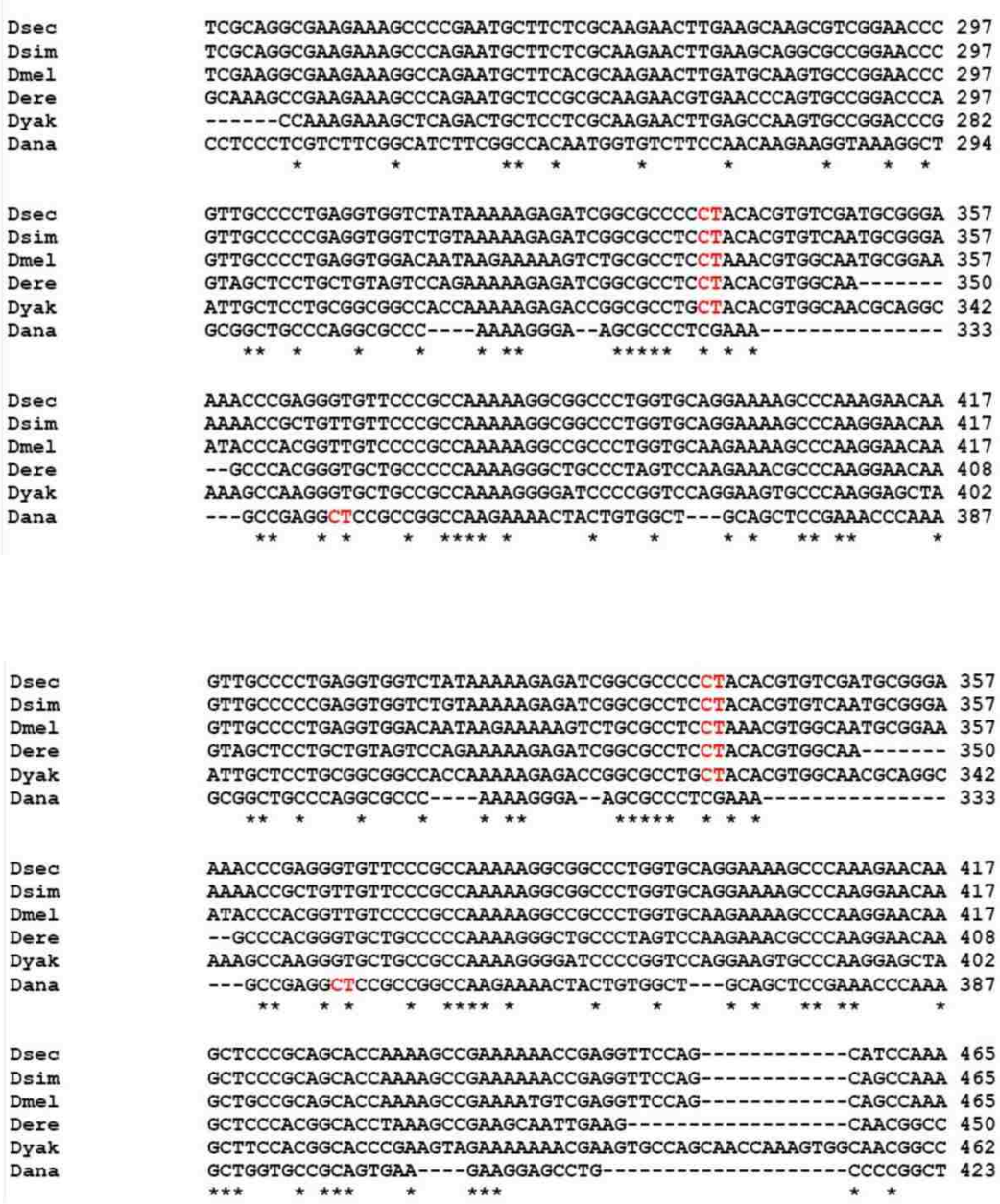

Figure 2.14. Clustal W alignment of *rpL22e-like-PA* nucleotide sequences from the *Drosophila melanogaster* group (found in FlyBase: FB2010_06). Other species found in FlyBase (not belonging to the melanogaster group) lack an RpL22e-like orthologue. Nucleotides in red represent conserved non-canonical splice sites. The position of the proposed splice sites in *D. ananasse* is based on the gaps within its alignment. Symbols

in the alignment denote the amount of nucleotide conservation observed in each column. "*" indicates that the nucleotides in that column are identical in all of the aligned sequences. ":" indicates conserved substitutions. "." shows semi-conserved substitutions. Dmel = *D. melanogaster* (FBtr0072049), Dsec = *D. sechellia* (FBtr0198555), Dsim = *D. simulans* (FBtr0224981), Dere = *D. erecta* (FBtr0140109), Dana = *D. ananassae* (FBtr0118008), Dyak = *D. yakuba* (FBtr0258110). Figure adapted from Kearse *et al*. (2011).

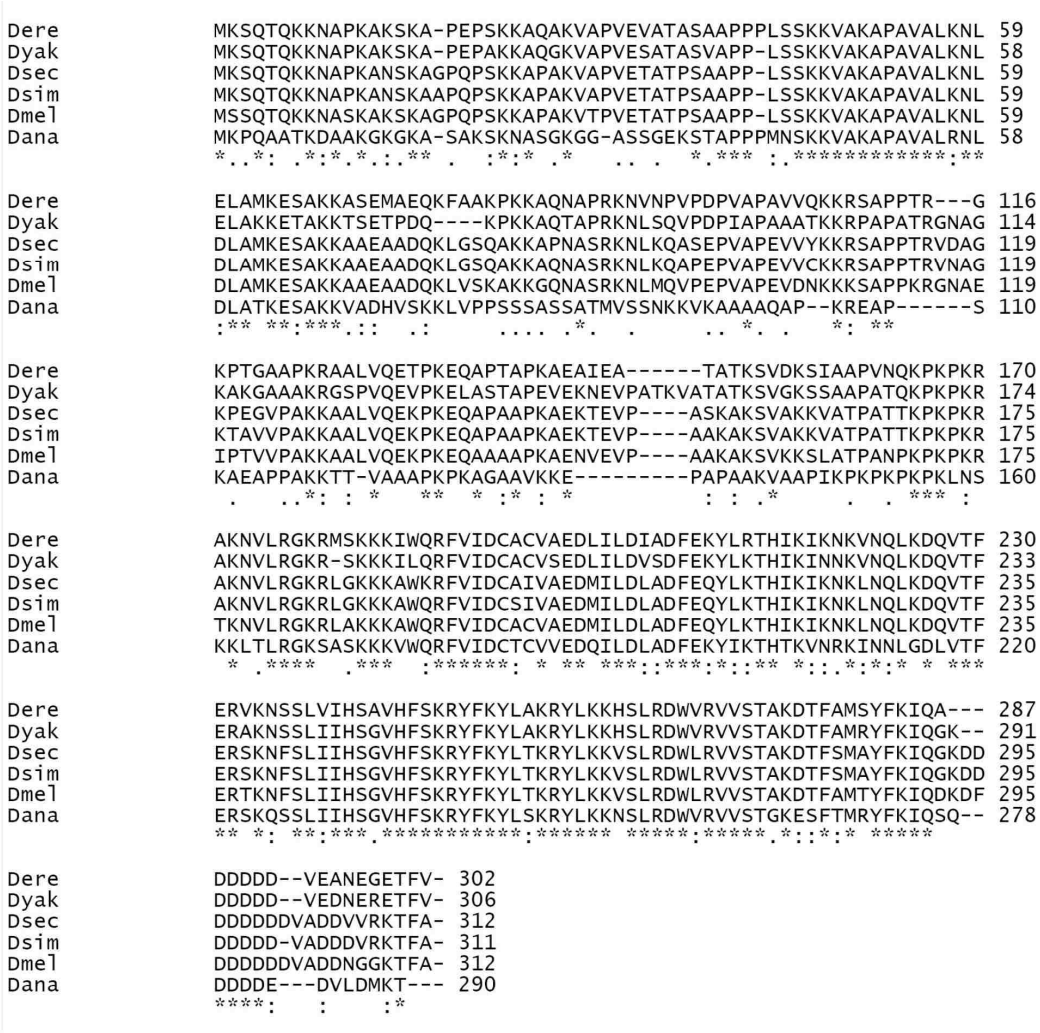

Figure 2.15. Clustal W alignment of RpL22e-like-PA amino acid sequences from the *Drosophila melanogaster* group (found in FlyBase: FB2010_06). Other species found in FlyBase (not belonging to the melanogaster group) lack an RpL22e-like orthologue. Symbols in the alignment denote the amount of amino acid conservation observed in each column. "*" indicates that the amino acids in that column are identical in all of the aligned sequences. ":" indicates conserved substitutions. "." shows semi-conserved substitutions. Dmel = *D. melanogaster*, Dsec = *D. sechellia*, Dsim = *D. simulans*, Dere = *D. erecta*, Dana = *D. ananassae*, Dyak = *D. yakuba*.

Sample	Fold Difference of *rpL22-like* in Testes compared to sample	Fold Difference of *rpL22-like short* in Testes compared to sample	Fold Difference of *rpL22-like* compared to *rpL22-like short*	Fold Difference of *rpL22-like* compared to *Vasa*	Fold Difference of *rpL22-like* compared to *β2-Tubulin*
Testes	-	-	9745 (7699-12335)	105 (83-133)	0.23 (0.18-0.29)
Ovaries	4296 (3394-5438)	181 (143-229)	411 (325-520)	0.0035 (0.0028-0.0044)	4 (3-6)
Male Heads	1551 (1225-1963)	18 (14-22)	111 (87-140)	-	-
Female Heads	3702 (2924-4685)	73 (58-92)	192 (151-243)	-	-
S2	15876 (12543-20095)	306 (241-387)	188 (148-237)	-	-

Table 2.1. Fold differences of *rpL22e-like* mRNA isoform compared to tissues and specific genes. Fold differences were calculated using the comparative C_T method ($\Delta\Delta C_T$ method). Levels of *rpL22e-like-PA*, normalized to *rpL32*, and relative to other tissues, *rpL22-like-PB*, *Vasa* (germline-specific; Qin *et al*., 2007; Sano *et al*., 2002), *or β2-Tubulin* (testis-specific; Kemphues *et al*., 1979; Rudolph *et al*., 1987), is determined by using the formula: $2^{-\Delta\Delta C_T}$. Values within parentheses indicate range of fold differences, as a result of incorporating the standard deviation.

Name	Sequence	Experimental Use
FDmL22likeBamHI	5′-GTCACGGATCCATGAGTTCCCAGACGCAGAAAAAGAATGCTTCCAA-3′	RT-PCR & Cloning; Bridge RT-PCR; FLAG-tagged constructs
RDmL22likeBamHI	5′-GTCACGGATCCTTAGGCAAAGGTTTTTCCGCCATTGTCGTCGGCAA-3′	RT-PCR & Cloning
RDmL22likeBamHI_shortened	5′-GTCACGGATCCTTAGGCAAAGGTTTTTCCGCCATTG-3′	RT-PCR & Cloning; Bridge RT-PCR
FL22like_exon1/2	5′-GATACTAATTTCTTTGGAGAATG-3′	Bridge RT-PCR
RL22like_novel exon2/3	5′-TTAGGCAAAGGTTTTTCCGCCATTGTCGTCGGCAAGAGG-3′	Bridge RT-PCR; Northern Analysis
RDmL22-likeFLAG-BamH1	5′-GTCACGGATCCTTACTTGTCATCGTCATCCTTGTAGTCGCCGCGGCCGATGGCAAAGGTTTTTCCGCCATTGTCGTCGGCAA-3;	FLAG-tagged constructs

FL22likeFull	5′-GCTCAACCAGCTGAAGGATCA-3′	qRT-PCR
RL22likeFull	5′-GAAGTAGCGCTTGGAGAAGTGC-3′	qRT-PCR
FL22likeShort	5′-CAGAATGCTTCACGCAAGAACTT-3′	qRT-PCR
RL22likeShort	5′-AATGTCGTCGGCAAGAAGC-3′	qRT-PCR
FBeta2Tubulin	5′-GTGCTGAACTGGTGGATTCCGT-3′	qRT-PCR
RBeta2Tubulin	5′-GGTCAGCTGGAAGCCCTGAA-3′	qRT-PCR
FVasa	5′-CTGTACGAAAACGAGGATGGTGA-3′	qRT-PCR
RVasa	5′-ACCACCGTCCCCTCTTTCA-3′	qRT-PCR
FrpL32	5′-CTAAGCTGTCGCACAAATGG-3′	qRT-PCR
RrpL32	5′-ACGCACTCTGTTGTCGATACC-3′	qRT-PCR

FL22-like_startcodon	5′-ATGAGTTCCCAGACGCAGAAAAAGAATGCTTCCAAGGCC-3′	Recomb. Expression
FL22	5′-AAGATGGCTCCTACCGCCAAGACCAACAAGGG-3′	Recomb. Expression
RL22	5′-TTACTCGGCATCGTCGTCCTCATCG-3′	Recomb. Expression

RL22like_exon1	5′-GGAAGCATTCTTTTTCTGCGTCTGGGAACTC-3′	Northern Analysis
RL22like_exon3	5′-TTAGGCAAAGGTTTTTCCGCCATTGTCGTCGGC-3′	Northern Analysis

Table 2.2. List of primers and oligonucleotides used in experiments described Chapter 2.

Accession Number	FlyBase ID	Protein	Residues Compared	Total Length (aa)
NP_477134	FBgn0015288	*D. melanogaster* rpL22e	6-132	299
NP_611771	FBgn0034837	*D. melanogaster* rpL22e-like	7-135	312
NP_523886	FBgn0026372	*D. melanogaster* rpL23a	5-130	277
NP_001027290	FBgn0053807	*D. melanogaster* histone H1	114-246	256
P15869	n/a	*S. purpuratus* histone H1	90-121	210

Sequence A	Sequence B	Sequence Identity	Sequence Similarity
S. purpuratus histone H1 (sea cucumber)	*D. melanogaster* rpL22e	46.5%	68.5%
	D. melanogaster rpL22e-like	26.8%	62.8%
	D. melanogaster rpL23a	35.7%	58.7%
	D. melanogaster histone H1	29.8%	62.4%
D. melanogaster histone H1	*D. melanogaster* rpL22e	25.5%	60.3%
	D. melanogaster rpL22e-like	15.6%	55.3%
	D. melanogaster rpL23a	27.7%	56.7%

Table 2.3. Comparison of *Drosophila* RpL22e paralogues and RpL23a N-termini to C-termini of sea cucumber (*S. purpuratus*) and *Drosophila* histone H1. Clustal W alignment was used to determine the amino acid sequence identity and sequence similarity between fruit fly histone H1-like domains found in the RpL22e paralogues and RpL23 to both sea cucumber and fruit fly histone H1 C-termini. The unique N-termini of the three *Drosophila* ribosomal proteins discussed here have higher homology to the C-terminus of the sea cucumber's histone H1, not to their own histone H1 orthologue. However, in both histone H1 comparisons, RpL22 has greater homology that RpL22-like.

Chapter 3:

RpL22e, but not RpL22e-like-PA, is SUMOylated and localizes to the nucleoplasm of meiotic spermatocytes

---

3.1 Introduction

Duplicated ribosomal protein (Rp) genes are prominent features of yeast, plant, and fly genomes. Many highly similar or identical Rp genes (demonstrated most notably in *Saccharomyces cerevisiae* and in *Arabidopsis thaliana*) appear to encode paralogues with functionally-distinct roles in several cellular, molecular, or developmental pathways in response to different environmental cues (Komili *et al.*, 2007; Kim *et al*., 2009; Hummel *et al*., 2012). These discoveries have stimulated an interest in determining if ribosome heterogeneity, in this case defined by Rp paralogue interchangeability, has an impact on translational regulation capacity (reviewed by Xue and Barna, 2012). Differences in ribosomal RNA composition, tissue-specific expression of Rp paralogues, and Rp post-translational modifications (PTMs) also contribute to ribosome heterogeneity and may broaden the translational regulatory spectrum in cells under certain physiological conditions.

Noteworthy is the fact that some Rps perform extra-ribosomal functions in addition to their roles in translation (reviewed by Warner and McIntosh, 2009); certainly through the course of evolution, a duplicated Rp paralogue may have acquired a new role distinct

from its presumed original canonical role as a structural component of the ribosome. Notwithstanding the acquisition of a new function, some degree of functional redundancy between Rp paralogues might also have been retained.

Given that different functional roles have often been attributed to structurally similar paralogues, it is reasonable to propose that disparate functions could be ascribed to structurally dissimilar paralogues, particularly in instances where tissue-specific expression patterns accompany paralogue structural divergence. The conserved eukaryotic-specific RpL22e family in *Drosophila melanogaster* represents a model protein family whose structurally divergent members may have evolved disparate functions.

The fly RpL22e family includes two genes, *rpL22e* and *rpL22e-like*. A single protein product was previously annotated for each gene, but recent evidence demonstrates that the *rpL22e-like* gene is alternatively spliced, giving rise to two protein products, "pL22e-like-PA and a novel protein isoform called RpL22-like-PB (Kearse *et a*l., 2011). Previous work by others determined that *rpL22e-like* mRNA is expressed in embryonic and adult gonads and germline cells (gonads: Shigenobu *et al*., 2006a, 2006b; primordial germ cells: Shigenobu *et al*., 2006a; adult ovary germline stem cells: Kai *et al*., 2005), and in adult testes, but not adult ovary from microarray analyses (FlyAtlas: Chintapalli *et al*., 2007). On the other hand, RpL22e is ubiquitously expressed (e.g., Shigenobu *et al*., 2006a, b) in embryos and adults. With paralogue-specific antibodies (Abs), we

determined that RpL22e-like-PA is expressed in a tissue-specific manner, found only in germ cells in adult testes and in fly heads of both sexes (Kearse *et al*., 2011). Thus the gonadal protein expression pattern aligned well with previously reported mRNA expression patterns.

Well established as a 60S ribosomal subunit protein (Lavergne *et al*., 1987), RpL22e is only 37% identical in amino acid (aa) sequence to RpL22e-like-PA (Marygold *et al*., 2007). Both proteins share a Rp signature with rRNA binding motifs (as defined for human RpL22e) at the C-terminal end (Houmani and Ruf, 2009). Our previous ribosomal profile analyses confirm RpL22e-like-PA co-sediments with monosomes and polysomes (Kearse *et al*., 2011), though other possible functions cannot be excluded at this time. A fly-specific N-terminal extension (of unknown function) with homology to the C-terminal end of histone H1 (previously described only for RpL23a and RpL22e by Koyama *et al*., 1999) is clearly the most divergent structural feature between the two proteins. Therefore, any potential functional differences between these proteins might be mediated through interactions in the N-terminal domain.

In the male reproductive system of the fly, RpL22e is expressed in the testis, accessory gland, seminal vesicle, and the ejaculatory duct. RpL22e-like-PA is only expressed within germ cells throughout spermatogenesis; therefore, RpL22e paralogues are co-expressed within germ cells (Kearse *et al*., 2011). The significance of the overlapping expression pattern within germ cells is yet to be uncovered.

Unexpectedly in the testis and in other tissues, we discovered additional immunoreactive species (using paralogue-specific Abs) at a higher molecular weight (MW) of ~50kD than would be predicted (33kD) for RpL22e (Figure 2.6; Kearse *et al*., 2011). In the testis, RpL22e-like-PA was detected at its predicted MW of 34kD, with no indication of stable higher MW species. We proposed that the high MW, SDS-resistant species might represent post-translationally modified RpL22e (Kearse *et al*., 2011). If so, an array of RpL22e PTMs sufficient to account for a minimum MW differential of ~20kD would have to be proposed. In the male germline where both paralogues are co-expressed, PTM of RpL22e, but not of RpL22e-like-PA would further distinguish these paralogues not only structurally, but most likely functionally as well. Such a distinction in PTM between Rp paralogues would bring to the forefront a new mechanism not widely explored as a means to regulate paralogue functions within the same cell.

Numerous examples of Rps serving as substrates for PTM machinery for methylation, acetylation, ubiquitylation, addition of *O*-linked β-D-*N*-acetylglucosamine, phosphorylation, and SUMOylation have been described (see Xue and Barna, 2012 for a brief review of this subject overall; e.g., see Matafora *et al*. [2009] for SUMOylation). Much remains to be uncovered about the importance of PTMs in controlling the dynamics of ribosome assembly (reviewed by Staley and Woolford, 2009) and in altering Rp function in translation or in other cellular pathways. Modification of eukaryotic Rps in the context of the ribosome adds a layer of translational regulation that has stimulated

numerous lines of investigation (e.g., Young *et al*., 2012; Koc and Koc [2012] for PTM review of mitochondrial Rps; Xue and Barna [2012] for PTM review) and in some instances, an impact on translation has been documented, albeit mechanistically not fully understood. A notable example is that incorporation of polyubiquitinated RpL28 (a component of the peptidyl transferase center) into ribosomes may have a stimulatory effect on translation (Spence *et al*., 2000).

PTMs of some Rps may be significant in defining extra-ribosomal roles for these proteins; for example, regulated phosphorylation of RpS6 affects cell size and glucose metabolic regulation in murine cells but does not affect mRNA translational control (Ruvinsky *et al*., 2005). Further, for RpS3, the DNA repair activities (Yacoub *et al*., 1996, Sandigursky *et al*., 1997, Deutsch *et al*., 1997) and the most recently described regulatory activities affecting mitotic spindle dynamics (Jang *et al*., 2012) appear to be controlled by PTMs that include regulated phosphorylation as well as SUMOylation (Kim *et al*., 2005; Kim *et al*., 2009; Jang *et al*., 2011).

For RpL22e and RpL22e-like-PA, little is known about PTMs, with a few exceptions for RpL22e. RpL22e is a substrate for casein kinase II with phosphorylation sites located at the C-terminal end (Zhao *et al*., 2002). Previous proteomics studies have identified numerous Rps as SUMO (small ubiquitin-like modifier) targets (e.g., Matafora *et al*., 2009; Nie *et al*., 2009), implicating involvement of the SUMOylation pathway in ribosome assembly (Matafora *et al*., 2009; Shcherbik and Pestov, 2010) or in the

degradation of unassembled Rps (Galisson *et al*., 2011). RpL22e was identified as a possible SUMOylation substrate based on its recovery in a complex containing multiple SUMO substrates (Nie *et al*., 2009); however, no definitive evidence that RpL22e itself is a target of SUMOylation has as yet been reported. SUMO, encoded by *smt3* (single SUMO gene in *Drosophila*), is a reversible protein modifier of ~10kD that can be added as a single entity or in multiples to acceptor lysines in protein targets through a series of enzymatic reactions (reviewed by Geiss-Friedlander and Melchior, 2007). The addition of SUMO chains to RpL22e could account for MW differences previously observed (Figure 2.6; Kearse *et al*., 2011).

Computational analyses to predict conserved recognition motifs within proteins reveal a putative strong SUMOylation site within RpL22e and RpL22e-like-PA located within the N-terminal domain but at a different location within each paralogue (Eukaryotic Linear Motif resource for Functional Sites in Proteins; http://elm.eu.org/). It is known that SUMOylation can impact subcellular localization, activity, and/or stability of modified substrates by altering intra- or intermolecular protein interactions (Geiss-Friedlander and Melchior, 2007). Further, the SUMOylation pathway is critical at multiple stages of spermatogenesis in several species, including *Drosophila* (reviewed by Lomelí and Vazquez, 2011).

Together with the detection of higher MW immunoreactive RpL22e species with paralogue-specific, peptide-derived Abs, computational predictions of a SUMO motif

within the N-terminal region of RpL22e, and proteomics evidence for association of RpL22e in complexes with other SUMO substrates (Nie *et al*., 2009), we have proposed that RpL22e is a SUMO substrate. To investigate this possibility, we used a combination of biochemical, molecular, and genetic approaches that included co-immunoprecipitations from S2 cells using anti-SUMO and anti-RpL22e Abs, a bacterial-based SUMOylation assay, and *in vivo* germline-specific RNAi depletion of SUMO. Another goal was to determine if high MW immunoreactive RpL22e species associate with 60S subunits, 80S monosomes, and/or polysomes in ribosome profiles from S2 cells. Such an association would support involvement in translation. On the other hand, lack of co-sedimentation with ribosomal components would favor involvement in extra-translational pathways. Further, using immunohistochemistry (IHC) we refine the cellular and subcellular localization patterns for both paralogues in the male reproductive tract, previously described by Kearse *et al*. (2011). Collectively, these investigations provide insights into mechanistic processes that specify RpL22e paralogue functions within the testis.

3.2 Results

We have previously reported the tissue- and sex-specific expression of the duplicated member of the RpL22e family, RpL22e-like-PA (Kearse *et al.*, 2011). In the adult testis, RpL22e-like-PA protein is detected at its predicted MW of 34kD and has an electrophoretic pattern identical to recombinant protein. However, we noted that the ubiquitously expressed RpL22e (expressed from the ancestral gene) was detected predominantly at a MW of ~ 50kD, greater than its predicted MW of 33kD. Here we further refine this observation by characterizing RpL22e in various tissues and show evidence for RpL22e PTM.

Comparing RpL22e electrophoretic patterns between *Drosophila* S2 tissue culture cells and adult gonads, variation in accumulating proteins is seen in the ~33-55kD range (Figure 3.1A). To facilitate protein comparative analysis, we established a protein nomenclature based on the approximate observed MW. The predicted MW protein from the annotated coding sequence is 33kD and is seen in all tissues. Two additional proteins, designated 43α and 43β, accumulate at varying amounts at the ~43kD range in S2 cells, ovaries, as well as testes. The abundance of 43α,β varies between samples, suggesting it may be an intermediate and/or not as stable. Immunoreactive proteins migrating in the ~55kD range are also evident, with 55α present in all tissues examined. Interestingly, testis tissue contains two additional immunoreactive proteins, designated 55β and 55γ. Western analysis of accessory glands (removed during testes dissections) suggests 55β and 55γ are testis-specific RpL22e species within the male reproductive

tract (Figure 3.2). Furthermore, comparison of RpL22e immunodetection patterns between whole testis tissue and isolated apical tip tissue suggests that 55γ is restricted to mitotic spermatogonia and/or early primary spermatocytes (Figure 3.3). The absence of these species from ovary and S2 cells (this report) as well as from salivary glands and head tissue (Kearse *et al*., 2011) suggests that these species may indeed be unique to testis tissue.

Initially, to confirm higher MW proteins as *bona fide* RpL22e gene products, we first performed pre-immune (Kearse *et al*., 2011) and then peptide inhibition experiments (Figure 3.1B). When anti-RpL22e polyclonal Ab was pre-incubated with a blocking peptide (a C-terminal peptide originally used for Ab production – Kearse *et al*., 2011), detection of all proteins was significantly reduced compared to protein detection in the absence of the blocking peptide. That the specific peptide acts to block detection of the higher MW proteins as well as RpL22e at 33kD favors the interpretation that the Ab is detecting RpL22e proteins. To provide additional support that high MW products detected with the RpL22e polyclonal Ab are RpL22e proteins, we next attempted to express FLAG-tagged RpL22e in S2 cells. While the addition of the FLAG-tag did not hinder protein stability, only minimal amounts of protein with a higher MW than the predicted RpL22e (33kD) accumulated in some experiments (Figure 3.4). More definitive support was provided by RNAi knockdown of RpL22e in S2 cells. By treating cells with dsRNA targeting codons 1-100 of RpL22e, the predicted MW (33kD) and all higher MW immunoreactive proteins are significantly reduced over time compared to

dsRNA GFP controls (Figure 3.1C). Taken together, we conclude that immunoreactive proteins in the 33, 43, and 55kD range are true RpL22e proteins.

By RT-PCR, we eliminated the possibility that alternative splicing of the *rpL22e* gene could produce transcripts that would encode higher MW proteins, as amplicons larger than those that would be predicted from the coding sequence are not evident (data not shown). We therefore hypothesize that the accumulation of higher MW RpL22e proteins is a result of PTM. Initial investigation of PTMs by *in silico* probing (via Eukaryotic Linear Motif scanner) for conserved modification motifs predicts multiple modifications for RpL22e (Figure 3.5, Table 3.1). Seven putative phosphorylation targets are predicted in RpL22e, however, the small MW of such a modification (95Da per phosphate group), even if combined, would not account for the observed ~10 and ~20kD increase in MW (Figure 3.1). However, a conserved SUMOylation motif was predicted for RpL22e and if covalent attachment of the 10kD SUMO protein does occur, this could account for the observed electrophoretic shift seen by immunodetection.

Given that initial expression of FLAG-tagged RpL22e in S2 cells did not produce an abundance of high MW products, we surmised that if RpL22e is SUMOylated, then its overexpression in S2 cells would produce unequal stoichiometry between the target protein and SUMO, likely resulting in relatively little SUMO-modified FLAG-tagged RpL22e. To rectify this imbalance, it is common to overexpress elements of the SUMOylation pathway, including the E2 conjugating enzymes (Ubc9 in *Drosophila*) and

SUMO itself (Bhaskar *et al*., 2002; Mauri *et al*., 2008; Smith *et al.*, 2011). Therefore, we used the previously developed 529SU S2 stable cell line (Bhaskar *et al*., 2002), which harbors expression vectors for FLAG-SUMO and HA-Ubc9, both under the control of the Cu^{2+} inducible metallothionein promoter for FLAG-tagged RpL22e expression experiments. Western analysis of FLAG-RpL22e transfections shows accumulation of FLAG proteins with MWs of 33kD, as well as (although at lower quantities) ~43kD and ~55kD (Figure 3.6A). High levels of endogenous RpL22e may hinder FLAG-RpL22e modification in S2 cell-based assays. Although SUMO is FLAG-tagged in the cell line and we would expect any FLAG-SUMO conjugate to be detected with anti-FLAG Ab, we note that FLAG-SUMO conjugates are present at MWs (43-55kD) consistent with known higher MW RpL22e species. Additionally, these FLAG-SUMO conjugates are only detected when RpL22e, but not GFP, is transiently expressed. These data are consistent with the hypothesis that high MW species could be SUMOylated RpL22e proteins or alternatively yet less likely, RpL22e expression (but not GFP expression) may stimulate SUMO modification in this cell line for unknown proteins whose MWs coincide with those of higher MW RpL22e species. In either case, more direct evidence for RpL22e SUMO modification would be required.

Drosophila RpL22e has been identified in the first purification step of a TAP-tagging proteomics study identifying SUMO targets in embryos (Nie *et al*., 2009). In this study, the initial purification by Ni-NTA chromatography was performed under strong denaturing conditions (8M urea), eliminating any non-covalent interactions. Identifying

RpL22e from purified tagged-SUMO under these conditions does provide preliminary evidence that RpL22e can be SUMOylated in *Drosophila*. Based on the observed MW, we predict at least two SUMO moieties are covalently attached to RpL22e, with 43α and/or 43β containing a single moiety and 55α representing attachment of two SUMO moieties. While only one conserved major motif is found by the *in silico* analysis, SUMO has been shown to form chains in yeast and humans (reviewed by Ulrich, 2008) and evidence does suggest SUMO chain formation can occur in *Drosophila* as well (Reo *et al*., 2010).

We next assessed RpL22e SUMOylation by co-immunoprecipitation (co-IP) experiments. Using S2 cell lysates, SUMOylated proteins were immunoprecipitated using anti-*Drosophila* SUMO. The 55α RpL22e species was captured in IP reactions containing anti-*Drosophila* SUMO, but not in control reactions with beads alone (Figure 3.6B). Additionally, a SUMO immunoreactive protein of 55kD is captured from S2 cell lysates in IP reactions with anti-RpL22e, but not in control reactions (Figure 3.7).
To further test if RpL22e is a SUMOylation substrate, we used the previously developed bacterial-based SUMOylation assay utilizing the *Drosophila* SUMOylation pathway enzymes and SUMO protein (Nie *et al*., 2009). *E. coli* were co-transformed with plasmids encoding FLAG-RpL22e and either an incompetent ($Q^{\Delta GG}$) or competent (Q^{SUMO}) form of SUMO. Western analysis shows a 20kD electrophoretic shift of FLAG-RpL22e when co-transformed with a competent from of SUMO (Q^{SUMO}), but not with an

incompetent form ($Q^{\Delta GG}$) (Figure 3.8A). Based on the observed MW, we conclude the modification is due to the addition of two SUMO moieties (55α).

In an attempt to gain evidence for functional diversification between the RpL22e paralogues, we extended the *in silico* investigation of predicted PTMs of RpL22e-like-PA (Figure 3.5, Table 3.1). Interestingly, although located at a separate location within the N terminus, a conserved major SUMO motif is predicted in RpL22e-like-PA. We have not detected RpL22e-like-PA above its predicted MW in testis protein lysates (Kearse *et al*., 2011); thus, if modified, proteins are either not stable or do not accumulate to detectable levels. Nevertheless, we tested if RpL22e-like-PA is a SUMO substrate using the bacterial-based SUMOylation assay. Consistent with *in vivo* testis results, SUMOylation of RpL22e-like-PA is not evident in this bacterial SUMO assay (Figure 3.8B). Positioning of the predicted motif and/or its structural context may render this SUMO motif inaccessible or nonfunctional not only in the bacterial assay, but in the testis environment as well. Alternatively, additional essential factor(s) and/or conditions may be required for RpL22-like-PA SUMOylation that are neither present in the bacterial system or by inference, in the testis germline environment as well.

In many instances SUMOylation is known to impact target protein stability (reviewed by Geiss-Friedlander and Melchior, 2007). RpS3 stability is enhanced by SUMOylation (Jang *et al*., 2011). In order to determine if a similar effect could be demonstrated for RpL22e, we used an *in vitro* proteolytic assay described by Jang *et al*. (2011), previously

used to assess SUMOylated RpS3 stability. We did not observe an impact of SUMOylation on the stability of RpL22e, previously expressed and SUMOylated in a bacterial assay. The proteolytic sensitivity of unmodified and SUMOylated RpL22e was equivalent in this assay (Figure 3.9). We do conclude, however, that SUMOylated RpL22e from S2 cells and testis is highly stable, as revealed by Western blot analysis (Figure 3.1A and C).

Male germline-specific modifications include specific phosphorylation of SUMOylated RpL22e.

To characterize the testis-specific RpL22e modifications (Figures 3.1-2), we proceeded to investigate possible phosphorylation and additional SUMOylation events. Using *in vitro* calf-intestinal alkaline phosphatase treatments, we assessed the phosphorylation state of RpL22e in S2 cells and testis. Western analysis of extracts treated with phosphatase shows a significant reduction of the testis-specific 55γ species exclusively compared to control reactions (Figure 3.10A). Thus, the 55γ species is a phosphorylated form of SUMOylated RpL22e. Whether this 55γ contains a single or multiple phosphate moieties is not addressed here. Additionally, other lower MW RpL22e species (e.g., 43β) may also be phosphorylated but not accessible to the phosphatase *in vitro*.

Multiple phosphorylation targets are predicted in both RpL22e and RpL22e-like-PA (Figure 3.5, Table 3.1). No evidence for significant modification of germline-expressed RpL22e-like-PA has been observed (Kearse *et al*., 2011; this study). Phosphatase

treatments of testis extracts did not result in any discernible electrophoretic shifts in Western analysis of RpL22e-like-PA (Figure 3.10B), supporting the conclusion that RpL22e-like-PA is not phosphorylated at accumulating levels in the testis.

Further evidence of RpL22e SUMOylation in testis and the male germline is provided by SUMO knockdown. Using the UAS-GAL4 binary system and the pVALIUM20 RNAi vector to express a miR1 cassette for knockdown, *smt3* (encodes SUMO) was specifically targeted in the male germline using the *bam*-GAL4-VP16 driver (Chen and McKearin, 2003; White-Cooper, 2012). Western analysis of testis tissue from F1 males when compared to control tissue shows a strong reduction in the amount of testis-specific 55β and 55γ RpL22e protein species (Figure 3.10C). Depletion of the 55β species in response to SUMO knockdown suggests that this species may arise from an additional SUMO residue added to SUMOylated 55α RpL22e. Depletion of the phosphorylated 55γ would be expected if derived from the phosphorylation of the 55β species. Furthermore, quantitative changes in modified RpL22e proteins in the 43kD range (43α and 43β), as well as for 55α RpL22e further support the conclusion that RpL22e is a SUMO substrate.

In vivo knockdown of SUMO also provides evidence that the phosphorylated 55γ species is found in germ cells, as the *bam*-GAL4-VP16 driver has a restricted expression pattern confined to the germline. Although the presence of the 55γ species within somatic cyst cells cannot be excluded, it is apparent that the majority of the 55γ species in the testis is contributed by germ cells. Taking these data together, we propose that testis-specific

modifications result from an additional SUMOylation event on 55α RpL22e (containing two SUMO moieties) to yield a 55β species containing three SUMO moieties. Subsequent phosphorylation events on the 55β substrate give rise to the 55γ species.

Unmodified RpL22e associates with the translation machinery.

Phosphorylation and methylation are among the most common PTMs seen in eukaryotic Rps (Lee *et al*., 2002; Young *et al*., 2012). Such modifications typically have roles in ribosome biogenesis, as opposed to active translation (Bachand *et al*., 2006; Ren *et al*., 2010; Webb *et al*., 2010). In some cases, modification (e.g., ubiquitylation) of the Rp occurs on polysomes, suggesting a role for the modification in active translation (Panasenko and Collart, 2012). Accumulation of unmodified or modified Rp within a particular type of ribosomal particle provides insight into a putative role in assembly or active translation. Conversely, the lack of accumulation in ribosomal particles would provide evidence for an extra-ribosomal function.

To assess a role for RpL22e in translation, we performed polysome analysis in S2 cells, using the distribution of a known large ribosomal subunit protein (RpL23a) for comparison. In cycloheximide-treated cells, unmodified RpL22e (seen at 33kD) co-sediments with the 60S large subunit, 80S monosomes, as well as polysomes, supporting its role as a ribosomal component and as a component of actively translating ribosomes (Figure 3.11A). A similar distribution pattern is seen for endogenous RpL23a. Notably, all modified RpL22e (43α, 43β and 55α), representing the majority of this protein in S2

cells, accumulates at the top of the gradient, well segregated from ribosomal subunits and active translation machinery, strongly indicative of a role apart from translation. Unlike modified RpL22e, no RpL23a accumulated at the top of the gradient.

Further, to confirm that unmodified RpL22e (33kD) is associated with the translation machinery, cells were treated with the chain terminator puromycin, resulting in dissociation of polysomes and accumulation of 80S monosomes. Similar to what is seen for RpL23a, sedimentation of unmodified RpL22e protein shifts from polysomes to the 80S monosome region with puromycin treatment (Figure 3.11A). Taken together, we conclude that only unmodified RpL22e associates with ribosomal subunits and is part of the active translation machinery. We find that modified RpL22e (43α, 43β and 55α) in S2 cells does not co-sediment at detectable levels with ribosomal particles and remains distributed at the top of ribosome gradient profiles.

To determine if SUMOylation of RpL22e has a role in ribosome assembly, we investigated a mutant that lacks all predicted SUMO motifs. Initial experiments mutating the predicted major acceptor lysine (K39R) did not completely abolish SUMOylation in the *in vitro* bacterial assay (Figure 6.1) and led us to develop a mutant (consisting primarily of the C-terminal domain that harbors the rRNA binding signature) that lacks any SUMO motifs. Mutagenesis of proposed SUMO acceptor sites in RpL22e will be instrumental in dissecting further biochemical details of paralogue modification, but will be addressed in future studies. Uniquely, the fly-specific N-terminal histone H1-like

domain (Koyama *et al*., 1999) harbors all putative SUMO motifs (Figure 3.5). Deleting the N-terminal domain (residues 1-175) results in a sequence that is highly conserved between all metazoans and closely resembles orthologues from yeast, *C. elegans*, and human. Noteworthy is the fact that no SUMO modification motifs are predicted by ELM (data not shown) in these RpL22e orthologues. The resulting coding sequence, RpL22eΔH1-FLAG (residues 176-299), can be expressed in S2 cells at similar levels as the full length protein, suggesting that deletion of the domain does not hinder stability (Figure 3.11B). Polysome analysis of full length (RpL22e-FLAG) and truncated RpL22e (RpL22eΔH1-FLAG) shows that both have a similar distribution pattern as endogenous RpL23a and both co-sediment with the active translation machinery (Figure 3.11C). Modified FLAG-RpL22e does significantly accumulate in S2 cells (Figure 3.4) and the unmodified form of RpL22e is expected to migrate with the polysomes and not be free at top of the gradient. Therefore, we postulate that stable modification of RpL22e, most notably SUMOylation, is not required for RpL22e assembly into the 60S ribosomal subunit or for ribosome function. Instead, SUMOylation of RpL22e likely shunts the protein into an extra-ribosomal pathway.

RpL22e paralogues are differently localized in the male germline.

In yeast, localization of 54 out of the 59 pairs of duplicated ribosomal proteins, typically encoding identical or nearly identical proteins, has been studied using a GFP fusion approach (Huh *et al*., 2003). Of the 54 pairs investigated, only five pairs had paralogues with unique, separate localization patterns, suggesting possible non-redundant roles (Huh

et al., 2003; Kim *et al*., 2009). We have previously reported that within the male reproductive system, RpL22e-like-PA is specifically localized to the male germline and RpL22e is ubiquitously localized throughout the male reproductive tract (Kearse *et al*., 2011). Insights into redundant or novel functions of both paralogues may be provided by comparing subcellular localization. Using paralogue-specific Abs and confocal microscopy, we assessed the distribution pattern of the RpL22e family in the male germline.

Drosophila male germline development is a coordinated event requiring somatic and germline stem cell signaling cascades that steer germ cells toward sperm cell differentiation, as well as testis-specific gene expression and dramatic changes in nuclear and cytoplasmic morphology in germ cells (reviewed by de Cuevas and Matunis, 2011; White-Cooper, 2009, 2010). Briefly, germ cells originate from a set of germline stem cells (GSC) in close contact with somatic precursor cells (SPC) at the apical tip. Each daughter cell from GSCs is surrounded by two somatic cyst cells (derived from SPCs) forming a spermatogonial cyst that proceeds through four rounds of mitosis with incomplete cytokinesis to generate a 16-cell spermatogonial cyst. Spermatogonia enter meiosis I after a prolonged G1 phase, increasing in volume approximately 30 times to form primary spermatocytes. Upon completion of meiosis II, spermatocytes elongate forming axonemes, followed by individualization to form separated spermatids. A gradient of germ cell maturation emerges with the most immature cysts residing at the apical tip and mature spermatids with elongated tails positioned near the distal end of the

testis to move into the seminal vesicle. Stages of germline development are therefore easily distinguishable by cellular morphology as well as by their general position within the testis. Notably, nuclei are very distinct in phase contrast microscopy (and when immunostaining cytosolic proteins) can be counted within cysts to identify the mitotic spermatogonial stage. Additionally, maturing meiotic spermatocytes are distinguishable as nuclei enlarge during the prolonged G1 phase before meiosis I.

IHC reveals distinct and separate subcellular localization patterns for RpL22e paralogues in the mitotic and meiotic male germ line. Indicative of a ribosomal protein, nucleolar and strong cytoplasmic localization is evident for RpL22e-like-PA- in mitotic spermatogonia (Figure 3.12A). In early primary spermatocytes (before first meiotic division), nucleolar accumulation of RpL22e-like-PA is still evident although less pronounced; abundant cytoplasmic staining is still apparent. Nucleolar accumulation of RpL22e-like-PA in mature primary spermatocytes is absent, as only strong cytoplasmic staining is seen (Figure 3.12A). Notably, immunostaining is not seen in the somatic cells within the testis. Furthermore, these data provide evidence that RpL22e-like is a male germ cell marker in *Drosophila*.

Interestingly, RpL22e has a predominant nuclear localization pattern in both mitotic and meiotic germ cells, with some cytoplasmic staining most evident in mitotic germ cells. Strong cytoplasmic staining is also apparent in somatic cyst cells (Figure 3.12). There is, however, a clear difference in the nuclear distribution of RpL22e within mitotic cells

compared to meiotic germ cells. Nucleolar localization is seen in mitotic spermatogonia, partially co-localizing with RpL22e-like, with partial immunostaining in the cytoplasm. Nucleolar localization was confirmed by co-localizing RpL22e with the nucleolar protein nucleostemin1 (Figure 3.13A), shown to be enriched in the granular component of the nucleolus in *Drosophila* (Rosby *et al*., 2009). GFP-tagged nucleostemin1 (Rosby *et al*., 2009) was expressed specifically in the early male germline using the GAL4-UAS binary system with the germline specific *bam*-GAL4-VP16 driver.

The punctate nucleolar RpL22e pattern seen in the mitotic germ line dissipates and becomes increasingly nucleoplasmic as development continues. Using phase contrast microscopy of tissue immunolabeled for RpL22e, we observed distinct segregation (although still close proximity) of RpL22e from the nucleolus within primary spermatocytes (Figure 3.13B). We further confirmed the RpL22e nucleoplasmic pattern by co-staining for fibrillarin, a marker for the dense fibrillar center of the nucleolus. Confocal microcopy confirms the close proximity, but separate localization of RpL22e and fibrillarin, as co-localization is not evident (Figure 3.13C). In more mature spermatocytes, the RpL22e staining pattern becomes less uniformly diffuse in the nucleoplasm and includes focused, punctate staining in the nuclear periphery. As spermatogenesis continues, sperm cell nuclei become increasingly compact. It is unclear how the RpL22e staining pattern is modified in this maturing population of cells (as images of this population were difficult to capture), but it is notable that the axonemes of individual sperm cells show strong RpL22e and/or RpL22e-like-PA staining (Kearse *et*

al., 2011). For RpL22e, it is unclear if axoneme staining results from extrusion of RpL22e from the nucleoplasm into the cytoplasm as the sperm nucleus undergoes compaction or if new RpL22e protein synthesis in the cytoplasm provides the explanation.

RpL22e may be a ribosomal component in mitotic spermatogonia, as higher levels of cytoplasmic staining are seen. Co-localization of RpL22e and GFP-nucleostemin1, a protein localized to the granular component of the nucleolus (Rosby *et al*., 2009), further supports a possible ribosomal role for RpL22e during mitotic stages of spermatogenesis. The function of nucleoplasmic RpL22e in meiotic spermatocytes remains unknown, but nucleoplasmic immunolocalization favors the hypothesis that in the meiotic germline, the bulk of RpL22e does not have a role in ribosome biogenesis or in active translation. The predominant nucleoplasmic immunostaining pattern for RpL22e in the absence of strong cytoplasmic staining in meiotic germ cells correlates well with results from S2 cells showing that modified RpL22e does not co-sediment with polysomes, but instead sediments at the top of ribosomal profile gradients (Figure 3.11). These data favor the proposal for an extra-ribosomal role for modified RpL22e in the testis as well.

SUMO knockdown perturbs RpL22e localization in the meiotic germline.

We next determined the impact of SUMO knockdown on RpL22e localization. As previously seen in Figure 3.10C, knockdown of SUMO causes a drastic change in RpL22e modification. Immunostaining shows that RpL22e becomes more widely

nucleoplasmic, as compared to the control (Figure 3.14). The characteristic punctate staining near the nuclear periphery is not observed, but staining remains more diffuse within the nucleoplasm. Whether or not this change in nucleoplasmic localization is a direct effect of the altered RpL22e modification pattern or of subsequent nuclear defects from SUMO knockdown is unclear, but will be addressed in future studies. Nevertheless, RpL22e nucleoplasmic localization is sensitive to SUMO protein levels.

3.3 Discussion

RpL22e is differentially post-translationally modified in different tissues.

Evidence from S2 cell-based expression assays and *in vivo* expression analyses in several tissues shows that RpL22e is expressed not only at its predicted MW of 33kD, but also at higher MWs of ~43-55kD. Collectively, co-IPs and bacterial SUMOylation assays favor the conclusion that higher MW RpL22e is attributable to PTMs that include SUMOylation, with the amount of SUMO-conjugated RpL22e accumulating in varying amounts in different tissues. These results extend the proteomics report of Nie *et al.* (2009) and show that RpL22e is a direct SUMO target.

How RpL22e function changes in response to SUMOylation is unknown, but in S2 cells, SUMOylated RpL22e is not found in association with ribosomal subunits or translating ribosomes nor is SUMOylation required for RpL22e incorporation into ribosomes or for ribosome function, the latter based on our analysis in S2 cells of the expression and gradient sedimentation of an N-terminal RpL22e truncation in which all predicted SUMO motifs were deleted (RpL22eΔH1-FLAG). Thus, we conclude that RpL22e has no less than a dual cellular role including an extra-ribosomal function(s), regulated by SUMOylation.

Testis expression of RpL22e paralogues is further distinguished by a unique pattern of PTMs for RpL22e but not for RpL22e-like-PA. Additional testis-specific RpL22e modifications include phosphorylation and may include conjugation of an additional

SUMO moiety. Phosphorylation of the 55β species of SUMOylated RpL22e appears to give rise to the 55γ moiety. Based on its absence from testis apical tip extracts and from day 1 *smt3* (SUMO)-depleted testis extracts (that primarily accumulate primary spermatocytes), the 55γ species may be a unique component generated only in post-mitotic cells. More definitive evidence of phosphorylation timing requires more extensive biochemical investigation of cohorts of cells at different spermatogenesis stages.

Specific machinery responsible for phosphorylation is unknown; however, a testis-specific isoform of casein kinase II β subunit 2 (a component of the casein kinase holoenzyme) has been described in flies and is expressed in post-mitotic spermatogenesis stages (Kalmykova *et al*., 2002). Expression of this subunit in meiotic cells would position the enzymatic activity in spermatogenesis stages where phosphorylated SUMOylated RpL22e is prevalent. As a known substrate of casein kinase II (Zhao *et al*., 2002), RpL22e phosphorylation may be mediated by the β regulatory subunit isoform in meiotic cells. Previous attempts by Kalmykova *et al*. (2002) to knockdown expression of this β subunit by RNAi were not reproducible, not allowing the impact of β subunit depletion on spermatogenesis or fertility to be assessed. Revisitation of this approach may be useful, however, to determine if isoform depletion impacts phosphorylation of SUMOylated RpL22e.

The function of phosphorylated forms of SUMOylated RpL22e is unknown. One hypothesis is that this modification alters SUMOylated RpL22e interactions (and distribution) that subsequently affect RpL22e function in meiotic cells. In *smt3* (SUMO)-depleted testes, the 55γ phosphorylated moiety is diminished in immunoblots. RpL22e does not show a punctate staining pattern within the nucleoplasm, as is the case in control testes. Instead, RpL22e nuclear staining remains diffuse. In control testes, relatively little unconjugated RpL22e is present in immunoblots. Therefore, it is reasonable to propose that the majority of nuclear staining visualized within germ cells is SUMOylated RpL22e. While it is tempting to speculate that the 55γ species is contained within nucleoplasmic foci and that 55β phosphorylation is causative in promoting the redistribution of a fraction of RpL22e from its diffuse nucleoplasmic pattern, stronger evidence for this proposal must await more rigorous biochemical characterization of RpL22e at specific stages of spermatogenesis. Alternatively, the change in RpL22e localization in meiotic cells and phosphorylation of SUMOylated RpL22e may be unrelated events.

Differential sub-compartmentalization of RpL22e paralogues and its functional implications.

Our IHC data show that both paralogues are co-expressed within germ cells, but paralogue localization changes as germ cells mature. We have previously determined that RpL22e-like-PA is a *bona fide* testis Rp (Kearse *et al*., 2011). Within mitotic germ cells closest to the apical tip, both paralogues are distributed within the nucleolus and

cytoplasm. This localization pattern is consistent with a ribosomal function for both paralogues within mitotic germ cells. If so, then two different ribosomal populations based on RpL22e paralogue content could be identified, and may constitute a class of "specialized ribosomes" (as recently proposed by Xue and Barna, 2012) with unique translational roles at mitotic stages of spermatogenesis.

In primary spermatocytes, the cytoplasmic localization pattern for RpL22e-like-PA is retained; however, the RpL22e pattern is primarily nuclear; relatively little cytoplasmic staining is noted at this stage, but may still signal that a fraction of the RpL22e pool is incorporated into cytoplasmic ribosomes. RpL22e nuclear staining appears uniformly diffuse at this stage except that staining is generally excluded from nucleoli. Primary spermatocytes undergo tremendous cellular growth and increases in protein synthesis as they enter meiosis. It is unclear what novel interactions for newly synthesized RpL22e or previously synthesized RpL22e account for the observed change in nuclear distribution in primary spermatocytes. Redistribution of human RpL22e from nucleoli into the nucleoplasm in Epstein Barr virus-infected cells is mediated through binding of virally-encoded EBER1 RNA with RpL22e (Houmani *et al*., 2009). Future efforts to identify effectors that interact with RpL22e and impact its nuclear distribution should consider both protein and RNA components.

SUMOylation has been linked to regulating localization of nuclear proteins and formation of nuclear bodies. The small GTPase-activating protein RanGAP was the first

SUMO substrate identified (Matunis *et al*., 1996) and its localization is regulated by SUMOylation. Unmodified RanGAP is cytoplasmic, but SUMOylated RanGAP localizes to nuclear pores (Matunis *et al*., 1996; Mahajan *et al*., 1997). The formation of PML nuclear bodies is dependent on SUMOylation of the PML protein (Zhong *et al*., 2000). We show that the nucleoplasmic localization of RpL22e in the meiotic germline is sensitive to SUMO levels. Whether this redistribution is a direct effect from interfering with RpL22e SUMOylation or the result of a change in nuclear architecture due to SUMO knockdown remains to be investigated. Future studies identifying SUMO acceptor lysines in RpL22e may allow for further characterization of its nucleoplasmic distribution and SUMOylation dependence.

Many studies have found mechanisms that rapidly degrade excess Rps (e.g., Lam *et al*., 2007; reviewed by Perry, 2007). It is likely that RpL22e accumulates within meiotic cell nuclei for a specific, functional role. Ni *et al*. (2006) reported a chromatin-RpL22e association in a transcriptional repressor complex with histone H1 in *Drosophila* Kc cells, suggesting that RpL22e has an alternate function in transcriptional regulation aside from its function as an Rp. We note that no higher MW RpL22e species were identified in immunoblots in this report and thus it is unclear if SUMOylated RpL22e is a contributing effector in these studies. Differences may be attributed to polyclonal Ab specificity in that study compared to the current investigation. Recent studies in *Schizosaccharomyces pombe* reported that other Rp-chromatin complexes are enriched at

tRNA genes and centromeres, implicating Rps as effectors in tRNA biogenesis and centromere functions (De *et al*., 2011).

Mounting evidence therefore positions numerous Rps in nuclear locations that suggest alternate Rp roles. We speculate that in a variety of cell types, SUMOylated RpL22e may associate with chromatin as cells undergo nuclear architectural changes, chromatin remodeling, and/or transcriptional silencing. In the male germline additional PTMs would further regulate and expand the role of RpL22e beyond functions found in other cells and tissues. Within post-meiotic cells undergoing extensive nuclear remodeling, SUMO accumulates in chromatin during histone removal (Rathke *et al*., 2007), but its role and targets are unknown. Whether or not testis-specific modification of SUMOylated RpL22e is part of the mechanism to promote chromatin condensation and/or transcriptional repression in maturing germ cells awaits determination. Alternatively, SUMOylated RpL22e may be stored in chromatin complexes with other Rps as pre-ribosomal complexes awaiting assembly into 60S ribosomal subunits although the SUMOylation step can clearly be bypassed. If so, a rationale for RpL22e sequestration away from the nucleolus for ribosome assembly may be an equally important problem to comprehend.

Overall, this study finds additional evidence to support the proposal that RpL22e paralogues have evolved disparate functions within the male germline. That these paralogues are partitioned into different biochemical pathways leading to differential

PTM and different subcellular accumulation within germ cells makes a compelling argument for the pursuit of RpL22e function within the male germline.

3.4 Material and Methods

Drosophila Stocks

Unless noted, all flies used were wildtype Oregon R from Carolina. The *bam*-GAL4-VP16 driver was a kind gift from Marina Wolfner (Cornell), but originally developed by Dennis McKearin (Chen and McKearin, 2003). The GFP-Nucleostemin1 stock was a kind gift from Pat DiMario (Rosby *et al*., 2009). The *smt3* (SUMO) RNAi line, originally developed by the TRiP, uses the pVALIUM20 vector to generate a hairpin and was obtained from Bloomington Stock Center (#36125). We thank the TRiP at Harvard Medical School (NIH/NIGMS R01-GM084947) for providing transgenic RNAi fly stocks and/or plasmid vectors used in this study. All stocks were kept at room temperature on standard cornmeal media.

Fly *in vivo* RNAi and Ectopic Expression

SUMO (*smt3*) knockdown was performed using the UAS-GAL4 binary system. UAS-VALIUM20-*smt3* females were crossed with *bam*-GAL4-VP16, UAS-Dicer2 males at 25°C to drive SUMO (*smt3*) knockdown in the male germline. 1 day old F1 males were collected and used for analyses.

Similarly, GFP-Nucleostemin1 (NS1) was expressed in the male germline by crossing UAS-GFP-NS1 females with *bam*-GAL4-VP16 males at 25°C. 1 day old F1 males were collected and used for immunohistochemical analysis.

Antibodies

The rabbit polyclonal anti-*Drosophila* RpL22e and mouse polyclonal anti-*Drosophila* RpL22e-like antibodies (Kearse *et al*., 2011) were used at 1:2000 for Western analysis and 1:100-200 for immunohistochemistry (IHC). The rabbit polyclonal anti-*Drosophila* SUMO was obtained from Abgent (#AP1287b) and used at 1:500 for Western analysis. The mouse monoclonal anti-FLAG antibody was obtained from SIGMA (#F3165) and used at 1:1000 for Western analysis. The mouse anti-GFP monoclonal antibody was obtained from Abgent (#AM1009a) and used at 1:500 for IHC. Mouse anti-fibrillarin was obtained from Abcam (#ab4566) and used at 1:200 for IHC. The mouse anti-β-tubulin antibody (E7) developed by M. Klymkowsky was obtained from the Developmental Studies Hybridoma Bank developed under the auspices of the NICHD and maintained by The University of Iowa, Department of Biology, Iowa City, IA 52242 and used at 1:500 for Western analysis.

HRP conjugated goat anti-mouse IgG and goat anti-rabbit IgG secondary antibodies were obtained from Promega and used at 1:50,000 for Western analysis. Goat anti-mouse/Alexa Fluor 488 and goat anti-rabbit/Alexa 568 were obtained from Invitrogen and used at 1:200 for IHC.

Cell Culture

S2 cells were obtained from the Drosophila Genetics Research Center and grown in Schidner's Media (Invitrogen, #21720024) supplemented with 10% head-inactivated fetal

bovine serum (Invitrogen) and grown at 26°C. The 529SU stable cell line was a kind gift from Albert Courey (UCLA) and was grown as above with the addition of 300µg/mL Hygromycin B as a selection agent.

Cells were seeded at 1.0 $x10^6$ cells/mL (3mL per well) for transfections. 24h post seeding, transient transfections were carried out using the calcium phosphate kit (Invitrogen) with 19µg DNA per well following manufacture guidelines. Cells were washed 24h post transfection and induced with 500µM $CuSO_4$ (final).

Preparation of Cell and Tissue Lysates

S2 cells were collected during log phase growth (2-3 d post seeding at 1.0 $x10^6$ cells/mL) or at designated time points after treatments, pelleted at 4°C, and then lysed in RIPA buffer (25mM Tris-HCl pH 7.6, 150mM NaCl, 1% Triton X-100, 1% sodium deoxycholate, 0.1% SDS) supplemented with 1mM PMSF for 10 min on ice. Gonads were dissected from wildtype adults in 1X PBS and immediately frozen on dry ice. Approximately 15 pairs were lysed in 30µL of RIPA buffer supplemented with 1mM PMSF for 10 min on ice. Lysates were centrifuged for 10 min at 16,000xg to clear cell debris, nuclei and mitochondria. The resulting supernatant was then quantified using the Bio-Rad *DC* Protein Assay Kit with BSA standards.

Western Analysis

SDS-PAGE was conducted under reducing (βME) conditions. Proteins were then electrotransferred onto a 0.2µm Westran-S PVDF membrane (Whatman) for 1h in chilled transfer buffer. Upon blocking in 5% non-fat dry milk (NFDM) for 1h, primary antibodies were incubated overnight at 4°C in 3% NFDM. HRP conjugated secondary antibodies were incubated for 2h at 4°C in 3% NFDM. ECL-Plus (GE Healthcare) was used for chemiluminescent detection on Kodak Bio-Max film as directed by the manufacturer.

Peptide inhibition experiments were completed by pre-incubating Ab with five-fold excess (by weight) of peptide used for antibody production (Kearse *et al*., 2011) in 500µl 1X PBS at room temperature for 2h before using for Western analysis. Addition of PBS in lieu of blocking peptide was used for negative control samples.

S2 cell RNAi

Knockdown of RpL22e by RNAi was achieved by serum-starvation induced uptake of dsRNA (final 37nM) as described by Clemens *et al*. (2000). dsRNA was generated using PCR amplicons with T7 recognition sites at 5' and 3' ends with the MEGAscript T7 *in vitro* transcription kit (Invitrogen/Ambion) and purified as described by manufacturer's recommendations. Annealing of dsRNA was achieved by incubation 30-60 min at 65ºC and allowed to cool slowly at room temperature. Samples were taken at designated time

points, pelleted and frozen for subsequent analysis. Samples were lysed and quantitated as described above.

Cloning and Mutagenesis

A FLAG tag was added to the N-terminus by PCR for RpL22e and RpL22e-like-PA (cDNA was previously cloned, Kearse *et al*., 2011) and cloned into pMT/V5-His-TOPO (Invitrogen) for expression studies in S2 cells and pEXP5-CT/TOPO (Invitrogen) for expression in *E. coli*. The RpL22e^{K39R} mutation was generated using the Change-IT Multiple Mutation Site Directed Mutagenesis Kit (Affymetrix) following manufacturer's recommendations using the following forward primer: $PO_4$5'-AAGGTGGAGAAGCCGCGCGCTGAGGCCGCCAAG-3'. The single codon change was confirmed by Sanger sequencing.

The RpL22e-FLAG and RpL22eΔH1-FLAG constructs for expression studies in S2 cells were constructed by standard PCR methods using previously cloned RpL22e cDNA (Kearse *et al*., 2011). A FLAG-tag was incorporated by inserting the FLAG coding sequence into the reverse primer sequence (5'-GTACGAATTCTTACTTGTCATCGTCATCCTTGTAGTCGCCGCGGCCGATCTCGGCATCGTCGTCCTCATCGTCG-3') using Platinum Taq DNA Polymerase High Fidelity (Invitrogen, #11304011) and cloned into pMT/V5-His-TOPO following the manufacturer's recommendations. Subsequently, to create RpL22eΔH1-FLAG, a methionine codon (ATG) was added upstream of the coding sequence starting at amino

acid 176 in the forward primer (5'-GAATTCATGAAGAACGTGCTGCGTGGCAAGGGACAGAAGAAGAAG-3') and cloned into pMT/V5-His-TOPO. Proper FLAG-tag fusion and construct sequence was confirmed at each cloning step by Sanger sequencing.

Bacterial SUMOylation Assay

Assay was performed essentially as previously reported by Nie *et al*. (2009). Q^{SUMO} and $Q^{\Delta GG}$ plasmids were a generous gift from Albert Courey (UCLA).

For RpL22e, BL21 Star (DE3) *E. coli* cells (Invitrogen) were co-transformed with pEXP-5/FLAG-RpL22e^{WT} or pEXP-5/FLAG-RpL22e^{K39R} along with Q^{SUMO} or $Q^{\Delta CC}$ and plated on to double selective media (LB agar with 100µg/mL Ampicillin and 50µg/mL Kanamycin) at 37°C. Resistant transformants were selected to inoculate overnight seed cultures in LB broth with Ampicillin and Kanamycin at 37°C. 100µL of seed culture was used to inoculate 50mL auto-inducing media (Studier, 2005) with antibiotics in 500mL baffled flasks at 200rpm. Cultures were incubated in a 26°C shaking water bath at 200rpm until 10.0 OD_{600}. For protein prep, 10mL of culture was pelleted and resuspended in 1mL sonication buffer (1X PBS, 0.1% Triton X-100, 1mM PMSF). Samples were lysed with three 10 second sonication cycles with 1 minute intervals resting ice followed by a 10 minute centrifugation step (16,000xg at 4°C) to clear debris. Lysates were quantified and used for SDS-PAGE and Western analysis as described above.

For RpL22e-like-PA, the assay was performed identically with pEXP-5/FLAG-L22e-like-PA.

In vitro Proteolysis

Proteolysis assays of bacterial SUMOylation assay lysates (see above) using purified trypsin (Sigma) was performed as previously described (Jang *et al*., 2011). Reactions were stopped by the addition of an equal volume of reducing sample buffer and boiled for 5 min. Subsequently, 5µg of lysate was used for SDS-PAGE and Western analysis.

Immunoprecipitation

Indirect immunoprecipitation (IP) protocols were adapted from Sanz *et al*. (2009) for S2 cells. 10mLs of S2 cells were seeded at 1.0 x10^6 cell/mL in T25 flasks and incubated for 3 days at 26°C. Cells were pelleted at 100 x g for 5 min, washed with PBS, and lysed in 1mL of IP lysis buffer (10mM Tris-HCL [pH 7], 100mM KCl, 5mM $MgCl_2$, 1mM DTT, 100µg/mL cycloheximide) for 10 min on ice. A post-mitochondrial fraction was created by centrifugation at 16,000 x g for 10 min in a microcentrifuge at 4°C. 20µg anti-*Drosophila* SUMO antibody (Abgent, #AP1287b) incubated with 400-500µL of lysate overnight at 4°C with constant agitation. Antibody-antigen complexes were captured by the addition of 40µL of prepared magnetic protein A beads (Millipore, #LSKMAGA02) as recommended by the manufacture with constant agitation for 20 min at RT. Upon three washes with high salt IP wash buffer (300mM KCl), captured proteins were eluted

by incubation of excess free peptide at 4°C for 30 min (two rounds of 200µL free peptide at 100mg/mL with constant agitation). Eluates were pooled, TCA precipitated (as described in Houmani and Ruf, 2009), resuspended in reducing SDS-sample buffer, separated by SDS-PAGE, and probed for RpL22e in Western analysis.

RpL22e IP reactions were performed as described above, but capture used 20µg anti-RpL22e. Eluates were subjected to Western analysis and probed with anti-*Drosophila* SUMO.

Phosphatase Treatment

10µL reactions using Calf Intestinal Alkaline Phosphatase (New England Biolabs) were set up as suggested by New England Biolabs. Protein samples were diluted to 1-2 µg/10 µL in 1X NEBuffer 2. Upon the addition of 1 unit of CIP/1 µg protein, reactions were incubated at 37°C for 60 minutes. PBS was added to negative control samples in lieu of phosphatase. Reactions were either frozen on dry ice and stored at -80°C or directly used for SDS-PAGE by adding equal volume of reducing SDS-sample buffer and boiled.

Sucrose Gradient Ultracentrifugation

S2 cells were seeded at $1x10^6$ cells/mL (9mLs per drug treatment) and allowed to grow for 3 days at 26ºC. Cells were then treated with 100µg/mL cycloheximide or 300µg/mL puromycin for 10 min on ice, pelleted and washed with ice-cold 1X PBS containing cycloheximide or puromycin. Cells were then lysed in 1mL of ribosome lysis buffer and

layered on top of a 10-50% buffered sucrose gradient as described by Houmani and Ruf (2009). Gradient preparation, centrifugation conditions and subsequent protein extraction by TCA precipitation was performed as previously described by Houmani and Ruf (2009). Gradients were fractionated using a Brandel syringe pump and Foxy Jr. R1 gradient fractionators along with an Isco UA-6 detector for continuous absorbance reading at 254nm. Fractions were collected in 0.5mL volumes with 40 sec fraction collection times set with 0.75mL/min pump speed).

For analysis of RpL22e-FLAG and RpL22eΔH1-FLAG, three wells of S2 cells were transfected as described above. 48h post-induction, wells were pooled, treated with cycloheximide, lysed, and subjected to sucrose gradient ultracentrifugation as described above.

Immunohistochemistry

Testis squashes and immunostaining was performed as previously described for all analyses (Kearse *et al*., 2011).

3.5 Figures and Tables

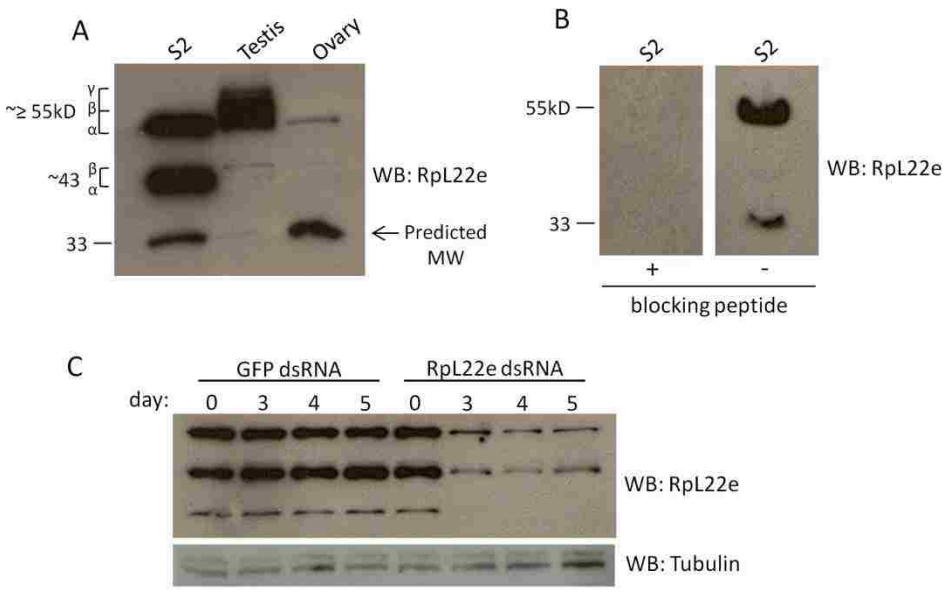

Figure 3.1. RpL22e is detected at various MWs in multiple *Drosophila* tissues. A) Using a peptide-derived polyclonal antibody, RpL22e is detected in S2 tissue culture cells, testis and ovary tissue at its predicted MW of 33kD, but also at higher molecular mass, designated as 43α,β and 55α,β,γ (increasing in molecular mass). B) Peptide inhibition experiments confirm specificity of polyclonal antibody. C) Immunodetection of 33kD RpL22e, as well as novel slower migrating species (43α,β and 55α) is reduced in S2 cells via RNAi by incubation of dsRNA targeting codons 1-100 of RpL22e, but not by targeting GFP (negative control). Tubulin was used as a loading control.

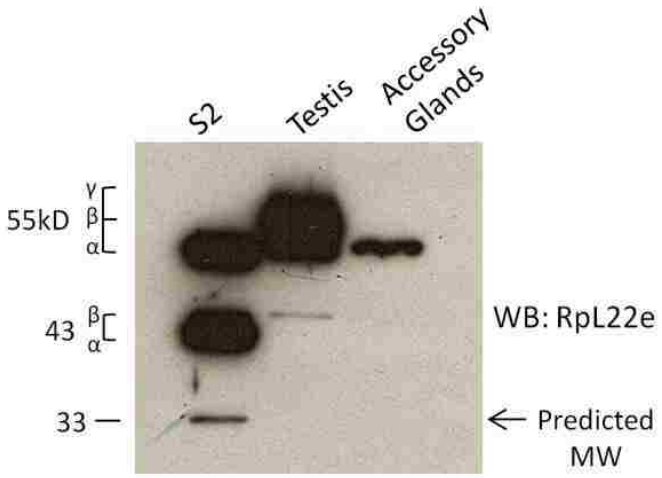

Figure 3.2. 55β,γ RpL22e are specific to testis, but not the associated accessory gland. Accessory glands were dissected from the male reproductive tract and treated as described in material and methods for testis tissue. Western analysis of S2 cells, testis and accessory glands confirms 55β,γ are unique to the testis of the male reproductive tract.

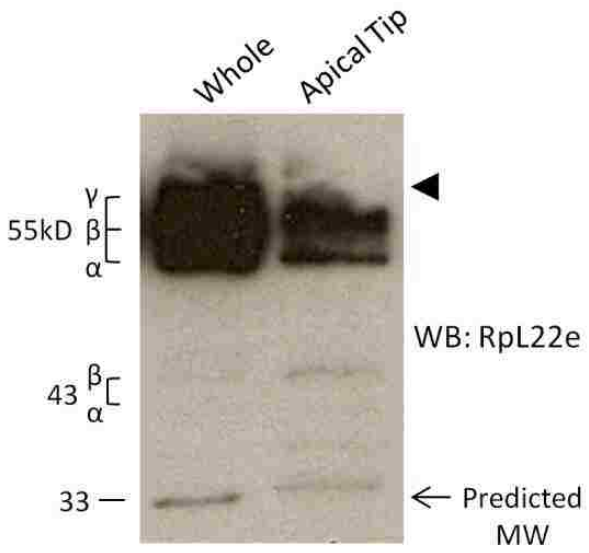

Figure 3.3. 55γ RpL22e accumulates in mitotic germline-enriched samples. Apical tips, which contain the germline stem cells, mitotic spermatogonia, and early/immature primary spermatocytes, were dissected from whole testis tissue and treated as described in material and methods for testis tissue. Western analysis of whole testis tissue and apical tips show a significant decrease in immunodetection of 55γ RpL22e (arrowhead).

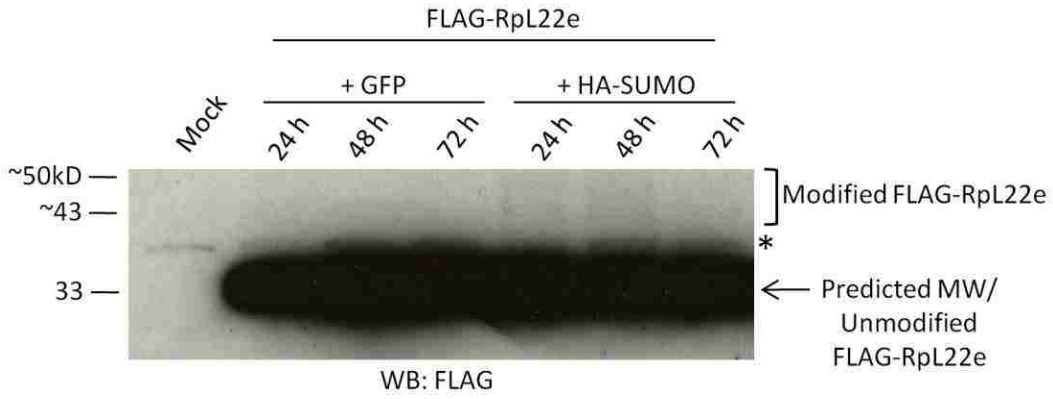

Figure 3.4. High MW FLAG-RpL22e can be detected when co-expressed with HA-SUMO in S2 cells. FLAG-RpL22e was co-expressed in S2 cells with either GFP or HA-SUMO and induced for 24, 48, or 72h. Western analysis shows accumulation of higher MW FLAG immunoreactive proteins in the 40-50kD range with co-expression of HA-SUMO, but not GFP. A non-specific endogenous FLAG immunoreactive protein is seen in all lanes (asterisk).

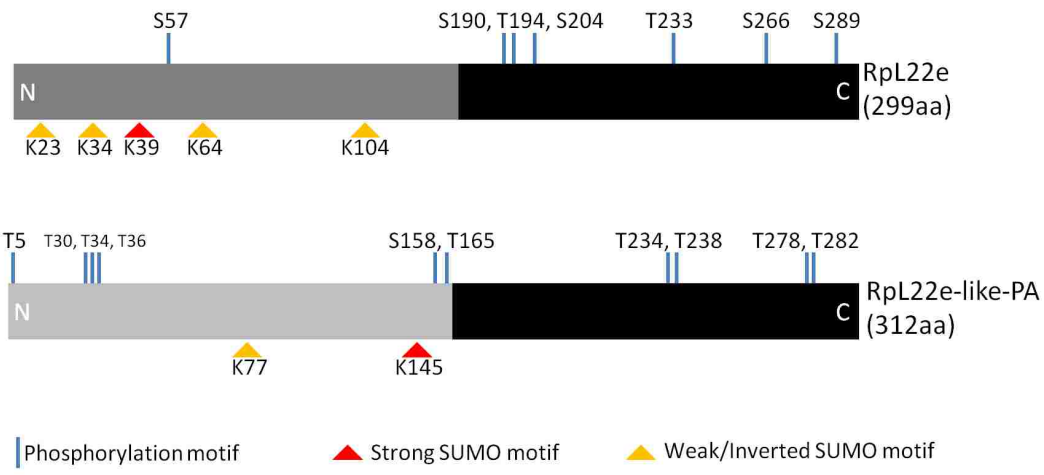

Figure 3.5. Computational predictions of post-translational modifications within the RpL22e family. Eukaryotic Linear Motif (ELM) scanner predicts multiple modifications in both RpL22e (FBgn0015288; FBpp0070143) and RpL22e-like-PA (FBgn0034837; FBpp0071958) as consensus sequences were conserved for various phosphorylation and SUMOylation motifs. The black domains represent the conserved region between the fly paralogues and other eukaryotic RpL22e proteins. Dark and light gray domains represent the fly-specific histone H1-like N-terminal extension that has less homology between the paralogues. Consensus sequences and motifs within the RpL22e family members are found in Table S1.

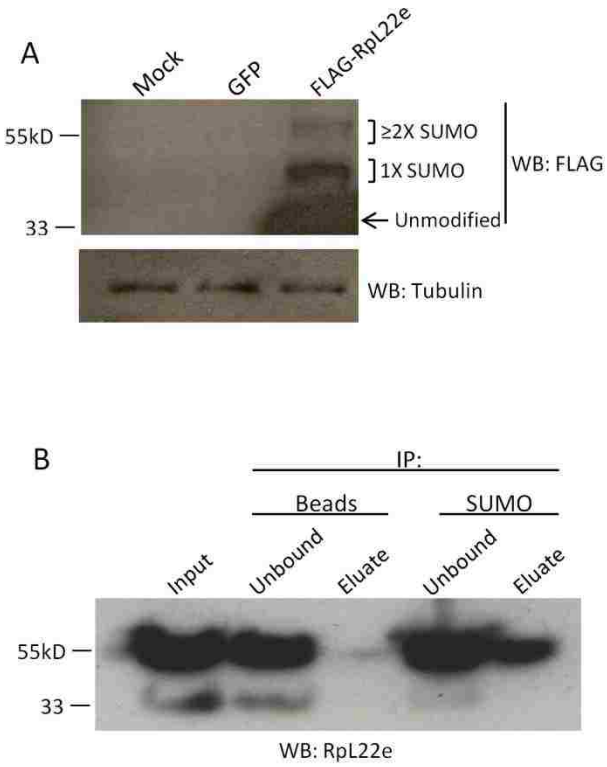

Figure 3.6. Higher MW RpL22e is detected when FLAG-tagged and co-immunopurifies with SUMO. A) FLAG-RpL22e is detected above its predicted MW of 33kD in the 43-55kD range in the 529SU S2 cell line, which harbors inducible expression of the SUMO protein (as FLAG-SUMO) and the E2 SUMO conjugating enzyme Ubc9 (as HA-Ubc9). Tubulin was used as a loading control. B) 55α RpL22e can be co-immunopurified from S2 cells using anti-*Drosophila* SUMO, but not with beads alone.

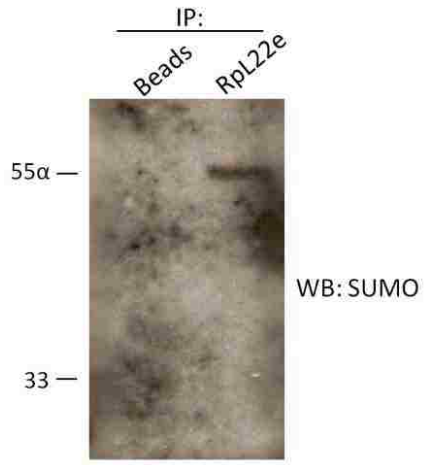

Figure 3.7. Anti-RpL22e immunoprecipitated a SUMOylated protein of ~ 55kD. Using anti-RpL22e for capture, an anti-*Drosophila* SUMO immunoreactive protein at ~55kD is immunoprecipitated from S2 cells. This capture is not evident in bead alone control reactions.

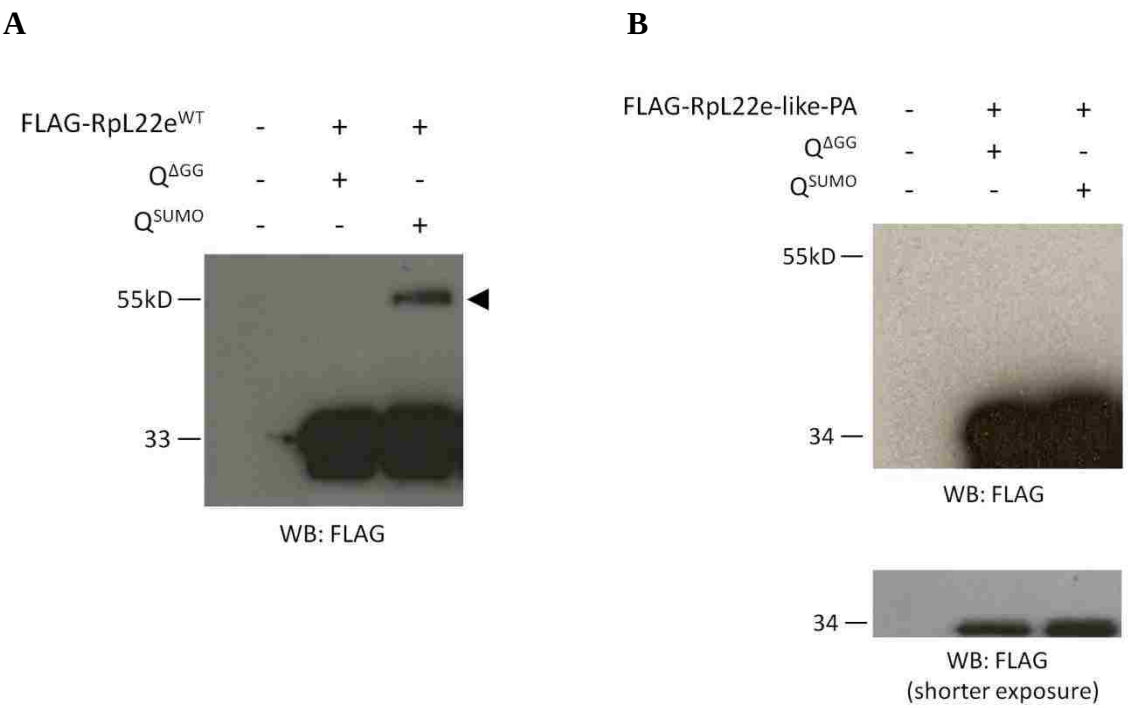

Figure 3.8. FLAG-RpL22e, but not FLAG-RpL22e-like-PA, can be SUMOylated *in vitro*. A) When co-expressed in *E. coli* harboring the *Drosophila* SUMOylation machinery (the E1 heteromeric activating enzyme and E2 conjugating enzyme) with an attachable competent SUMO protein (Q^{SUMO}), but not with an incompetent SUMO mutant ($Q^{\Delta GG}$), FLAG-RpL22e is detected above its predicted MW (33kD) at 55kD (arrowhead). Based on the MW shift, the addition of two SUMO moieties is predicted. B) Although harboring two predicted SUMO motifs (Figure 3.5, Table 3.1), FLAG-RpL22e-like-PA is not SUMOylated *in vitro*.

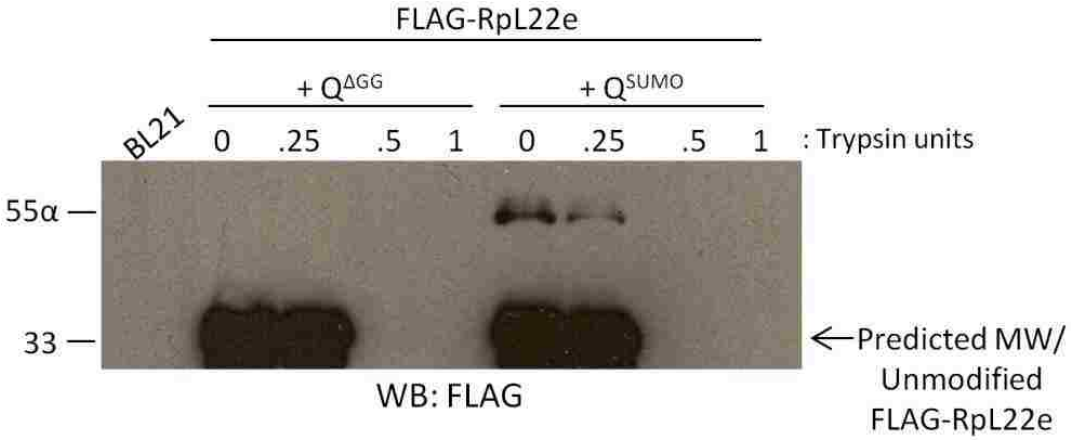

Figure 3.9. Unmodified and SUMOylated RpL22e are equally susceptible to *in vitro* proteolysis. Bacterial SUMOylation assay lysates were treated with varying amounts of trypsin to assess proteolysis susceptibility. No difference in trypsin proteolysis was seen between lysates containing unmodified and SUMOylated RpL22e. Units of trypsin were added accordingly to previously published assays (Jang *et al*., 2011). It was empirically determined that complete proteolysis was achieved with ≥0.25 units, but not with ≤0.20 units (data not shown).

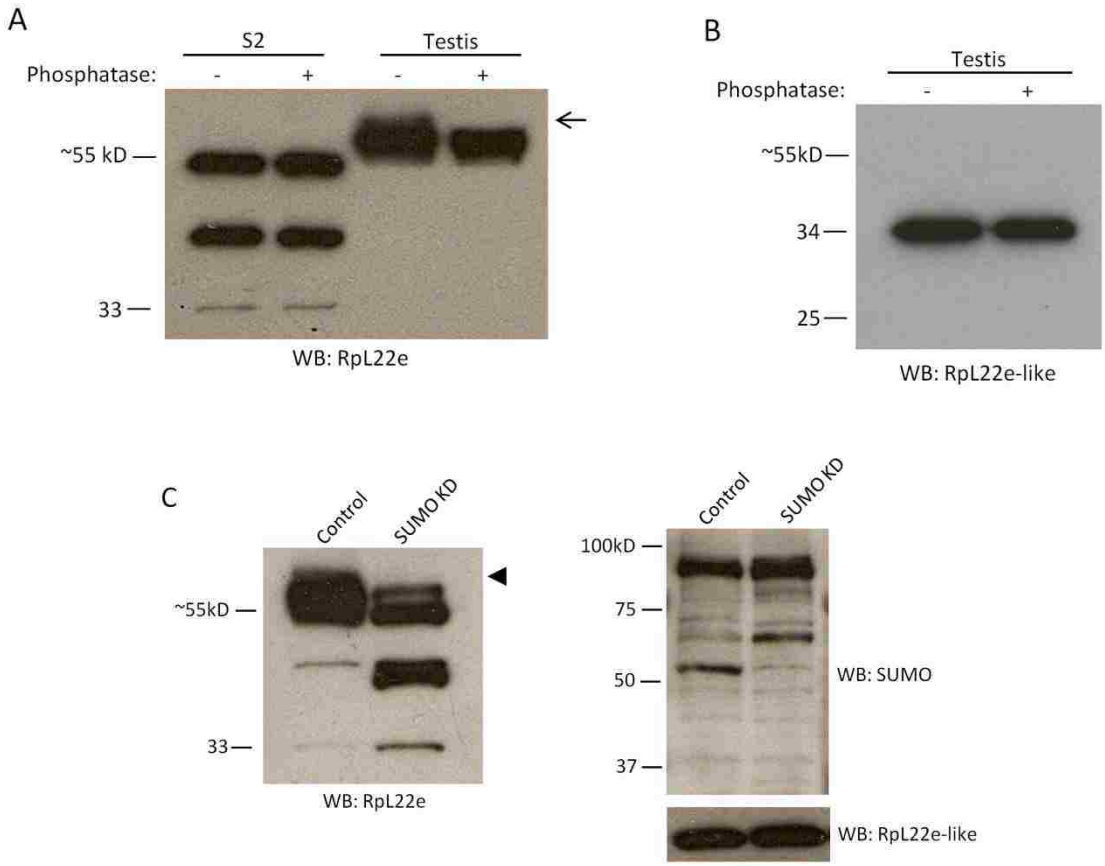

Figure 3.10. Testis RpL22e, but not FLAG-RpL22e-like-PA, is susceptible to phosphatase *in vitro* and *smt3* (SUMO) knockdown *in vivo*. A) Incubation of S2 cell and testis tissue extracts with calf-intestinal alkaline phosphatase *in vitro* significantly reduces immunodetection of the testis-specific 55γ RpL22e species (arrow). B) Phosphatase treatment has no effect on the RpL22e-like-PA immunodetection pattern in testis. C) *In vivo* knockdown of *smt3* (via UAS-GAL4 binary system) was achieved by expressing a miR1 cassette targeting *smt3* using a germline-specific GAL4 driver (*bam*-GAL4-VP16, UAS-Dicer2). The testis RpL22e immunodetection pattern is significantly altered upon *smt3* knockdown compared to control tissue. No change in RpL22e-like-PA

accumulating levels is seen. Immunodetection with anti-*Drosophila* SUMO confirms alteration of SUMOylation levels via *smt3* knockdown. Additional *smt3* knockdown experiments using *nos*-GAL4 (the only other male germline-specific driver; expressed in germline stem cells and very early mitotic spermatagonia) in attempt to achieve greater *smt3* knockdown resulted in complete perturbation of the germline (data not shown), making additional Western analyses impossible.

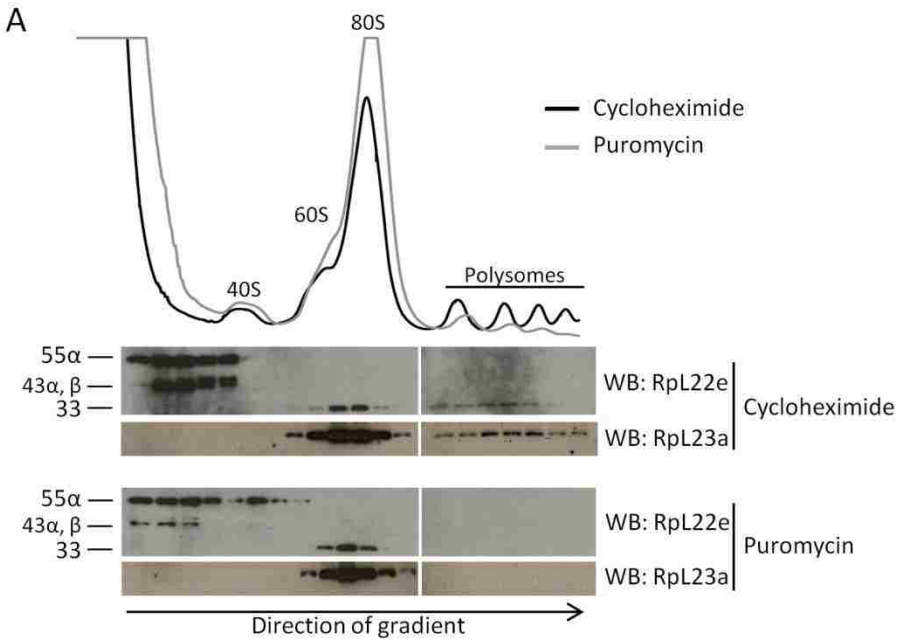
A
80S
60S
40S
Polysomes
Cycloheximide
Puromycin
55α
43α, β
33
WB: RpL22e
WB: RpL23a
Cycloheximide
55α
43α, β
33
WB: RpL22e
WB: RpL23a
Puromycin
Direction of gradient

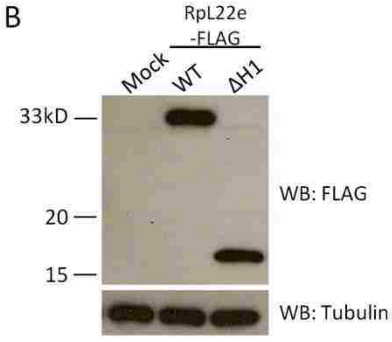
B
RpL22e
-FLAG
Mock
WT
ΔH1
33kD
20
15
WB: FLAG
WB: Tubulin

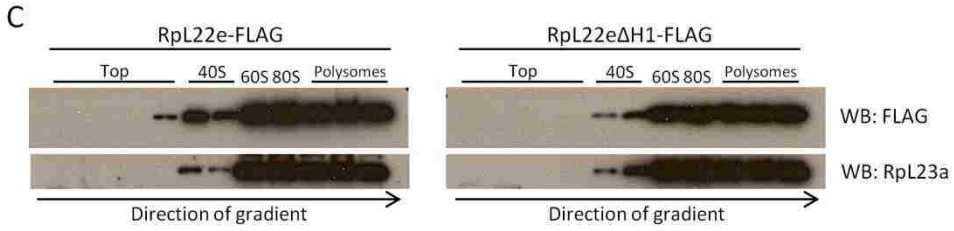
C
RpL22e-FLAG
Top
40S
60S 80S
Polysomes
RpL22eΔH1-FLAG
Top
40S
60S 80S
Polysomes
WB: FLAG
WB: RpL23a
Direction of gradient
Direction of gradient

Figure 3.11. Modified RpL22e does not co-sediment with the translation machinery. A) S2 cell extracts were separated in a 10-50% buffered sucrose gradient for polysome analysis to assess RpL22e co-sedimentation with ribosomal subunits, 80S monosomes, and polysomes. In cells treated with the elongation inhibitor cycloheximide, all modified RpL22e (43α, β and 55α) accumulates at the top of the gradient, and only the unmodified 33kD RpL22e co-sediments with the 60S large subunit, 80S monosomes, and polysomes. Treatment with the chain terminator puromycin (causing a disruption of polysomes and accumulation of 80S monosomes) shifts the immunodetection pattern of unmodified RpL22e from polysomes to monosomes. Endogenous RpL23a was used was a positive control. B) Deletion of fly-specific histone H1-like domain that harbors five putative SUMOylation motifs (ΔH1; residues 176-299) results in stable protein in S2 cells. Full length (residues 1-299) is represented as WT. Tubulin was used as a loading control. C) Polysome analysis of S2 cells expressing RpL22e-FLAG (full length) or RpL22eΔH1-FLAG shows an equal distribution pattern, as both were found to co-sediment with the translation machinery. Endogenous RpL23a was used as a positive control. Similar deletion experiments for RpL22e-like also show the histone H1-like domain is non-essential for RpL22e-like ribosome incorporation (Figure 6.3).

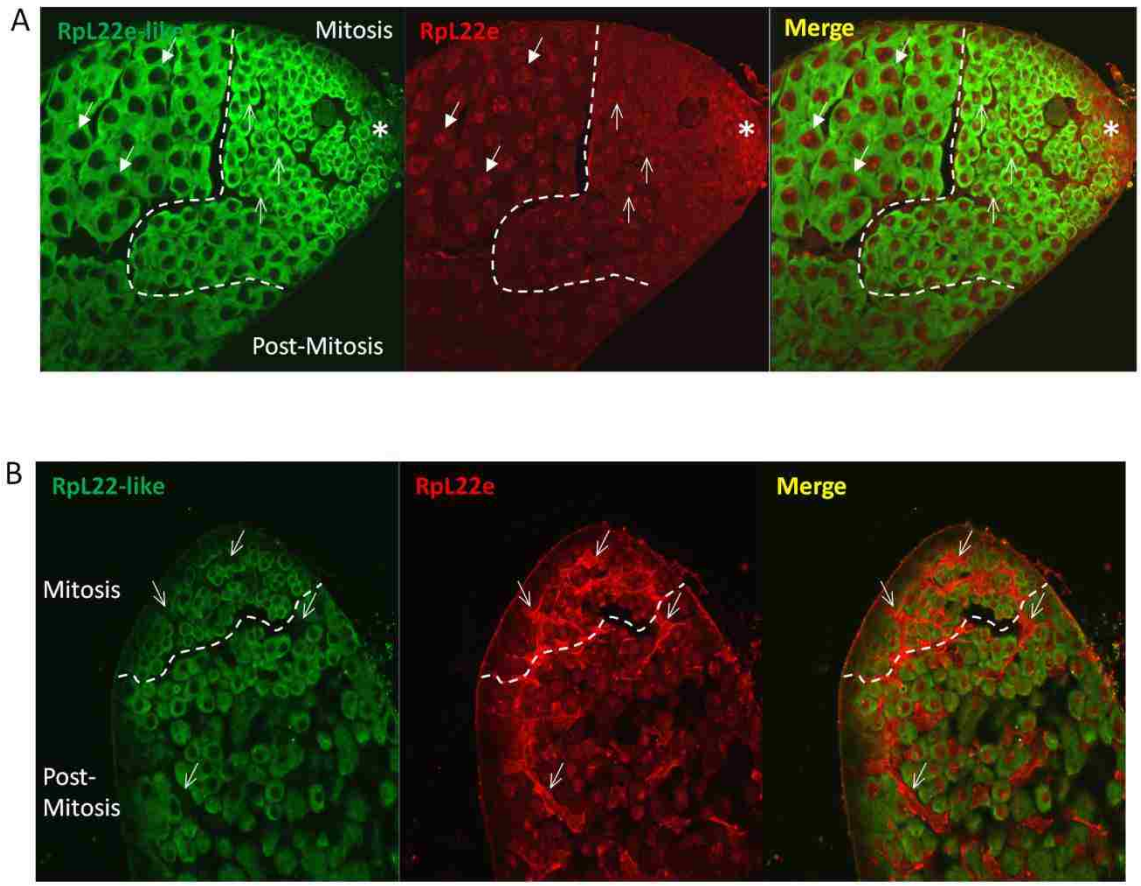

Figure 3.12. RpL22e family members are differently localized in the male germline. A) The mitotic and post-mitotic germline are separated by a dashed line. Mitotic spermatogonia are proximal to the apical tip (asterisk), where germline stem cells are located and germline development begins. Post-mitotic primary spermatocytes (will further develop and enter meiosis I) are found distal to the apical tip. Immunofluorescence (used to localize RpL22e family members) reveals distinct localization patterns in the male germline. RpL22e-like-PA (green) is primarily cytoplasmic, which some subnuclear accumulation (presumably in the nucleolus) in mitotic germ cells. Strong cytoplasmic localization is seen meiotic spermatocytes.

RpL22e (red) is primarily distributed in the nucleus. A punctate RpL22e localization is seen in the mitotic germline (open arrow), but becomes more nucleoplasmic in post-mitotic cells (closed arrow). Co-localization is only seen in the nucleus (presumably in the nucleolus) in mitotic spermatogonia (open arrows, merge). B) RpL22e (red) is also detected in somatic cyst cells (arrow) that surround spermatogonial cysts. RpL22e-like-PA (green) is a distinct germline marker. Although the anti-RpL22e-like Ab detects both spliced isoforms (-PA and -PB), staining intensity is consistent with the relative accumulation of RpL22e-like-PA (based on Western analysis) compared to RpL22e-like-PB in the testis (Kearse *et al*., 2011). RpL22e-like-PA is far more abundant (~10,000X) than RpL22e-like-PB in the testis (Kearse *et al*., 2011).

A

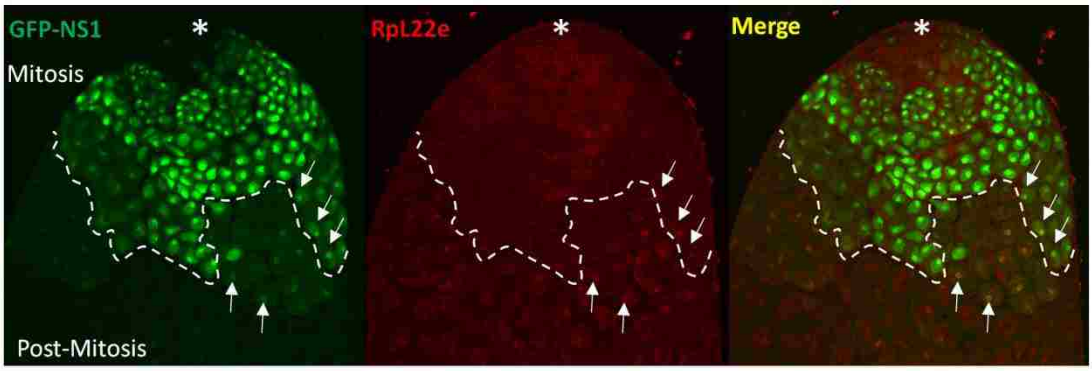
GFP-NS1
Mitosis
Post-Mitosis
RpL22e
Merge

B

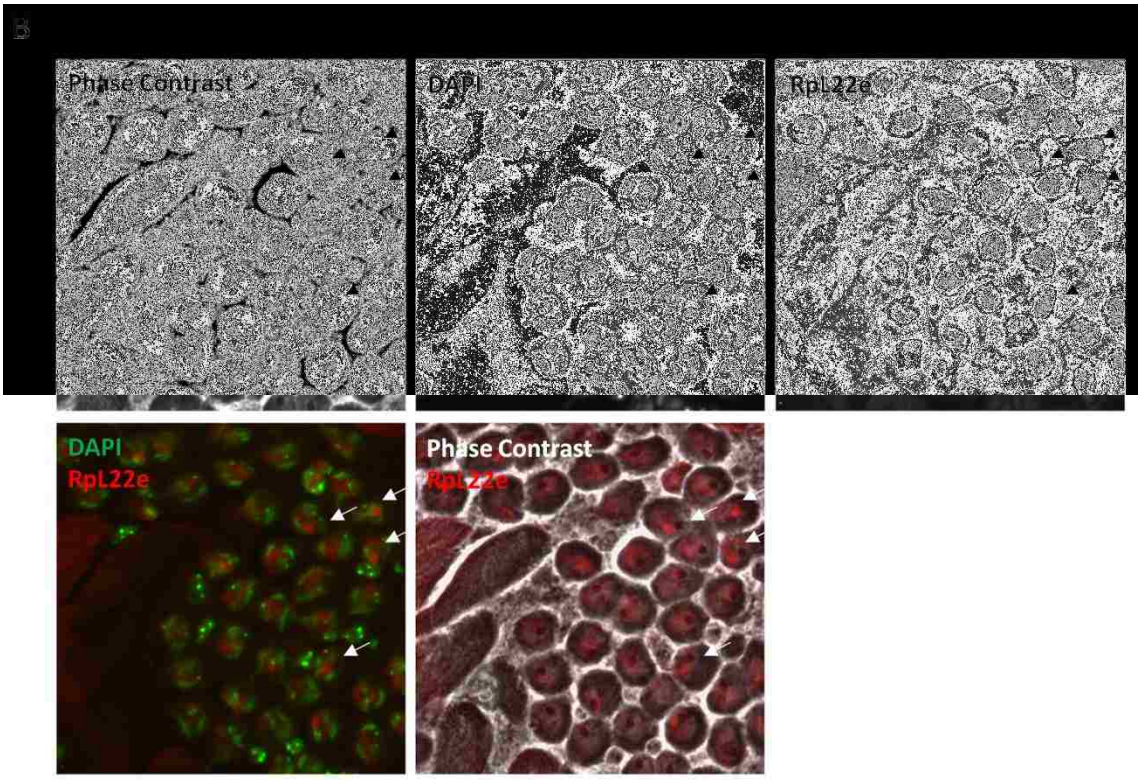
Phase Contrast
DAPI
RpL22e
DAPI
RpL22e
Phase Contrast
RpL22e

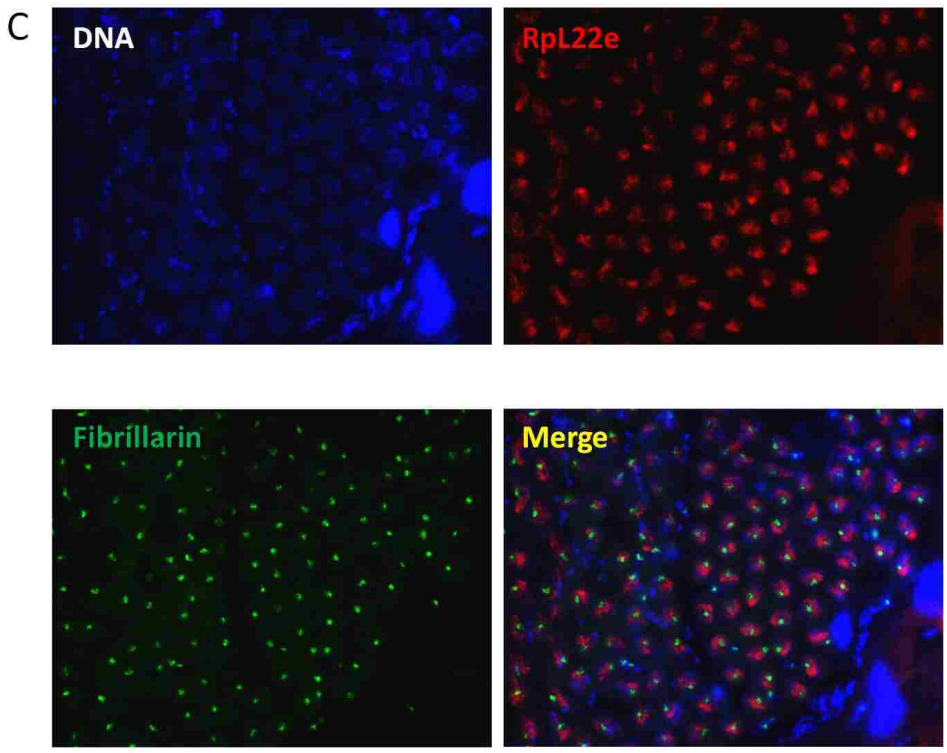

Figure 3.13. RpL22e co-localizes with nucleolar markers in mitotic spermatogonia, but not in mature meiotic spermatocytes. A) GFP-tagged Nucleostemin1 (GFP-NS1) was expressed *in vivo* in the early germline using the germline-specific *bam*-GAL4-VP16 driver. Co-localization of GFP-NS1 (green) nucleolar foci with RpL22e (green) subnuclear immunostaining is evident in mitotic spermatogonia and early primary spermatocytes (arrows). Mitotic spermatogonia are proximal to the apical tip (asterisk), where germline stem cells are located and germline development is initiated. Post-mitotic primary spermatocytes are found distal to the apical tip. B) Phase contrast and immunohistochemistry of mature meiotic primary spermatocytes shows juxtaposition, but not co-localization, of the phase dark nucleoli and RpL22e (red) immunolocalization

(arrows). DAPI staining (green) was used to confirm nuclear co-localization. C) Co-immunolocalization of the nucleolar marker fibrillarin (green) and RpL22e (red) in mature meiotic primary spermatocytes confirms RpL22e is nucleoplasmic, not nucleolar. DAPI staining (blue) was used to confirm nuclear co-localization.

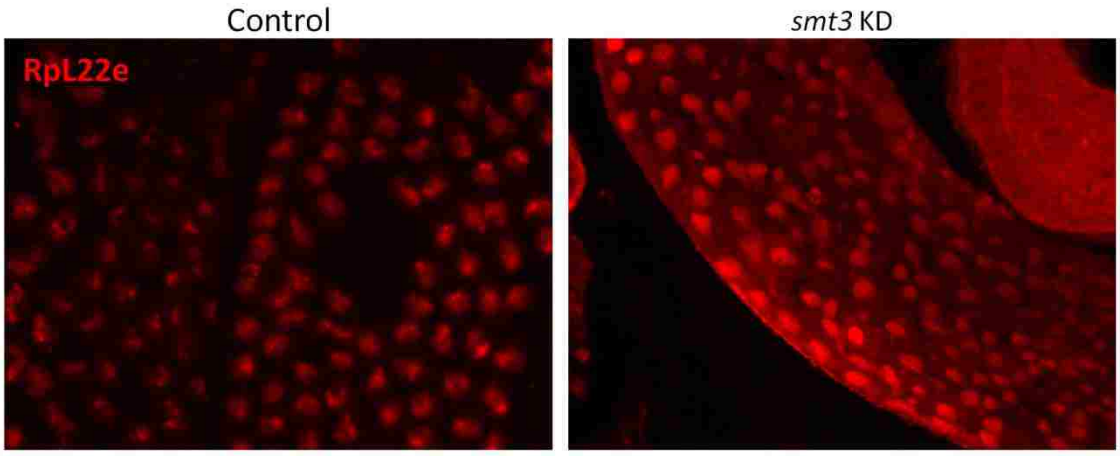

Figure 3.14. RpL22e localization in mature spermatocytes is sensitive to SUMO levels. *In vivo* knockdown of SUMO (*smt3*) was achieved by expressing a miR1 RNA cassette targeting *smt3* (Figure 3.10C). Nucleoplasmic RpL22e immunolocalization (red) in mature meiotic spermatocytes is generally widespread as a result of the *smt3* knockdown, as compared to control tissue where the RpL22e nucleoplasmic pattern is more punctate.

Description	Consensus Motif	Motif in RpL22e	Residues
GSK3 phosphorylation site	...([ST])...[ST]	KKVSLRFT LRFTIDCT NNVTFERS	187-194 191-198 230-237
Main preference for PKA-type AGC kinase phosphorylation	[RK][RK].([ST])[^P]..	KKASEAA KKVSLRF KKNSLRD	54-60 187-193 263-269
Secondary preference for PKA-type AGC kinase phosphorylation	.R.([ST])[^P]..	LRFTIDC FRISSND	191-197 286-292
Site phosphorylated by the Polo-like-kinase	.[DE].([ST])[ILFWMVA]..	AEDSIMD	201-207
Proline-Directed Kinase	...([ST])P..	AASTPAA	120-126
Strong SUMOylation motif	[VILMAFP](K).E	GKVE PKAE	38-41
Weak SUMOylation motif	[GAVILMAFP](K).E	GKVE	33-36
Inverted SUMOylation motif	[DE].(K)[AVILMAFP]	EKKA DVKA DAKA	21-24 62-65 102-105

Description	Consensus Motif	Motif in RpL22e-like-PA	Residues
CK1 phosphorylation site	S..([ST])...	SSQTQKK SLATPAN	2-8 162-168
CK2 phosphorylation site	...([ST])..E	AKVTPVE	27-33
GSK3 phosphorylation site	...([ST])...[ST]	KNASKAKS AKVTPVET PVETATPS KAKSVKKS DQVTFERT FERTKNFS VVSTAKDT AKDTFAMT	8-15 27-34 31-38 155-162 231-238 235-242 275-282 279-286
(ST)Q motif which is phosphorylated by PIKK family members	...([ST])Q..	SSQTQKK	2-8
Main preference for PKA-type AGC kinase phosphorylation	[RK][RK].([ST])[^P]..	KKKSAPP KKVSLRD	107-113 265-271
Proline-Directed Kinase	...([ST])P..	AKVTPVE ETATPSA SLATPAN	27-33 33-39 162-168
Strong SUMOylation motif	[VILMAFP](K).E	PKAE	144-147
Inverted SUMOylation motif	[DE].(K)[AVILMAFP]	DQKL	75-78

Table 3.1. Post-translational modification motifs predicted by Eukaryotic Linear Motif scanner found in the *Drosophila* RpL22e family. Amino acid sequences used were obtained from Flybase.org: RpL22e (FBgn0015288; FBpp0070143), RpL22e-like-PA (FBgn0034837; FBpp0071958). Nomenclature follows ELM, but is derived by Aasland et al. (2002). Weak and inverted SUMOylation motifs were expanded by results published by Matic et al. (2010). ELM (http://elm.eu.org/) is publically available.

Chapter 4:

RpL22e paralogues are unequally required *in vivo*

4.1 Introduction

Duplicated ribosomal protein (Rp) genes are found throughout eukaryotic genomes, including yeast (Wapinski *et al*., 2010), plants (Barakat *et al*., 2001; Whittle and Krochko, 2009), flies (Marygold *et al*., 2007) and to a much lesser extent, mice (Sugihara *et al*., 2010) and humans (Lopes *et al*., 2010). Additionally, the human genome contains >2,000 Rp pseudogenes (Zhang *et al*., 2002; Tonner *et al*., 2012; Balasubramanian *et al*., 2009). High conservation between paralogues suggests a common role as a component of the translation machinery, but relaxed selective pressure on the duplicated gene will allow for divergence and subsequently, for the possible development of new functions that are not limited to translation.

Interestingly, recent work has shown that certain duplicated Rps in plants (Whittle and Krochko, 2009), flies (Kearse *et al*., 2011), and mammals (Lopez *et al*., 2010; Sugihara *et al*., 2010) are expressed in a tissue-specific manner. Studies in yeast have shown significant differences in phenotypes between Rp paralogue knockout strains containing highly identical paralogous genes, leading authors to suggest a 'ribosome code' (Komili *et al*., 2007). Similar to the histone code, ribosome composition—mainly due to heterogeneity in Rps from duplicated genes—may provide a new level of gene regulation (Komili *et al*., 2007). Recently, Xue and Barna (2012) have similarly proposed

"specialized ribosomes." Ribosome heterogeneity derived from rRNA and variable/specific expression of Rp genes and Rp paralogues, along with post-translational modification may lead to an intrinsic layer of gene regulation previously unappreciated, as unique ribosomes may translate a set of mRNAs selectively (Xue and Barna, 2012). Diseases or phenotypes associated with disruption of Rp (or Rp paralogue) expression may allow for better understanding of this new proposed facet of gene regulation.

Ribosome-related diseases—termed "ribosomopathies"—have been increasingly studied in recent years and are associated with various steps of rRNA maturation, Rp expression, and subunit assembly (reviewed by Narla and Ebert, 2010). Interestingly, many Rp genes are associated with tissue-specific phenotypes. The Minute phenotype in *Drosophila*—characterized by prolonged development, low fertility and viability, altered body size and abnormally short, thin bristles on the adult body—is closely linked to many Rp genes (Lambertsson *et al*, 1998; Marygold *et al*., 2007). Multiple small and large subunit Rp genes are associated with Diamond-Blackfan anemia and other blood-related human genetic diseases (Boria *et al*., 2010; Narla and Ebert, 2010). Mutations in many zebrafish Rp genes leads to malignant peripheral nerve sheath tumors (Amsterdam *et al*., 2004; Lai *et al*., 2009). Mammalian models also support a tissue-specific sensitivity for some Rp genes. Mouse *rpL28* has a highly specific expression pattern in embryos leading to unique developmental defects when deleted (Kondrashov *et al*., 2011). While mechanisms are still yet to be determined, a strong link exists between certain cell- and tissue-specific diseases and Rps. Further investigation of Rp paralogues is therefore

warranted and may be crucial to provide insight into how Rps may have a tissue-specific, developmental, or conditional (e.g. spatial-temporal, environmental cues) role in gene regulation.

The eukaryotic-specific RpL22e family consists of two members in *Drosophila melanogaster*: the ancestral gene *rpL22e* and the duplicated gene *rpL22e-like* (Flybase.org: Crosby *et al.*, 2007). We have previously reported the tissue-specific expression of *rpL22e-like* in the adult male germline (Kearse *et al*., 2011, 2013 *in review*). *In situ* hybridization shows *rpL22e-like* mRNA in pole cells, embryonic gonads, and stomatogastric nervous system in developing embryos (Shigenobu *et al*., 2006). The ancestral *rpL22e* gene has a ubiquitous expression profile in embryos (Shigenobu *et al*., 2006; Crosby *et al*., 2007) and in larval (Crosby *et al*., 2007) and adult stages of both males and females (Crosby *et al*., 2007, Kearse *et al*., 2011).

Drosophila rpL22e is an X-linked gene, shown to be essential *in vivo* (Bourbon *et al*., 2002) and in S2 tissue culture cells (Boutros *et al*., 2004). However, *rpL22e* is non-essential for translation *in vitro* (rat; Lavergne *et al*., 1987), yeast (Deutschbauer *et al*., 2005), and mice (Anderson *et al*., 2007), but is essential in the nematode *C. elegans* (Kamath *et al*., 2003). Whether or not the duplicated *rpL22e-like* is also essential is not known. Although disruption of *rpL22e-like* expression in embryonic pole cells and gonad expression may only impact germline development and fertility, expression of *rpL22e-like* in the somatogastric nervous system during embryonic development may be

more significant for embryonic viability. A P-element transposon insertion 156 nucleotides upstream of the transcription start site of *rpL22e-like* is homozygous lethal while heterozygous males and females that reach adulthood are fertile. Whether this insertion lies within regulatory elements of *rpL22e-like* or other *cis*-elements remains unexplored, but the lack of annotated genes near this insertion site suggests the gene is essential (closest genes are 2.5 Mb downstream and 15.4 Mb upstream; FlyBase.org).

In this report, we utilize *in vivo* paralogue-specific RNAi depletion of *rpL22e* and *rpL22e-like* to test the requirement for these paralogues in *Drosophila* development, spermatogenesis, and fertility.

4.2 Results

rpL22e, but not *rpL22e-like,* is essential in the fly

Using the UAS-GAL4 binary system, we tested the requirement of *rpL22e* and *rpL22e-like* separately in *Drosophila* development by expressing inverted repeats (IR) forming shRNA to drive RNAi. Homology between the *RpL22e* paralogues is lowest at the 5' end of the coding sequence (Kearse *et al*., 2011), allowing for separate targeting by RNAi. Hereafter, the *rpL22e* RNAi line is referred to RpL22e.IR and the *rpL22e-like* RNAi line is referred as RpL22e-like.IR. As the most appropriate genetic control available, we obtained a GFP expressing line that harbors the identical expression construct backbone as our developed RNAi lines, all of which have been integrated at the attP2 locus on chromosome 3. To test whether each *rpL22e* paralogue is essential for development, we compared the F1 ratios between the genetic control, RpL22e.IR, and RpL22e-like.IR when crossed with *Act*-GAL4 for ubiquitous knockdown. F1 progeny carrying both UAS-GAL4 elements (unbalanced) are distinguished from other F1 progeny by the absence of dominant wing markers (*CyO* and *TM3*, *Ser*).

We hypothesize that ubiquitous knockdown of *rpL22e* is lethal, as it has been reported by P-element gene disruption (Bourbon *et al*., 2002) and by RNAi in S2 cells (Boutros *et al*., 2004) that *rpL22e* is an essential gene. Our data show that ubiquitous knockdown of *rpL22e* in *Drosophila* is lethal, as F1 males or females harboring both the RpL22e.IR and GAL4 elements (unbalanced F1) were not found (Figure 4.1A), confirming that *rpL22e* is

an essential gene in males and females. We suspect that *rpL22e* depletion is embryonic lethal, as an accumulation of non-developing larva or pupae was not evident.

Whether *rpL22e-like* is also essential has not been thoroughly investigated. FlyBase reports that a P-element insertion 156 nucleotides upstream of the *rpL22e-like* transcription start site is homozygous lethal, suggesting that *rpL22e-like* is essential. We tested this by ubiquitous knockdown of *rpL22e-like* using the *Act*-GAL4 driver. Our results show that *rpL22e-like* is dispensable *in vivo*. *Act*>RpL22e-like.IR adult F1 ratios are comparable to the genetic control (Figure 4.1A) The *CyO* balancer and a genotype harboring both elements necessary for knockdown (UAS.IR and GAL4; seen as unbalanced) segregated equally between males and females (Figure 4.1A) in the expected developmental time frame. To confirm knockdown, we analyzed protein levels of RpL22e-like in control and *Act*>RpL22e-like.IR testis tissue. Western analysis shows a significant reduction (~60% KD) in RpL22e-like protein levels in F1 *Act*>RpL22e-like.IR testes compared to the control (Figure 4.1B). Therefore, we conclude that *rpL22e-like* is dispensable in males and females. Whether the P-element insertion upstream of *rpL22e-like* transcription start site affects other *cis*-regulatory elements still remains to be determined, but our data suggest the associated lethality is unlikely to be due to an impact on *rpL22e-like*.

Taking these data together, we conclude there is an unequal requirement for *rpL22e* paralogues in *Drosophila* developmental; *rpL22e*, but not *rpL22e-like*, is dispensable for male and female development.

Depletion of RpL22e-like does not permanently impair sperm development and fertility

We have previously reported that RpL22e-like expression is primarily restricted to the male germline and is part of the active translation machinery (Kearse *et al*., 2011). Whether *rpL22e-like* is required for male germline development and fertility is unknown. Furthermore, recent work (Kearse *et al*., 2013, *in review*) has shown RpL22e undergoes extensive post-translational modification and is primarily localized to the nucleoplasm in meiotic spermatocytes, suggesting a role outside of translation in this cell type. To test the requirements of each paralogue in germline development (spermatogenesis) and fertility, we used the germline-specific *bam*-GAL4-VP16 driver (Chen and McKearin, 2003) for germline-specific RNAi knockdown.

Western analysis of testis tissue from *bam*>RpL22e-like.IR tissue compared to control shows significant reduction (~80% KD) of RpL22e-like protein levels, confirming knockdown (Figure 4.2A).

On the other hand, Western analysis shows that *rpL22e* knockdown with *bam*-GAL4-VP16 is less significant, as only minimal reduction of the predicted molecular weight,

unmodified RpL22e is seen compared to control (Figure 4.2B). Similar knockdown patterns are seen for both genes with a second germline-specific driver is used, *nos*-GAL4 (data not shown). Additionally, qRT-PCR shows no significant change in testis *rpL22e* mRNA levels with *bam*-GAL4-VP16 driven knockdown of *rpL22e* compared to control (data not shown). We suspect the minimal *rpL22e* knockdown is due to the restricted expression pattern limited to the early mitotic germline of the two germline specific GAL4 drivers (*bam*-GAL4 and *nos*-GAL4; White-Cooper, 2012). This conclusion is further supported by the minimal knockdown results when using an independently developed second-generation *rpL22e* RNAi line (designated as VAL20-RpL22e miR1 RNAi) that uses a miR1 scaffold for increased RNAi knockdown (used with *bam*-GAL4-VP16; Figure 4.2C). Other testis-specific GAL4 drivers with various expression profiles are available, but are not specific to the germline alone (Hrdlicka *et al*., 2002; Bunt *et al*., 2012); therefore, these GAL4 drivers would not be useful to compare paralogue requirements in the developing germline. Additionally, significant levels of modified RpL22e accumulate in the testis, suggesting that protein turnover rates of modified RpL22e may significantly affect the efficiency of RNAi knockdown effect in this tissue. To further investigate the role of *RpL22e* in the male germline, genetic mosaics would provide the opportunity to tract individual cysts lacking a functional *rpL22e* gene. This approach, however, is beyond the scope of this report.

As a result of the small amount of *rpL22e* knockdown, we therefore have focused on exploring the requirement of *rpL22e-like* in the male germline. Various levels of severity

are seen in testis-specific gene mutations, disruptions, deletions, or knockdown with phenotypes characterized by the impact on germline development. In *aly*, *can*, *mia* or *sa* mutants, spermatocytes arrest in the G2/M transition of meiosis I with partial chromosome condensation, accumulating enlarged post-mitotic spermatocytes (Lin *et al*, 1996). Sperm individualization defects are also evident and are associated with *soti* mutations (Barraeu *et al*., 2010; Kaplan *et al*., 2010) and *Gld2* knockdown (Sartain *et al*., 2011). In addition, some mutations in testis-specific or -enriched genes are associated with accumulating apoptotic (*aya* and *sa*; Fabrizio *et al*., 2003) and degenerating, necrotic cells (*comr*; Jiang and White-Cooper, 2003).

Examining testes from *bam*>RpL22e-like.IR F1 males, the complete line of spermatogenic cells is seen. Phase contrast microscopy shows complete male germline development with the presence of long individualized sperm in *rpL22e-like*-depleted tissue (Figure 4.3). To assess if *rpL22e-like* knockdown has an impact on male reproduction, we assayed for sperm motility and fertility. Motile sperm were seen in all F1 males tested (Table 4.1), showing the presence of sperm that should be competent for fertilization and also confirming complete germline development. We then assayed individual F1 males for their ability to mate and fertilize eggs from wildtype females. No differences were seen in the percentage of fertile *rpL22e-like* depleted males compared to controls (Table 4.1).

Taking these data together, we conclude that depletion of *rpL22e-like* (~80% KD) is dispensable in the male germline and does not have a longstanding impact on sperm maturation or fertility. Preliminary immunohistochemical analysis of *rpL22e-like* depleted tissue shows the possibility that a small proportion of mitotic cysts are disrupted (data know shown); however, further investigation is needed to confirm and characterize the observed cysts. Nevertheless, *rpL22e-like* depletion in the male germline has no overall impact on male germ cell development or fertility.

Individual germline depletion of the *rpL22e* family members alters the expression levels of their paralogues.

To explore possible compensatory mechanisms or to determine if RpL22e acts to rescue the germline from the effect of *rpL22e-like* knockdown, we assessed RpL22e expression levels in *rpL22e-like* RNAi-depleted tissue (knockdown seen in Figure 4.2A). Interestingly, RpL22e protein levels at all molecular weights (although at varying amounts) increase in RpL22e-like depleted tissue when compared to the control (Figure 4.4A). Notably, the unmodified 33kD (known to be in polysomes in S2 cells; Kearse *et al*., 2013, *in review*) and 55kD (SUMOylated and phosphorylated; Kearse *et al*., 2013, *in review*) RpL22e species are the most upregulated. However, RpL23a levels are not altered (Figure 4.4A), suggesting a specific effect rather than a global increase in ribosomal protein expression.

To further characterize this effect, we analyzed *rpL22e* mRNA levels to determine if the increase in RpL22e protein level correlates with an increase in mRNA level. Increased mRNA levels would suggest an increase in gene transcription and/or an increase in mRNA stability. Steady mRNA levels would suggest regulation at a post-transcriptional level. qRT-PCR shows a statistically significant 31% increase (average) in testis *rpL22e* mRNA levels when *rpL22e-like* is depleted in the male germline when compared to control (Figure 4.4B), suggesting an increase in gene transcription and/or mRNA stability.

To determine if a similar effect is also seen when *rpL22e* is targeted for RNAi knockdown, we assessed the levels of endogenous RpL22e-like protein and mRNA when *rpL22e* is targeted for RNAi knockdown to see if. Although we conclude *rpL22e* knockdown is inefficient in the testis (Figure 5.2B-C), Figure 4.5A shows a marked decrease in testis RpL22e-like compared to control when *rpL22e* is targeted for knockdown. However, *rpL22e-like* mRNA levels remain constant, suggesting regulation at a post-transcriptional level (e.g. translation) (Figure 4.5B).

4.3 Discussion

rpL22e paralogues are not equally required for viability or for male germline development

Many Rp genes contain snoRNAs within their introns. As is the case with *rpL22e*, the locus contains two snoRNAs (Ψ18S-531 and Ψ28S-2179) nested within the second intron. Additionally, a ncRNA (CR42491) of unknown function is located within the *rpL22e* locus (FlyBase.org). P-element disruption of *rpL22e* (within intron 1) is reported as homozygous lethal (Bourbon *et al*., 2002; Flybase.org). It is unknown whether the P-element insertion results in a transcriptionally silent or altered locus, but if so, snoRNAs Ψ18S-531 and Ψ28S-2179, as well as ncRNA CR42491 levels would be compromised. Consequently, phenotypes associated with the P-element disruption may not be properly assigned for the *rpL22e* gene itself, but rather the associated ncRNAs. Our RNAi data support the conclusion that the *rpL22e* gene is essential for *Drosophila* development, as mature mRNAs targeted for RNAi knockdown are targeted in the cytosol. snoRNAs and the ncRNA processed from intron 2 in the nucleus would remain unaltered by RNAi targeting in the cytosol.

Why *rpL22e* is only essential in the fly and in *C. elegans* remains to be investigated. The lack of conservation of its requirement for viability in other organisms may suggest that the gene provides an additional function outside of its known function as an Rp. We have previously shown that fly RpL22e undergoes extensive post-translational modification, including SUMOylation and phosphorylation, and localizes to the

nucleoplasm of primary spermatocytes in the male germline – the latter, suggesting a role outside of translation (Kearse *et al*., 2013, *in review*). Although the nature of the extra-ribosomal function remains to be determined, it is possible that this auxiliary function in other cell types and tissues is required for *Drosophila* development. Additionally, *Drosophila* RpL22e harbors a fly-specific N-terminal extension of unknown function, but is homologous to the C-terminus of histone H1 (Koyama *et al*., 1999). Interestingly, our previous work has shown that deleting this N-terminal domain does not hinder incorporation of the residual, truncated protein into functional ribosomes (Kearse *et al*., 2013, *in review*), leading to the interpretation that this fly-specific extension is neither required for assembly into ribosomes or for ribosome function. The N-terminal extension may therefore support the proposed extra-ribosomal role of RpL22e. Whether this domain is essential for *Drosophila* development remains to be determined, but may provide an explanation as to why RpL22e is essential in the fly.

Our data also show RpL22e-like is dispensable for *Drosophila* development and does not perturb germline development when depleted ~60% and ~80%, respectively. This leads to the interpretation that RpL22e-like may be dispensable in the male germline or that the levels of RpL22e-like that remain after RNAi depletion are sufficient to sustain germline development. Finding that *rpL22e* mRNA and protein levels increase with RNAi depletion of *rpL22-like* provides preliminary support that RpL22e could be responding to the reduced level of RpL22e-like in the germline, acting to rescue translation (further discussion below). Nevertheless, it is clear from our data that a significant amount of

RpL22e-like can be depleted from the male germline without a lasting impact on germline development, sperm motility, or fertility.

Knockdown of both paralogues (double knockdown) would provide insight into whether an RpL22e paralogue is essential in the germline; however, knockdown of *rpL22e* using germline-specific *nos*-GAL4 or *bam*-GAL4-VP16 was inefficient (see Chapter 6.7). We are confident that our RNAi stock works well as our ubiquitous knockdown (*Act*-GAL4) confirms that *rpL22e* gene is essential. The FLP/FRT recombination system (described by Theodosiou and Xu, 1998) could be used to generate genetic mosaics in which a set of cells (in this case, a developing spermatogonia) is homozygous for a non-functional *rpL22e* with the remaining cells and tissues being heterozygous. Alternatively, developing new germline-specific GAL4 lines with more wide-spread expression in the male germline may provide new tools to revisit *rpL22e* knockdown.

Coordinated gene expression of the *rpL22e* paralogues

In yeast, ~70% of yeast duplicated Rp genes are asymmetrically expressed and are generally regulated to maintain the expression ratio, rather than the dose of Rps (Parenteau *et al*., 2011). Whether this regulatory pattern is similar in higher eukaryotes remains to be determined. Parenteau *et al*. (2011) has determined that yeast RpL22e paralogues (84.4% sequence identity and 95.6% sequence similarity; Nakao *et al*., 2004) display intergenic intron-dependent regulation (e.g. the intron of RpL22eA regulates the expression of RpL22eB, and vice versa). Furthermore, deleting the introns from both

genes leads to increased expression of both paralogues at a level of 2-6 fold (Parenteau *et al*., 2011). Coordinated gene expression between RpL22e paralogues is clearly evident in yeast, but whether this is similar in *Drosophila* or higher eukaryotes has not been investigated. In *Drosophila*, testis-specific (or testis-biased) genes with paralogues are often coordinated in *Drosophila* (Mikhaylova *et al*., 2008), but specific mechanisms remain to be determined.

Our knockdown experiments show that *rpL22* gene expression increases when *rpL22e-like* is depleted in the male germline. Stable RpL23a protein levels maintained in this experiment support a specific RpL22e paralogue effect, rather than a global increase in Rp synthesis. Additionally, endogenous RpL22e-like levels were decreased upon *rpL22e* knockdown (mRNA levels remained constant). Whether or not RpL22e paralogues can bind their own mRNA or the opposing paralogue mRNA has not been investigated, but this may provide insight into the mechanism(s) by which paralogue expression levels are regulated. Additionally, paralogue overexpression (see chapter 6.6 for preliminary data) and expression of paralogue mutations (including deletions) may give further insight into regulatory mechanisms controlling coordinated expression and protein domains involved in this regulatory response, respectively.

Our previous work has shown that RpL22e may be assembled into ribosomes within mitotic germ cells, but may have a role outside of active translation in maturing meiotic germ cells, based on its predominant localization to the nucleoplasm (Kearse *et al*., 2013,

in review). Additionally, we have shown that all unmodified RpL22e in S2 cells co-sediments with the translation machinery (Kearse *et al*., 2013, *in review*). Increased levels of unmodified RpL22e upon *rpL22e-like* depletion may be interpreted as RpL22e responding and serving as a ribosomal component to rescue translation, replacing RpL22e-like. If so, is there a selective advantage in *Drosophila* related to the expression of male-germline specific *rpL22e-like*? This remains unclear, however our data suggest that *rpL22e-like* is dispensable in the male germline, with no discernible negative impact on reproduction when depleted ~80%. Further investigation of the precise role of post-translationally modified RpL22e (Kearse *et al*., 2013, *in review*) will be crucial to determine if RpL22e assembles into ribosomes at specific stages of male germline maturation.

Alternatively, the increase in *rpL22e* expression upon *rpL22e-like* depletion could be a response based on shared regulatory elements for the two genes derived from gene duplication. Regulatory elements (genomic and mRNA) in the *rpL22e* gene family have not been reported in any model system. Rp promoter elements have been studied in *Drosophila*, but those for *rpL22e* paralogues or other Rp paralogues have not investigated (Ma *et al*., 2009). Eukaryotic Rp mRNAs, particularly in mammals, often contain 5'-TOP (5' terminal oligopyrimidine tract) regulatory elements that respond to cellular growth cues (Meyuhas, 2000) and have recently been identified as targets for miRNA regulation (Ørom *et al*., 2008). However, *Drosophila* Rp regulation through 5'-TOP motifs has not been thoroughly investigated (Qin *et al*., 2007). Exploring *cis*-regulatory

elements, shared or unique to each paralogue, may provide insight to the coordinated gene expression of the *rpL22e* paralogues.

4.4 Materials and Methods

Plasmid construction and injection

For RNAi, we utilized the pVALIUM10 strategy developed by the TRiP at Harvard Medical School (flyrnai.org). We thank the TRiP at Harvard Medical School (NIH/NIGMS R01-GM084947) for providing transgenic RNAi fly stocks and/or plasmid vectors used in this study.

Codons 1-100 were used to target RpL22e and RpL22e-like mRNAs separately because of lower homology at the N-terminus. Off target hits were ruled out of the selected targeted region by analysis with the SnapDragon dsRNA design tool provided by the TRiP. Construction followed a two-stage gateway cloning procedure provided by the TRiP. Briefly, the targeted regions were subcloned from cDNA (Kearse *et al*., 2011) into the directional entry vector pENTR/D-TOPO (Invitrogen). Sequences of selected clones were confirmed by Sanger sequencing and cloned into the designation vector pVALIUM10 (TRiP) using LR clonase (Invitrogen). Clones were selected and sequenced to confirm proper orientation and sequence. pENTR/D-TOPO and pVALIUM10 were propagated in TOP10 *E. coli* cells (Invitrogen) and ccdB Survival $T1^R$ *E. coli* cells (Invitrogen), respectively. TOP10 *E. coli* cells were used for all cloning steps.

Plasmid DNA was purified using the QIAGEN plasmid maxiprep kit and resuspended in sterile dH_20 for phiC3-integrase-mediated site-specific transgenesis. Plasmid DNA was injected into *y, v, nanos-integrase; attP2* embryos for integration into chromosome 3L.

Transgenics were selected, backcrossed, and balanced to homozygosity with *y v; Sb/TM3, Ser*. Injection and balancing was performed by Genetic Services and was funded by a National Academy of Science Grant-In-Aid of Research (G20100315152292) administrated by Sigma Xi to MGK.

Fly stocks

All stocks were kept at room temperature on standard cornmeal media. The *Act*-GAL4 driver (*y[1] w[*]; P{Act5C-GAL4-w}E1/CyO*), *nos*-GAL4 driver (*P{w[+mC]=UAS-Dcr-2.D}1, w[1118]; P{w[+mC]=GAL4-nos.NGT}40*) UAS-VAL10-GFP stock (*y[1] v[1]; P{y[+t7.7] v[+t1.8]=UAS-GFP.VALIUM10}attP2*), and VAL20-L22e RNAi stock (*y[1], sc[*], v[1]; P{TRiP.HMS00143}attP2*) were obtained from the Bloomington Stock Center. The *bam*-GAL4-VP16, UAS-Dicer2 (*y, w; bam-GAL4, UAS-Dicer2*) driver was a kind gift from Marina Wolfner (Cornell), but was originally developed by Dennis McKearin (Chen and McKearin, 2003). The RpL22e.IR line (*y[1], v[1]; pVALIUM10{UAS-RpL22e.IR} attP2/TM3, Ser)* was kept over the TM3, Ser balancer due to it being male sterile when homozygous. The RpL22e-like.IR line (*y[1], v[1]; pVALIUM10{UAS-RpL22e-like.IR} attP2*) could be propagated as a homozygous line without any noticeable effect on development or fertility.

Crosses

All RNAi crosses were set up at 27-29°C to achieve maximum GAL4 activity without inducing heat stress. In all cases unless noted (see sperm motility and fertility assays),

two 0-5 day males harboring the desired GAL4 driver were mated with four 0-5 day old virgin females harboring the desired UAS element. 0-1 day old F1 males were used for Western analysis and phase contrast microscopy. Western analysis, including antibody specifications, was completed as previously reported (Kearse *et al*., 2013, *in review*). For phase contrast microscopy, testes were dissected in 1X PBS and gently squashed with a cover slip and imaged with a Nikon Eclipse TE200U.

Sperm Motility and Fertility Assays

Crosses were set up at 27-29°C with two 3 day old males harboring GAL4 drivers and four 2-4 day old virgin females harboring desired UAS element. For assessing sperm motility, virgin F1 males were collected and kept isolated from females for three days before scoring sperm motility in gentle squashes and visualizing under standard phase contrast microscopy. Scoring was performed blindly.

Fertility assays were completed as previously described by Metzendorf and Lind (2010). Briefly, single three day old virgin F1 males (as describe above) were mated with three 2-4 day old virgin wildtype females at 25°C. After 15 days, vials were scored for larvae. Presence of larvae represents a fertile male. Crosses and analysis were performed blindly.

qRT-PCR

RNA isolation, cDNA preparation and qRT-PCR specifications were completed as previously described (Kearse *et al*., 2011). Expression levels were normalized to A*ct5C*. Primers used can be found in Table 4.2.

4.5 Figures and Tables

A

B

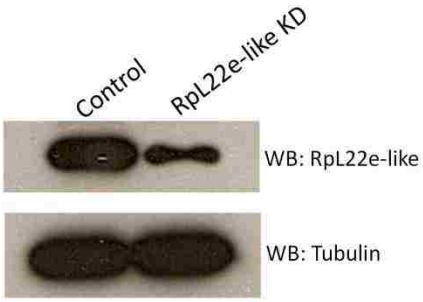

Figure 4.1. *rpL22e*, but not *rpL22e-like*, is essential for fly development. A) F1 progeny were scored to assess the impact of *rpL22e* paralogue knockdown on development. Equal representation of the CyO balancer and *Act*-GAL4 driver, as wells as similar female:male ratios, suggests *rpL22e-like* is dispensable for viability (left). The lack of F1 adults harboring *Act*-GAL4 and RpL22e.IR represented as unbalanced progeny (lacking the CyO and TM3 balancers) suggests *rpL22e* is an essential gene (right). F: Females; M: Males. B) Western analysis of testis tissue confirms *rpL22e-like* knockdown (*Act* > RpL22e-like.IR). Tubulin was used as a loading control.

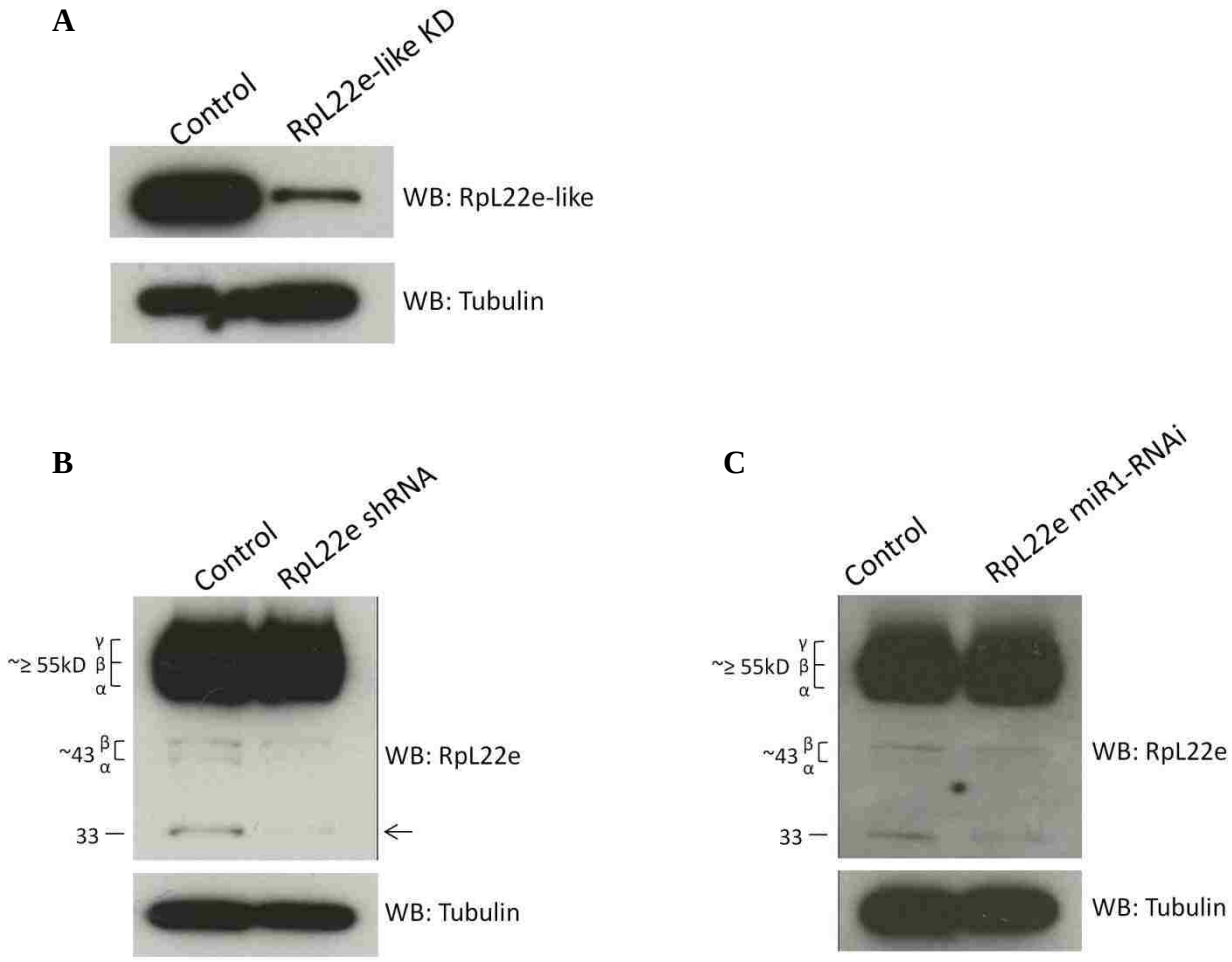

Figure 4.2. *rpL22-like*, but not *rpL22e*, can be depleted in the male germline with *bam*-GAL4-VP16. A) Western analysis confirms *rpL22e-like* knockdown in the male germline (*bam* > RpL22e-like.IR). B) Minimal knockdown (*bam* > RpL22e.IR) of testis RpL22e when targeted with shRNA. Significant reduction is only seen of the predicted MW/unmodified protein (arrow) when compared to control. Modified proteins (43-55kD) remain comparable to control. C) The second generation VALIUM20-RpL22e miR1 RNAi line utilizing a miR1 scaffold is inefficient with *bam*-GAL4-VP16 as testis RpL22e proteins levels are comparable to control. Tubulin was used as a loading control.

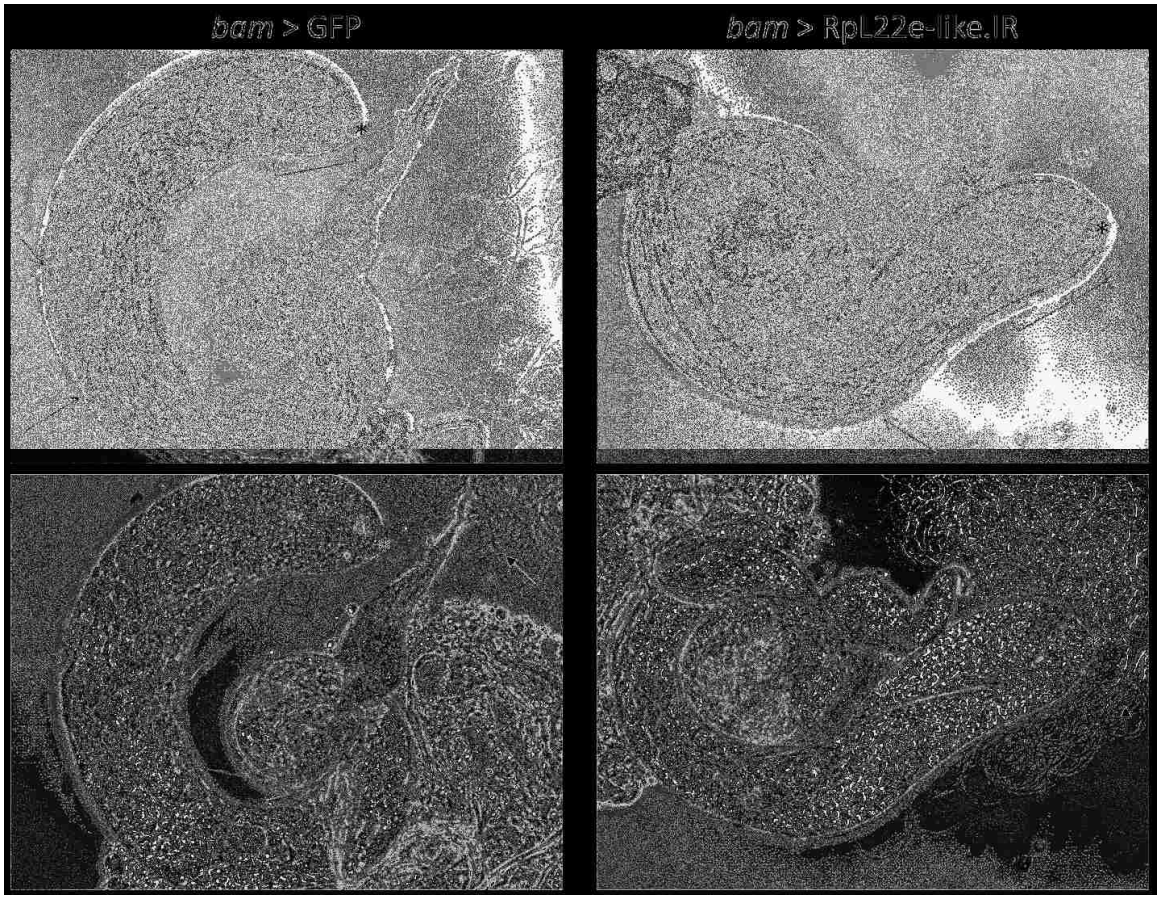

Figure 4.3. *rpL22e-like* depletion results in complete germline development. Phase contrast microscopy of light (top) and heavy (bottom) testis squashes shows the various stages of germline development in *rpL22e-like*-depleted tissue, including mitotic cells and primary spermatocytes (bracket), secondary spermatocytes (short open arrow), sperm bundles (long open arrow), and mature individual sperm (closed arrow). Asterisk denotes the apical tip, where germline stem cells are located and germline development begins. Images were taken at 10X magnification.

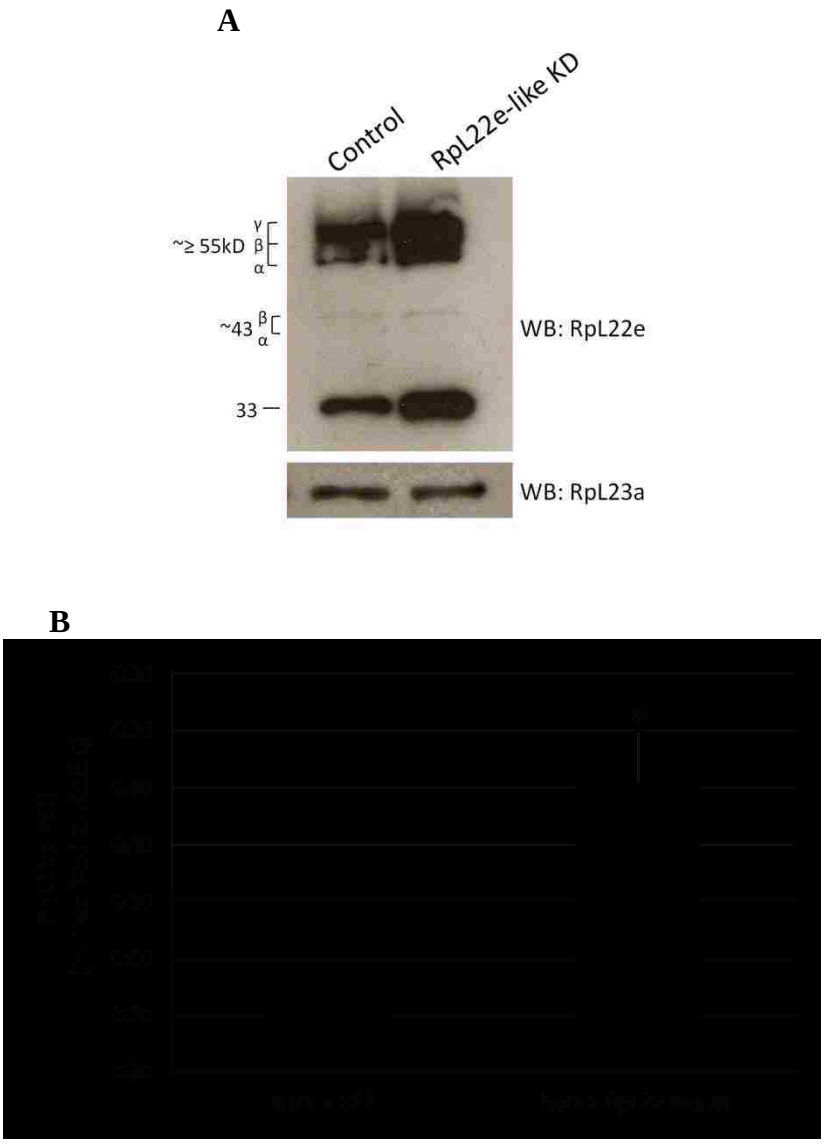

Figure 4.4. Testis *rpL22e* mRNA and protein levels increase in *rpL22e-like*-depleted tissue. A) An increase in testis RpL22e protein levels is seen when *rpL22e-like* is specifically depleted in the male germline (*bam*-GAL4-VP16; see Figure 4.2A for knockdown) when compared to control. Testis RpL23a levels remain constant. B) qRT-PCR shows a statistically significant increase (average : 31%; range: 17-47%) in testis *rpL22e* mRNA levels when *rpL22e-like* is depleted from the germline. Error bars represent standard error, n=3, *p<0.01

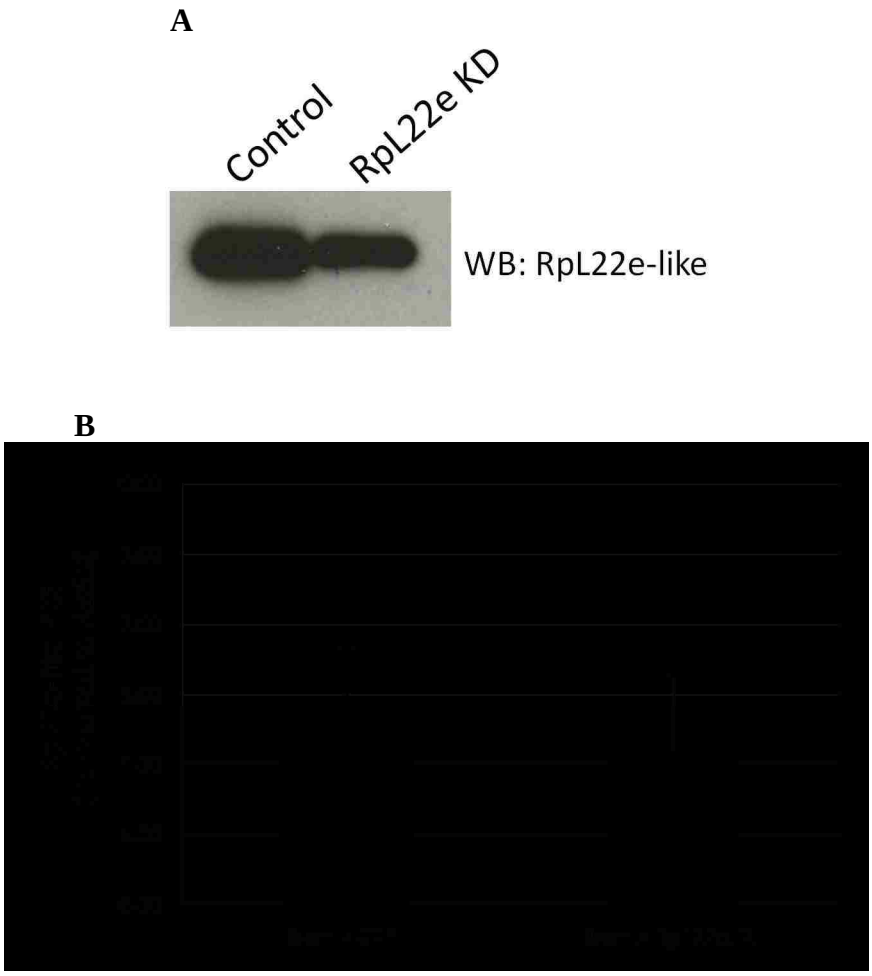

Figure 4.5. Germline knockdown of *rpL22e* alters RpL22e-like protein levels, but not mRNA levels. A) A decrease in testis RpL22e-like levels is seen when *rpL22e* is targeted for RNAi knockdown in the male germline (*bam*-GAL4-VP16; see Figure 4.2B for knockdown) when compared to control. B) qRT-PCR shows no statistical change in testis *rpL22e-like* mRNA levels compared to control. Error bars represent standard error, n=3.

Table 4.1. Assay of male reproductive health after *rpL22e-like* depletion.

F1	*n*	# males with motile sperm	% males with motile sperm		*n*	# fertile males	% fertile males
bam > GFP	40	40	100		49	48	98.0
bam > RpL22e-like.IR	40	40	100		49	47	95.6

Table 4.2. Primers used for qRT-PCR in Chapter 4.

Forward_Act5C	5’-GAGCGCGGTTACTCTTTCAC-3’
Reverse_Act5C	5’-GCCATCTCCTGCTCAAAGTC-3’
Forward_RpL22e	5’-TGCTGAGGATAGCATCATGG-3’
Reverse_RpL22e	5’-AAAAGTGAACGTCGGAGCTG-3’
Forward_RpL22e-like	5’-CAAAAAGAAGGCTTGGCAAC-3’
Reverse_RpL22e-like	5’-TCCTTCAGCTGGTTGAGCTT-3’

Chapter 5:

Summary, Conclusions and Future Directions

5.1 Summary and Conclusions

Gene duplication is a contributing factor of genome evolution and results in reduced selective pressure when two functional copies are present, allowing for the accumulation of genetic variation in one copy and possibly the development of alternate or novel functions. Comparison of nucleotide and protein sequence between paralogues has been used to define homology and identity between closely related genes (Fitch, 1966a,b,c; Fitch and Margoliash, 1967; Margoliash *et al*., 1968; Margoliash, 1969; Haber and Koshland, 1970). Conservation between paralogues not only suggests the paralogous members have evolved from a common molecular ancestor, but that the paralogues also have similar functions. Conserved residues or stretches of amino acids between protein paralogues, resulting in identical or highly identical regions signify essential, functional residues (Haber and Koshland, 1970). Whether sequence divergence as result of evolution results in functionally distinct genes must be addressed empirically.

Focusing on the *Drosophila RpL22e* protein family, my proposed research objectives tested the hypothesis that structurally distinct ribosomal protein paralogues have distinct, tissue-specific roles which provide paralogue-specific functions (not limited to translation) in selected cells or tissues. Data in this dissertation support this hypothesis and provide evidence that although RpL22e paralogues may have overlapping functions

in the male mitotic germline, they have functionally diverse roles within the meiotic germline.

Duplication of *rpL22e* has produced paralogous *rpL22e-like,* which has evolved a primarily male germline-specific expression pattern. Additionally, *rpL22e-like* is alternative spliced using non-canonical splice sites that produce two mRNA isoforms and structurally diverse protein isoforms (RpL22e-like-PA and -PB). The role of the novel RpL22e-like-PB isoform remains enigmatic, but data in this dissertation confirm that although only 37% identical to its ancestral paralogue, RpL22e-like-PA (most abundant isoform) has maintained its ancestral function as a ribosomal component.

Further investigation has identified differential post-translational modification (PTM) of RpL22e paralogues. Data in this dissertation show that RpL22e is highly modified in the testis, including multiple SUMO moieties and at least a single phosphate addition, compared to other tissues. Biochemical analysis in S2 cells shows that only unmodified RpL22e co-sediments with polysomes, suggesting that modified RpL22e has an extra-ribosomal function. Conversely, although PTMs are predicted, modification of RpL22e-like is not evident, as the predicted MW protein accumulates comparably to recombinant protein in Western analysis and is not susceptible to modification *in vitro*.

Immunohistochemical (IHC) analysis shows distinct localization patterns of RpL22e paralogues in the male germline. RpL22e-like is germline-specific and has a localization

pattern indicative of an Rp throughout the germline, whereas RpL22e is seen in both somatic and germ cells. RpL22e primarily localizes to the nucleus in germ cells (some cytoplasmic staining is seen) and does co-localize with nucleolar markers in the mitotic and early/immature meiotic germ cells, raising the possibility that RpL22e is a ribosomal component in these cells. However, in maturing meiotic germ cells (primary spermatocytes; before meiosis I), RpL22e is strictly nucleoplasmic, suggesting a role outside of translation during meiosis. Therefore, data support the conclusion that in maturing meiotic male germ cells the RpL22e paralogues have distinct roles, with RpL22e-like serving as a ribosomal component.

The function of nucleoplasmic RpL22e remains to be determined, but germline-specific knockdown of *smt3* does suggest that RpL22e nuclear localization is SUMO-dependent, as paralogue nuclear distribution and RpL22e PTM pattern are affected. Uniquely, the N-terminus of *Drosophila* RpL22e has homology to histone H1 (Koyama *et al*., 1999), which itself has recently been shown to be a SUMOylation substrate *in vivo* and *in vitro* (Matafora *et al*., 2009). Moreover, RpL22e has been identified in chromatin complexes that alter gene expression globally in *Drosophila* Kc cells (Ni *et al*., 2006). It is possible that RpL22e, in a SUMO-dependent manner, associates with chromatin to regulate gene expression during the transition into meiosis. This remains to be explored, but may be addressed by chromatin immunoprecipitation and experiments testing the *in vivo* requirement for RpL22e.

This dissertation also shows that sequence divergence obtained through evolution has contributed to differential post-translational modification between protein paralogues, which has previously been unreported for Rp paralogues in metazoans (previously reported for the RpS6 paralogues in *Arabidopsis*; Chang *et al*., 2005). While conserved or semi-conserved amino acid substitutions may not greatly affect structure, polarity, or contribute to steric hindrance, single amino acids changes do have the ability to acutely affect post-translational modification motifs. For example, a conserved lysine to arginine substitution minimally affects size and/or charge, but abolishes both ubiquitination and SUMOylation as the ε-amino group is replaced by a guanidinium group, eliminating the capability to form an isopeptide bond with ubiquitin or SUMO, respectively. Functional and phenotypic differences seen between highly similar or identical Rp paralogues (as seen in Komili *et al*., 2007) may be explained in part by differential post-translational modification. A large comparative analysis of predicted or confirmed PTMs between Rp paralogues has not been reported, but is warranted.

As described in greater detail in Chapter 5.2, the work presented in this dissertation also provides a foundation for additional research, focusing on the *in vivo* requirement and functions of the RpL22e paralogues.

Overall, this dissertation has contributed to the better understanding of duplicated Rps, providing evidence that Rp paralogues can share a common function, but sequence divergence obtained through evolution can promote functional diversity in a tissue-

specific manner. Mechanisms that contribute to functional diversification that have not been previously reported for Rp paralogues in metazoans have also been identified, namely alterative splicing and post-translational modification.

5.2 Future Directions

Determining regulatory elements required for germline specificity of *rpL22e-like*

Gene structure between ancestral and duplicated genes may provide clues to the duplication mechanism. For example, genes derived from retrotransposition often lack introns (Harrison and Gerstein, 2002; Yu *et al*., 2007). In the case of the *Drosophila* RpL22e paralogues, divergence is not only seen in coding and amino acid sequence, but is also evident in codon usage and UTR elements. The ancestral *rpL22e* gene is ubiquitously expressed, but our data show that *rpL22e-like* expression is male germline-specific in the male reproductive system (Kearse *et al*., 2011). Mechanisms responsible for the male germline-specific expression of RpL22e-like remain unexplored.

Determining genetic regulatory elements required for the observed expression patterns for both RpL22e paralogues will provide insight into the evolution of the gene family. Sano *et al*. (2002) has used a deletion strategy to define both 5' and 3' regulatory regions needed for a wildtype expression pattern of the germline-specific *vasa* gene in the fly ovary. Specifically, several truncations and mutations were made of flanking genomic sequence (utilizing the presence of restriction endonuclease recognition sites or by PCR mutagenesis) to delineate regulatory elements.

In a similar approach, P[acman] cloning technology allows for large segments of *Drosophila* genomic sequence to be propagated in *E. coli* as bacterial artificial chromosomes and manipulated with standard molecular biology techniques to create

reporter and gene fusion (e.g. GFP, lacZ) constructs. Subsequently, the genomic sequence is subcloned by recombination into fly P-element transformation vectors for genomic integration by either random or site-directed insertion (see Venken *et al*., 2006 for vector information and a more detailed strategy).

Using this strategy with mutational analysis of flanking genomic regions and UTR sequences, regulatory elements for both RpL22e paralogues can be defined. Subsequent bioinformatic analysis will also be useful in comparing regulatory regions, to determine if sequence divergence has contributed to the tissue-specific expression of *rpL22e-like*.

Determining the role of RpL22e-like-PB

In our efforts to define and characterize the expression pattern of *rpL22e-like*, we discovered the novel alternatively spliced isoform *rpL22e-like-PB*, which encodes a polypeptide primarily consisting of the N-terminus of RpL22e-like-PA (full length protein) (Chapter 2.2; Figure 2.210; Kearse *et al*., 2011). While this domain (the fly-specific N-terminal extension) has homology to the C-terminal end of histone H1 (Figure 1.4; Koyama *et al*., 1999), its function has not been assessed. However, based on homology to histone H1, it can be proposed that RpL22e-like-PB binds to chromatin in association with histone H1. This possibility is supported by reports showing *Drosophila* RpL22e binds to chromatin by association with histone H1 and alters gene expression globally in cultured *Drosophila* Kc cells (Ni *et al*., 2006).

Our data strongly favor the conclusion that *rpL22e-like-PB* mRNA is translated (Figure 2.13; Kearse *et al*., 2011) and that RpL22e-like-PB can be detected by Western analysis when overexpressed in S2 cells (data not shown). Immunoprecipitation (IP) experiments purifying overexpressed RpL22e-like-PB-FLAG from S2 cells and assaying for co-immunopurified (co-IP) chromatin proteins (e.g. core histone proteins) may initially support the proposal that RpL22e-like-PB binds chromatin. Determining whether RpL22e-like-PB-FLAG associates with specific genomic regions (e.g. transcriptionally active or heterochromatic regions) can be assayed by confirming co-IP of specific histone modifications (as defined for RpL22e in Kc cells by Ni *et al*, 2006). On a larger scale, Chip-chip experiments utilizing the Affymetrix GeneChip Drosophila Tiling 2.0R Array platform could provide a detailed analysis of DNA regions bound by RpL22e-like-PB-FLAG.

Additionally, overexpression of RpL22e-like-PB-FLAG *in vivo* (see Chapter 6.4 for similar strategy) and subsequent cellular localization analysis and characterization of any associated phenotypes may provide insight into function. Similar co-IP and ChIP experiments as described above can be performed with testis tissue (Gan *et al*., 2010) for *in vivo* analysis.

Lastly, mass spectrometry identification (e.g. MALDI-TOF) of co-immunopurified proteins from immunopurified RpL22e-like-PB-FLAG from S2 cells or testis tissue can

provide initial insights into binding partners and function. Subsequent validation of each identified protein by traditional co-IP and Western analyses will be required.

Determining SUMO acceptor lysines in RpL22e

Chapter 3 provides evidence for SUMOylation (at least two moieties added, based on MW) and phosphorylation of RpL22e in the testis. We also see the abundance of RpL22e proteins in S2 cells that, based on MW, could resemble a single SUMO modification and subsequent phosphorylation (43α,β; Figure 3.1); however, bacterial-based SUMO assays and *in vitro* phosphatase assays do not provide support that RpL22e-like is modified *in vitro* (Figures 3.8 and 3.10). Initial MALDI-TOF analysis of immunopurified RpL22e (from S2 cells) to determine post-translational modifications were inconclusive due to high background levels (data not shown). Revisiting this approach may be the most advantageous and timely strategy to identify both SUMOylation acceptor lysine and phosphorylated residues.

Based on our bacterial-based SUMO assays (Figure 3.8) and observed MW, we conclude that 55α RpL22e is the product of dual SUMOylation. In this assay, mutating the predicted major SUMO acceptor lysine (K39R) had minimal effect on accumulating 55α FLAG-RpL22e (Figure 6.2), suggesting either that K39 is not a SUMO acceptor or that RpL22e is alternatively SUMOylated. Bielska *et al.* (2012) has shown that a polypeptide containing a single SUMO moiety has multiple functional acceptor lysines. Given the abundance of lysine residues in RpL22e, dissection of functional SUMO acceptor sites

will require a broad mutagenesis approach. *In silico* analysis predicts five SUMO motifs, resulting in 120 possible mutagenic combinations. This long term strategy will be laborious, but an initial approach to mutate all predicted SUMO acceptor lysines will confirm the *in silico* prediction. Additionally, confirming that a quintuple lysine to arginine mutant at all predicted SUMO motifs, referred hereafter as RpL22e(5xR), is not SUMOylated can be basis for future *in vivo* studies to determine the role of SUMOylated RpL22e.

Determining the post-translational modification pathway of RpL22e

Elucidating the post-translational modification (PTM) scheme and dynamics of RpL22e may provide insight into function and regulation of the observed modifications. As described in the previous section, determining the precise SUMO acceptor lysines will be essential for establishing experiments investigating the role of SUMOylated RpL22e. Similarly, identification of phosphorylated serine and threonine residues will be essential for the complete understanding of the role of modified RpL22e.

We cannot confidently predict the dynamics of RpL22e modification from our *in vitro* SUMO assay (Figure 3.8) or *in vivo* depletion of SUMO in testis tissue (Figure 3.10C). However, based on the observed MW, we can predict PTMs leading to 43α and/or β preclude 55α (species seen in *in vitro* SUMO assay). *In vivo* depletion of SUMO in testis tissue (Figure 3.10C) results in an accumulation of RpL22e at 43kD (43α,β) and a significant aberration of modified proteins at the 55kD range compared to the control,

supporting the conclusion that PTMs resulting in 43α,β preclude 55α,β,γ. Additionally, the abundance of 43α,β does appear to vary between samples (e.g. S2 cells in Figure 3.1), suggesting these modified proteins may be unstable intermediates.

Based on the observed MW and predicted modification motifs by ELM, 43β may be a phosphorylated form of 1X-SUMOylated RpL22 (43α). However, supporting biochemical evidence is lacking. Immunodetection of FLAG-RpL22e at 43kD is not evident in the *in vitro* SUMO assay (Figure 3.8), suggesting 43α,β are unstable, transient intermediates or do not accumulate unless utilized.

Similar conclusions can be extended to the testis-specific RpL22e modifications (55β,γ). Based on the observed MW and the *in vivo* depletion of SUMO in testis tissue (Figure 3.10C), 55β may be 3X-SUMOylated RpL22e. However, direct supporting biochemical evidence is lacking. Additionally, our *in vitro* phosphatase assay has identified that 55γ is a phosphorylated form of RpL22e (Figure 3.10A).

To determine the dynamics of RpL22e post-translational modification, traditional pulse-chase experiments using ^{35}S-labeled methionine and/or ^{35}S-labeled cysteine can be employed followed by immunopurification. In shorter chase times, the initial RpL22e modifications would accumulate. Subsequent PTMs would accumulate as the chase time is extended. However, this approach assumes all modified RpL22e species can be immunopurified with equal efficiency.

To overcome this possible hurdle, targeted gene replacement can be used to introduce mutated *FLAG-rpL22e* harboring mutated PTM sites (lysine to arginine mutations for SUMOylation motifs; serine/therione to alanine mutations for phosphorylation motifs) to test how a single or combination of mutated PTM sites affect the RpL22e modification pattern (determined by Western analysis). Published protocols are available for *in vivo* investigations (Gong and Golic, 2003), as well as approaches in cultured S2 cells using zinc-finger nuclease technology (Maeder *et al*., 2008; Santiago *et al*., 2008; Urnov *et al*., 2010). This strategy also allows for investigating the functional impact of such modifications *in vivo* under wildtype expression levels. Alternatively, rescue experiments (described in more detail in the following section) with mutated (PTM-deficient) RpL22e may provide insight into the RpL22e PTM pathway, as well as the developmental impact of RpL22e modification.

Is SUMOylation of RpL22e essential for development and male germline maturation *in vivo*?

Along with previously published data (Bourbon *et al*., 2002; Boutros *et al*., 2004), our ubiquitous knockdown of RpL22e (Figure 4.1; *Act*-GAL4 > RpL22e.IR) provides evidence that RpL22e is essential for fly development. However, RpL22e is dispensable *in vitro* (Lavergne *et al*., 1987) and *in vivo* in multiple eukaryotes (Deutschbauer *et al*., 2005; Anderson *et al*., 2007). Whether SUMOylation contributes to RpL22 being essential *in vivo* has not been addressed. Polysome analysis of RpL22eΔH1-FLAG in S2

cells suggests SUMOylation of RpL22e is not required for incorporation into polysomes (Figure 3.11B), suggesting modified RpL22e has an extra-ribosomal function, which may provide an explanation of why RpL22e is essential in the fly and not in most other eukaryotes.

To determine if SUMOylation of RpL22e is essential for development *in vivo*, we can perform rescue experiments utilizing a RpL22e gene disruption line (referred hereafter as *rpL22eΔ*) that is publically available from the Bloomington *Drosophila* Stock Center (#15203: $rpL22e^{KG09650}$). In an *rpL22eΔ* background, we can express FLAG-RpL22e(5xR) at wildtype levels using a P[acman] cloning strategy (see discussion above; Venken *et al*., 2006) or overexpress using the pVALIUM10-roe vector (provided by the *Drosophila* RNAi Screening Center) and assess if FLAG-RpL22e(5xR) can rescue viability.

Additionally, if FLAG-RpL22e(5xR) does rescue viability, the role of SUMOylated RpL22e can be assessed in the male germline. Assessing germline development by phase contrast microscopy, along with assaying sperm motility and male fertility, can provide insight into the requirement of SUMOylated RpL22e in germline development. Furthermore, our data shows the RpL22e nucleoplasmic localization in meiotic germ cells is sensitive to SUMO levels and SUMO modification (Figures 3.10 and 3.14). Immunohistochemical analysis (anti-FLAG) of FLAG-RpL22e(5xR) rescued males can

also provide insight into whether or not SUMOylation of RpL22e is necessary for the observed nucleoplasmic localization in meiotic germ cells.

Can RpL22e-like-PA-FLAG rescue *rpL22eΔ* lethality?

Although only 37% identical to RpL22e, our data show that RpL22e-like shares a conserved role as a ribosomal component (Figure 2.9; Kearse *et al*., 2011). Whether RpL22e-like can functionally replace RpL22e *in vivo* remains unknown, but can be addressed with similar rescue experiments as described above. Seeing rescue of viability when RpL22e-like-PA-FLAG is expressed ubiquitously in an *rpL22eΔ* background would suggest redundancy, at least in functions that are essential. Phenotypic analysis will be crucial to determine any tissue-specific aberrations, as this would suggest non-redundancy in function in these tissues. However, if rescue is not seen, RpL22e must provide an essential function that has either evolved separately from its paralogue or has been lost by its paralogue through evolution.

Is the fly-specific N-terminal extension of the RpL22e essential *in vivo*?

Uniquely, *Drosophila* RpL22e contains a fly-specific N-terminal extension that has no known function, but is homologous to the C-terminal end of histone H1 (Koyama *et al*., 1999; Figure 1.4). RpL22e-like also has this extension, but is divergent in sequence (Kearse *et al*., 2011; Figure 2.1). Mutational analysis shows that in both paralogues, this novel extension is non-essential for incorporation into ribosomes and polysomes (Figures 3.11B and 6.2, respectively; designated as RpL22eΔH1 and RpL22e-likeΔH1),

suggesting this novel extension may be involved in extra-ribosomal interactions or functions. We also show that *rpL22e*, but not *rpL22e-like,* is essential *in vivo*. Moreover, RpL22e is non-essential in most eukaryotes (Lavergne *et al*., 1987; Deutschbauer *et al*., 2005; Anderson *et al*., 2007). Whether the fly-specific histone H1-like extension contributes to the RpL22e *in vivo* requirement in *Drosophila* has not been addressed.

Utilizing a similar rescue experimental design as described above, the ability of RpL22eΔH1-FLAG to rescue viability in an *rpL22eΔ* background would demonstrate that RpL22e as a ribosomal component is truly essential in *Drosophila*, as opposed to the novel histone H1-like domain providing an essential function. Conversely, if rescue is not seen, the novel histone H1-like domain must provide an essential RpL22e function, most likely an extra-ribosomal one. Additional mutational analysis may identify essential domains and residues, providing insight into possible binding and interacting partners of this novel extension.

Is RpL22e essential for male germline development?

In attempt to assess if both RpL22e paralogues are equally required in the male germline *in vivo*, we established paralogue-specific RNAi lines (UAS/GAL4 binary system; Chapter 4). Our data suggest that *rpL22e-like* is dispensable in the male germline, as depletion of *rpL22e-like* had no observable effect on germline development or fertility (Figures 4.2A, 4.3, 4.4). Unfortunately, we were unable to assess the requirement of *rpL22e in vivo* due to low knockdown efficiency. Using the available germline-specific

GAL4 drivers (*nos*-GAL4 and *bam*-GAL4), two independent RpL22e RNAi lines (RpL22e.IR and VAL20-RNAi-RpL22e) had minimal effects on RpL22e levels (Figures 4.2B-C). As discussed in Chapter 4, we suspect this is due to the restricted expression pattern of the available germline-specific GAL4 drivers.

Using the FLP/FRT system (Theodosiou and Xu, 1998; Parks *et al*., 2004; used in testis in Zheng *et al*., 2011), genetic mosaics harboring gene deletions or null mutations can be created. Although created at a low efficiency, FLP/FRT allows for cells homozygous for a mutation or deletion to be easily identified in tissue (heterozygous) by visible markers, often GFP. Using this strategy, spermatogonial cysts homozygous for *rpL22eΔ* can be tracked by visualizing GFP and characterized to determine the requirement of RpL22e *in vivo*. If developmental effects are seen, additional analyses, including phase contrast microscopy to characterize developmental stages and nuclear morphology, may provide insight into the role of RpL22e in the male germline. Additionally, this strategy could also be combined with *rpL22e-like* mutants (if generated or obtained from others) to assess the impact of deleting both *rpL22e* paralogues from the male germline.

Chapter 6:

Appendix A

6.1 Primers for site-directed mutagenesis of RpL22e SUMO acceptor lysines

Using the Affymetrix Change-It site-directed mutagenesis kit, the primers below (along with the supplied Reverse_Amp^R primer) can be used to generate lysine to arginine mutants to assess the predicted SUMO acceptor lysines in either a bacterial-based SUMO assay (using pEXP-5/FLAG-RpL22e), S2 cells (pMT/FLAG-RpL22e) or *in vivo* (pVALIUM10-roe/FLAG-RpL22e).

Forward_L22e_K23R:
PO4-5'-GCCGCTAAGCCAGCGGAGCGCGCCGCTCCCGCAGCCGCC-3'

Forward _L22e_K34R:
PO4-5'-GCCGCCGCCGCCAAGGGCCGCGTGGAGAAGCCGAAGGC-3'

Forward_L22e_K39R:
PO4-5'-AAGGTGGAGAAGCCGCGCGCTGAGGCCGCCAAG-3'

Forward _L22e_K64R:
PO4-5'-GAGGCGGCCAAGGATGTACGCGCAGCCGCCGCTGCTGCC-3'

Forward _L22e_K104:
PO4-5'-GCTCCCAAGAAGGACGCCCGCGCTGCTGCTGCTCCGGC-3'

6.2 FLAG-RpL22e^{K39R} is a SUMO substrate *in vitro*

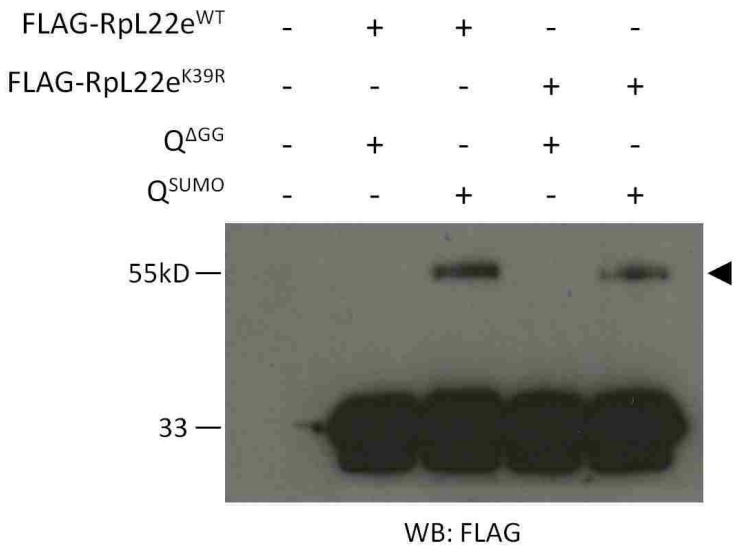

Figure 6.1. FLAG-RpL22e^{K39R} is a SUMO substrate *in vitro*. To further test if RpL22e is a SUMOylation substrate, we used the previously developed bacterial-based SUMOylation assay utilizing the *Drosophila* SUMOylation pathway enzymes and SUMO protein (Nie *et al*., 2009). *E. coli* were co-transformed with plasmids encoding FLAG-RpL22e and either an incompetent (Q$^{\Delta GG}$) or competent (Q^{SUMO}) form of SUMO. Western analysis shows a 20kD electrophoretic shift of FLAG-RpL22e when co-transformed with a competent from of SUMO (Q^{SUMO}), but not with an incompetent form (Q$^{\Delta GG}$). Based on the observed MW, we conclude the modification is due to the addition of two SUMO moieties. To test whether the major SUMO motif predicted (lysine 39) is a SUMO acceptor, the K39R mutation (lysine to arginine) was assayed. Accumulation of SUMOylated FLAG-RpL22e is observed but is less abundant than WT, suggesting

lysine39 may not be SUMO acceptor or RpL22e is alternatively SUMOylated. Bielska *et al.* (2012) has shown a polypeptide that contains a single SUMO moiety has multiple functional acceptor lysines. Furthermore, in assays where deSUMOylation enzymes, such as Ulp1, are depleted, stabilization of SUMOylation at arginine residues is noted (Smith *et al*., 2011). Such enzymes are not found in *E. coli* as SUMOylation is strictly a eukaryotic process; this may account for the stability of SUMOylation of the K39R mutant in this assay, raising the possibility that lysine39 may be a minor SUMO acceptor.

.

6.3 RpL22e-like-PB is a SUMO substrate *in vitro*

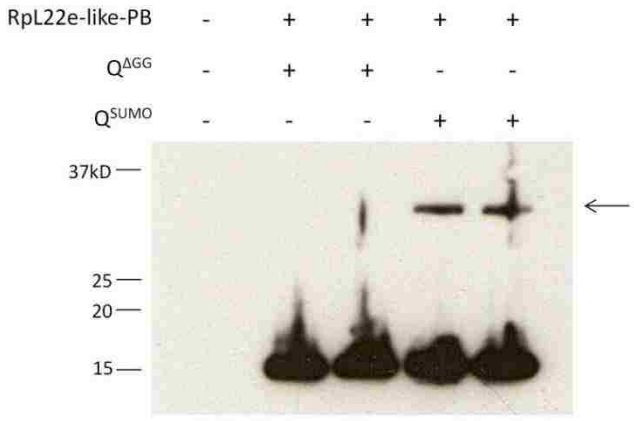

Figure 6.2. RpL22e-like-PB is a SUMO substrate *in vitro*. Chapter 2 provides evidence that *rpL22e-like* produces two structurally distinct proteins by alternative splicing, RpL22e-like-PA and -PB. Although conserved SUMOylation motifs are predicted, RpL22e-like-PA is not SUMOylated *in vitro* (Figure 3.8). RpL22e-like-PB also contains all of the predicted SUMO motifs, but whether it is a SUMO substrate has not been assessed. Using the previously described bacterial-based SUMO assay (Nie *et al*., 200; Figures 3.8 and 6.1), we show that RpL22e-like-PB is a SUMO substrate *in vitro* when co-expressed with a competent from of SUMO (Q^{SUMO}), but not with an incompetent form ($Q^{\Delta GG}$). Based on the MW shift from 15kD to ~35kD (arrow), we conclude RpL22e-like-PB is SUMOylated twice *in vitro*.

6.4 Polysome analysis of RpL22e-likeΔH1 in S2 cells.

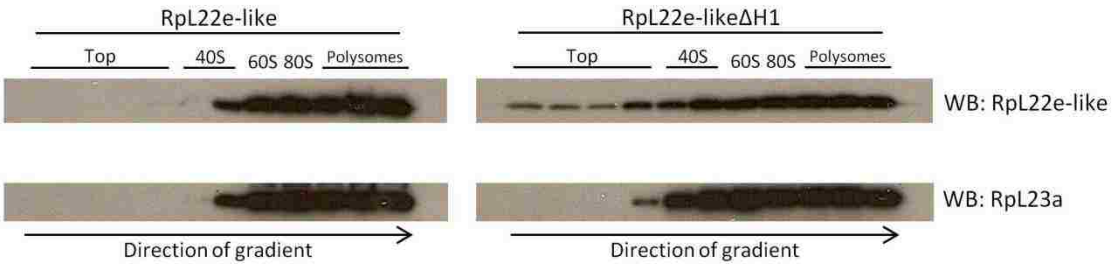

Figure 6.3. RpL22e-likeΔH1 co-sediments with polysomes in S2 cells. We have determined that fly-specific N-terminal histone H1-like domain of RpL22e is not essential for ribosome incorporation in S2 cells (Figure 3.11). Similarly, we assessed if the histone H1-like domain is essential for RpL22e-like-PA ribosome incorporation. Polysome analysis of S2 cells expressing RpL22e-like (full length; RpL22e-like-PA) or RpL22e-likeΔH1 shows both to co-sediment with polysomes, suggesting that the histone H1-like domain is not essential for RpL22e-like ribosome incorporation. However, unlike RpL22e-like, accumulating RpL22e-likeΔH1 is seen at the top of the gradient, suggesting that the histone H1-like domain may be needed for efficient ribosome incorporation. Endogenous RpL23a was used as a positive control.

6.5 Testis-Specific RpL22e Modifications May Occur After Meiosis I.

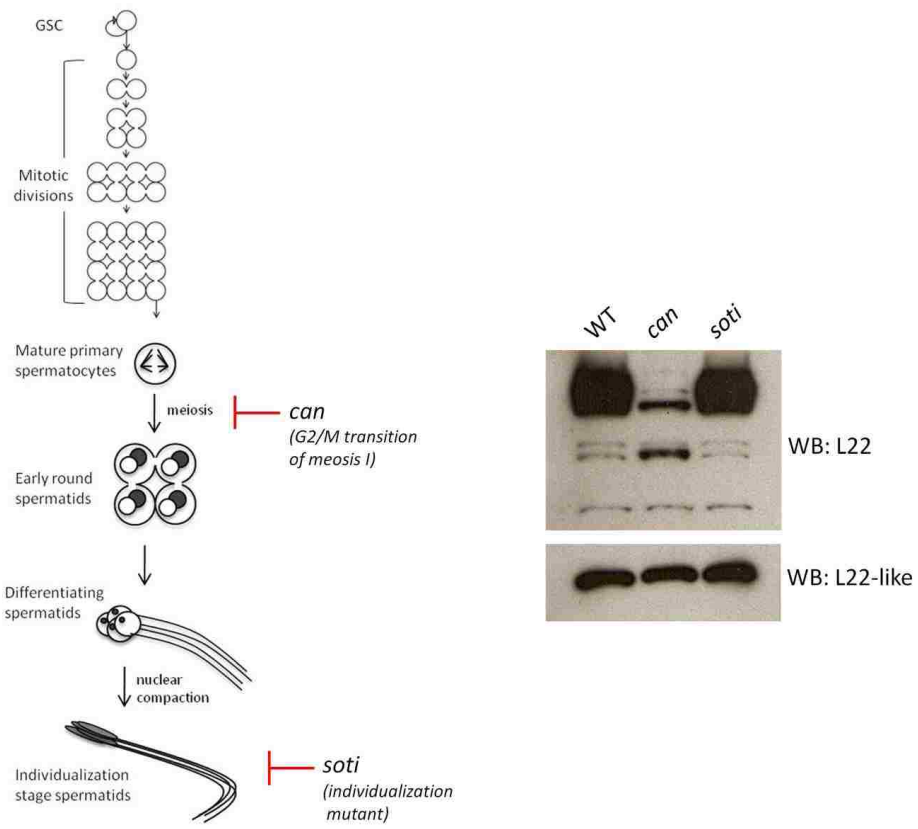

Figure 6.4. 55β,γ RpL22e accumulation is decreased in *can*, but not in *soti* mutants.

To investigate which developmental stage the testis-specific RpL22e modifications (Figures 3.1-3.3) may occur in, we assessed the RpL22e immunodetection pattern in meiotic and individualization mutants. *can* mutation cause spermatocytes to arrest in the G2/M transition of meiosis I with partial chromosome condensation, resulting in the complete absence of post-meiotic cells (Lin *e al*., 1996). *soti* mutant spermatids exhibit no gross defects during early and mid stages of spermatogenesis, severe defects are observed during spermatid individualization (Kaplan *et al*., 2010). Western analysis shows accumulation of 55β,γ RpL22e to be deficient in *can*, but not *soti* mutants,

suggesting the modifications resulting in 55β,γ RpL22e may occur after the G2/M transition of meiosis I. Additional male meiotic mutants can be tested (e.g. *aly*, *tomb*; different class than can) to confirm 55β,γ association with meiosis I.

The can^{12} stock (*w; can[12]/TM3, Sb*) was a kind gift from Minx Fuller (Standford). The $soti^{sik}$ stock (*soti[sik]/TM6B, Tb[1]*) was obtained from the Bloomington *Drosophila* Stock Center (#32124). Oregona R (Carolina Biolgocial) strains were used as wildtype. Stocks were kept on standard cornmeal media, but were kept at 18-20°C.

Spermatogenesis diagram adapted from Sartain *et al*. (2011).

6.6 Overexpression of FLAG-RpL22e and RpL22e-like-PA-FLAG *in vivo*

To determine if endogenous levels of the RpL22e paralogues are sensitive to the expression levels of their paralogues, we generated overexpression lines for FLAG-RpL22e and RpL22e-like-PA-FLAG. For each paralogue, previously clone cDNA (Kearse *et al*., 2011, 2013 in review) was used as templates for the addition of a FLAG tag by PCR with High Fidelity Platinum Taq Master Mix (Invitrogen) (see Table 6.1 for primers). Amplicons were cloned into pENTR/D-TOPO (Invitrogen), verified by Sanger sequencing, subsequently gateway-cloned into the destination vector pVALIUM10-roe (provided by the *Drosophila* RNAi Screening Center) with LR clonase (Invitrogen), and verified by Sanger sequencing. Injection into *y, v, nanos-integrase; attp2* embryos for site-directed insertion on chromosome 3 at the attP2 locus and balancing to homozygosity was performed by Genetic Services.

For ubiquitous overexpression, four virgin pVALIUM10-roe/FLAG-RpL22e females were mated with two Act-GAL4 males at 25°C. 0-1 day old males were used for testis dissection and body extracts.

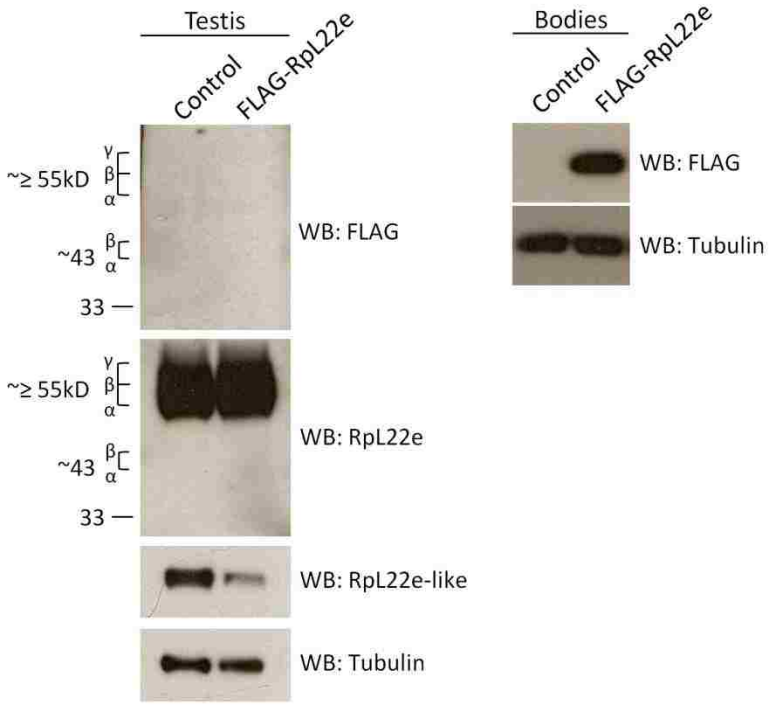

Figure 6.5. RpL22e-FLAG cannot be detected in testis tissue when overexpressed, but alters endogenous RpL22e-like protein levels. Using the *Act*-GAL4 driver to ubiquitously express RpL22e-FLAG *in vivo*, we assessed the expression levels of endogenous testis Rpl22e-like. Western analysis of day 0-1 F1 male testis tissue shows FLAG-RpL22e does not accumulate, but endogenous RpL22e-like levels are decreased. However, FLAG-RpL22e can be detected in whole body extracts from d0-1 males, confirming that the transgenic line is able to express FLAG-RpL22e. Tubulin was used as a loading control.

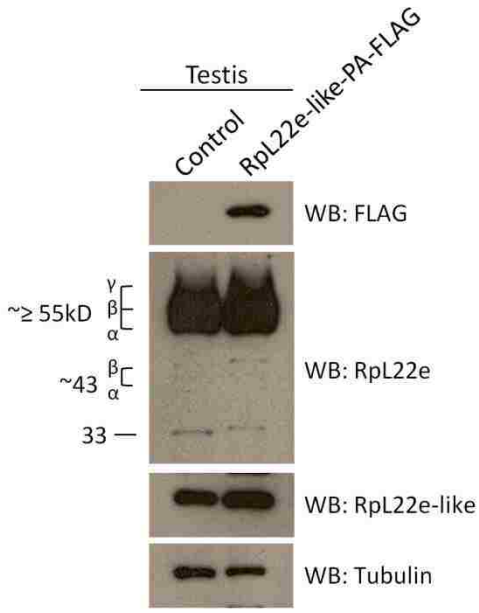

Figure 6.6. RpL22e-like-PA-FLAG can be overexpressed in the testis. RpL22e-like-PA-FLAG was expressed ubiquitously using the *Act*-GAL4 driver. Western analysis confirms RpL22e-like-PA-FLAG can be overexpressed in the testis, seen by the accumulation of RpL22e-like-PA-FLAG and increased levels of RpL22e-like-PA in F1 males. No significant change in endogenous RpL22e levels are seen when RpL22e-like-PA-FLAG is overexpressed. Tubulin was used as a loading control.

Table 6.1. Primers used to construct pVALIUM10-roe/FLAG-RpL22e and pVALIUM10-roe/RpL22e-like-PA-FLAG.

FLAG-RpL22e	
Forward_pENTR_FLAG:	5’-CACCATGATCGGCCGCGGCGACTACAAGGATGACGATGACAAG-3'
Reverse_RpL22e:	5’-GCCCTGAGGCTCTTGGGAGCAGCGGCAGC-3'

RpL22e-like-PA-FLAG	
Forward_RpL22e-like_pENTR:	5’-CACCGCGAGATCTATGAGTTCCCAGACGCAG-3'
Reverse_RpL22e-like_FLAG:	5’-GTCACGGATCCTTACTTGTCATCGTCATCCTTGTAGTCGCCGCGGCCGATGGCAAAGGTTTTTCCGCCATTGTCGTCGGCAA-3'

6.7 Double knockdown of *rpL22e* and *rpL22e-like* in the male germline

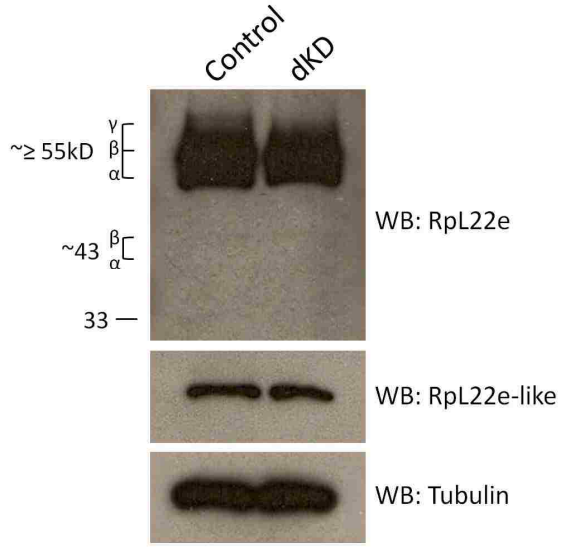

Figure 6.7. Double knockdown of *rpL22e* and *rpL22e-like* in the male germline with *nos*-GAL4 is inefficient. Using the *nos*-GAL4 driver (with UAS-Dicer2), *rpL22e* and *rpL22e-like* were targeted for germline depletion (*nos* > RpL22.IR, RpL22e-like.IR, Dicer2). Western analysis of testis tissue from F1 males shows inefficient knockdown of both RpL22e paralogues when targeted together. However, efficient RpL22e-like knockdown was previously seen with the *bam*-GAL4-VP16, *nos*-GAL4 drivers (both with UAS-Dicer2), and Act-GAL4 when targeted alone (Figures 4.1B, 4.2A). RpL22e has been difficult to knockdown with multiple drivers in the testis (Figure 4.2B-C.), but can be depleted with Act-GAL4 (Figure 4.1). Why targeting both paralogues results in inefficient knockdown of RpL22e-like remains unknown, but may be due to coordinated gene regulation. Preliminary evidence supports coordinated gene regulation, as altering levels of one paralogue affects the other (Figures 4.4, 4.5, 6.5). Nevertheless, additional investigations will be needed to provide confirmation and insight into a mechanism.

References

Aasland R, Abrams C, Ampe C, Ball LJ, Bedford MT, Cesareni G, et al. Normalization of nomenclature for peptide motifs as ligands of modular protein domains. FEBS Lett 2002; 513:141-144.

Agarwal D, Gregory ST, O'Connor M. Error-prone and error-restrictive mutations affecting ribosomal protein S12. J Mol Biol 2011; 410:1-9.

Amsterdam A, Sadler KC, Lai K, Farrington S, Bronson RT, Lees JA, Hopkins N. Many ribosomal protein genes are cancer genes in zebrafish. PLoS Biol 2004; 2:E139.

Anderson SJ, Lauritsen JP, Hartman MG, Foushee AM, Lefebvre JM, Shinton SA, Gerhardt B, Hardy RR, Oravecz T, Wiest DL. Ablation of ribosomal protein L22 selectively impairs alphabeta T cell development by activation of a p53-dependent checkpoint. Immunity 2007; 26:759-772.

Armache JP, Jarasch A, Anger AM, Villa E, Becker T, Bhushan S, et al. Localization of eukaryote-specific ribosomal proteins in a 5.5-Å cryo-EM map of the 80S eukaryotic ribosome. Proc Natl Acad Sci USA 2010; 107:19754-19759.

Babiano R, Gamalinda M, Woolford JL Jr, de la Cruz J. *Saccharomyces cerevisiae* ribosomal protein L26 Is not essential for ribosome assembly and function. Mol Cell Biol 2012; 32:3228-3241.

Bachand F, Lackner DH, Bähler J, Silver PA. Autoregulation of ribosome biosynthesis by a translational response in fission yeast. Mol Cell Biol 2006; 26:1731-1742.

Balasubramanian S, Zheng D, Liu YJ, Fang G, Frankish A, Carriero N, Robilotto R, Cayting P, Gerstein M. Comparative analysis of processed ribosomal protein pseudogenes in four mammalian genomes. Genome Biol 2009;10:R2.

Barakat A, Szick-Miranda K, Chang IF, Guyot R, Blanc G, Cooke R, Delseny M, Bailey-Serres J. The organization of cytoplasmic ribosomal protein genes in the *Arabidopsis* genome. Plant Physiol 2001; 127:398-415.

Barreau C, Benson E, Gudmannsdottir E, Newton F, White-Cooper H. Post-meiotic transcription in *Drosophila* testes. Development 2008; 135:1897-1902.

Bastian F, Parmentier G, Roux J, Moretti S, Laudet V, Robinson-Rechavi M. Bgee: integrating and comparing heterogeneous transcriptome data among species. DILS: LNCS 2008; 5109:124-131.

Baudin-Baillieu A, Fabret C, Liang XH, Piekna-Przybylska D, Fournier MJ, Rousset JP. Nucleotide modifications in three functionally important regions of the *Saccharomyces cerevisiae* ribosome affect translation accuracy. Nucleic Acids Res 2009; 37:7665-7677.

Baudin-Baillieu A, Tollervey D, Cullin C, Lacroute F. Functional analysis of Rrp7p, an essential yeast protein involved in pre-rRNA processing and ribosome assembly. Mol Cell Biol 1997; 17:5023-5032.

Beckmann R, Spahn CM, Eswar N, Helmers J, Penczek PA, Sali A, Frank J, Blobel G. Architecture of the protein conducting channel associated with the translating 80S ribosome. Cell 2011; 107:361-372.

Belin S, Beghin A, Solano-Gonzàlez E, Bezin L, Brunet-Manquat S, et al. Dysregulation of ribosome biogenesis and translational capacity is associated with tumor progression of human breast cancer cells. PLoS One 2009; 4:e7147.

Ben-Shem A, Garreau de Loubresse N, Melnikov S, Jenner L, Yusupova G, Yusupov M. The structure of the eukaryotic ribosome at 3.0 Å resolution. Science 2011; 334:1524-1529.

Bhaskar V, Smith M, Courey AJ. Conjugation of Smt3 to dorsal may potentiate the *Drosophila* immune response. Mol Cell Biol 2002; 22:492-504.

Bielska K, Seliga J, Wieczorek E, Kędracka-Krok S, Niedenthal R, Ożyhar A. Alternative SUMOylation sites in the *Drosophila* nuclear receptor Usp. J Steroid Biochem Mol Biol 2012; 132:227-238.

Boria I, Garelli E, Gazda HT, Aspesi A, Quarello P, Pavesi E, et al. The ribosomal basis of Diamond-Blackfan Anemia: mutation and database update. Hum Mutat 2010; 31:1269-1279.

Bortoluzzi S, d'Alessi F, Romualdi C, Danieli GA. Differential expression of genes coding for ribosomal proteins in different human tissues. Bioinformatics 2011; 17:1152-1157.

Bourbon HM, Gonzy-Treboul G, Peronnet F, Alin MF, Ardourel C, Benassayag C, Cribbs D, Deutsch J, Ferrer P, Haenlin M, et al. A P-insertion screen identifying novel X-linked essential genes in *Drosophila*. Mech Dev 2002; 110:71-83.

Boutros M, Kiger AA, Armknecht S, Kerr K, Hild M, Koch B, Haas SA, Paro R, Perrimon N; Heidelberg Fly Array Consortium. Genome-wide RNAi analysis of growth and viability in *Drosophila* cells. Science 2004; 303:832-835.

Bunt SM, Monk AC, Siddall NA, Johnston NL, Hime GR. GAL4 enhancer traps that can be used to drive gene expression in developing *Drosophila* spermatocytes. Genesis 2012; 50:914-920.

Burset M, Seledtsov IA, Solovyev VV. Analysis of canonical and non-canonical splice sites in mammalian genomes. Nucleic Acids Res 2000; 28:4364-4375.

Chang IF, Szick-Miranda K, Pan S, Bailey-Serres J. Proteomic characterization of evolutionarily conserved and variable proteins of *Arabidopsis* cytosolic ribosomes. Plant Physiol 2005; 137:848-862.

Chaudhuri S, Vyas K, Kapasi P, Komar AA, Dinman JD, Barik S, Mazumder B. Human ribosomal protein L13a is dispensable for canonical ribosome function but indispensable for efficient rRNA methylation. RNA 2007; 13:2224-2237.

Chen DH, McKearin DM. A discrete transcriptional silencer in the bam gene determines asymmetric division of the *Drosophila* germline stem cell. Development 2003; 130:1159-1170.

Chen D, Zhang Z, Li M, Wang W, Li Y, Rayburn ER, Hill DL, Wang H, Zhang R. Ribosomal protein S7 as a novel modulator of p53-MDM2 interaction: binding to MDM2, stabilization of p53 protein, and activation of p53 function. Oncogene 2007; 26:5029-5037.

Cheung PH, Culic O, Qiu Y, Earley K, Thompson N, Hixson DC, Lin SH. The cytoplasmic domain of C-CAM is required for C-CAM-mediated adhesion function: studies of a C-CAM transcript containing an unspliced intron. Biochem J 1993; 295:427-435.

Chintapalli VR, Wang J, Dow JA. Using FlyAtlas to identify better *Drosophila* melanogaster models of human disease. Nat Genet 2007; 39:715-720.

Clemens JC, Worby CA, Simonson-Leff N, Muda M, Maehama T, Hemmings BA, Dixon JE. Use of double-stranded RNA interference in *Drosophila* cell lines to dissect signal transduction pathways. Proc Natl Acad Sci USA 2000; 97:6499-6503.

Cmejla R, Cmejlova J, Handrkova H, Petrak J, Pospisilova D. Ribosomal protein S17 gene (RPS17) is mutated in Diamond-Blackfan anemia. Hum Mutat 2007; 28:117-1182.

Cocquet J, Chong A, Zhang G, Veitia RA. Reverse transcriptase template switching and false alternative transcripts. Genomics 2006; 88:127-131.

Copley RR, Goodstadt L, Ponting C. Eukaryotic domain evolution inferred from genome comparisons. Curr Opin Genet Dev 2003; 13:623-628.

Crosby MA, Goodman JL, Strelets VB, Zhang P, Gelbart WM; FlyBase Consortium. Flybase: genomes by the dozen. Nucleic Acids Res 2007; 35:D486-491.

Dai MS, Shi D, Jin Y, Sun XX, Zhang Y, Grossman SR, Lu H. Regulation of the MDM2-p53 pathway by ribosomal protein L11 involves a post-ubiquitination mechanism. J Biol Chem 2006; 281:24304-24313.

de Cuevas M, Matunis EL. The stem cell niche: lessons from the *Drosophila* testis. Development 2011; 138:2861-2869.

De S, Varsally W, Falciani F, Brogna S. Ribosomal proteins' association with transcription sites peaks at tRNA genes in *Schizosaccharomyces pombe*. RNA 2011; 17:1713-1726.

Degenhardt, R.F., and Bonham-Smith, P.C. *Arabidopsis* ribosomal proteins RPL23aA and RPL23aB are differentially targeted to the nucleolus and are disparately required for normal development. Plant Physiol 2008; 147:128-142.

Deschamps, J., and van Nes, J. Developmental regulation of the Hox genes during axial morphogenesis in the mouse. Development 2005; 132:2931-2942.

Deutsch WA, Yacoub A, Jaruga P, Zastawny TH, Dizdaroglu M. Characterization and mechanism of action of *Drosophila* ribosomal protein S3 DNA glycosylase activity for the removal of oxidatively damaged DNA bases. J Biol Chem 1997; 272:32857-32860.

Deutschbauer AM, Jaramillo DF, Proctor M, Kumm J, Hillenmeyer ME, Davis RW, Nislow C, Giaever G. Mechanisms of haploinsufficiency revealed by genome-wide profiling in yeast. Genetics 2005; 169:1915-1925.

Dobbelstein M, Shenk T. In vitro selection of RNA ligands for the ribosomal L22 protein associated with Epstein-Barr virus-expressed RNA by using randomized and cDNA-derived RNA libraries. J Virol 1995; 69:8027-8034.

Draptchinskaia N, Gustavsson P, Andersson B, Pettersson M, Willig TN, Dianzani I, et al. The gene encoding ribosomal protein S19 is mutated in Diamond-Blackfan anaemia. Nat Genet 1999; 21:169-175.

Duncan KA, Carruth LL. The sexually dimorphic expression of L7/SPA, an estrogen receptor coactivator, in zebra finch telencephalon. Dev Neurobiol 2007; 67:1852-1866.

Duncan KA, Jimenez P, Carruth LL. The selective estrogen receptor-alpha coactivator, RPL7, and sexual differentiation of the songbird brain. Psychoneuroendocrinology 2009; 34 Suppl 1:S30-38.

Doherty L, Sheen MR, Vlachos A, Choesmel V, O'Donohue MF, et al. Ribosomal protein genes RPS10 and RPS26 are commonly mutated in Diamond-Blackfan anemia. Am J Hum Genet 2010; 86:222-228.

Enerly E, Larsson J, Lambertsson A. Silencing the *Drosophila* ribosomal protein L14 gene using targeted RNA interference causes distinct somatic anomalies. Gene 2003; 320:41-48.

Eng FJ, Warner JR. Structural basis for the regulation of splicing of a yeast messenger RNA. Cell 1991; 65:797-804.

Fabrizio JJ, Boyle M, DiNardo S. A somatic role for *eyes absent* (*eya*) and *sine oculis* (*so*) in *Drosophila* spermatocyte development. Dev Biol 2003; 258:117-128.

Farrar JE, Nater M, Caywood E, McDevitt MA, Kowalski J, et al. Abnormalities of the large ribosomal subunit protein, Rpl35a, in Diamond- Blackfan anemia. Blood 2008; 112:1582-1592

Fewell SW, Woolford JL Jr. Ribosomal protein S14 of *Saccharomyces cerevisiae* regulates its expression by binding to RPS14B pre-mRNA and to 18S rRNA. Mol Cell Biol 1999; 19:826-834.

Fitch WM. The relation between frequencies of amino acids and ordered trinucleotides. J Mol Biol 1966a; 16:1-8.

Fitch WM. An improved method of testing for evolutionary homology. J Mol Biol 1966b; 16:9-16.

Fitch WM. Evidence suggesting a partial, internal duplication in the ancestral gene for heme-containing globins. J Mol Biol 1966c; 16:17-27.

Fitch WM, Margoliash E. Construction of phylogenetic trees. Science 1967; 155:279-284.

Fok V, Mitton-Fry RM, Grech A, Steitz JA. Multiple domains of EBER 1, an Epstein-Barr virus noncoding RNA, recruit human ribosomal protein L22. RNA 2006; 12:872-882.

Fumagalli S, Thomas G. The role of p53 in ribosomopathies. Semin Hematol 2011; 48:97-105.

Galisson F, Mahrouche L, Courcelles M, Bonneil E, Meloche S, Chelbi-Alix MK, Thibault P. A novel proteomics approach to identify SUMOylated proteins and their modification sites in human cells. Mol Cell Proteomics 2011; 10:M110.004796.

Gan Q, Schones DE, Ho Eun S, Wei G, Cui K, Zhao K, Chen X. Monovalent and unpoised status of most genes in undifferentiated cell-enriched *Drosophila* testis. Genome Biol 2010; 11:R42.

Gazda HT, Grabowska A, Merida-Long LB, Latawiec E, Schneider HE, et al. Ribosomal protein S24 gene is mutated in Diamond-Blackfan anemia. Am J Hum Genet 2006; 79:1110-1118.

Gazda HT, Sheen MR, Vlachos A, Choesmel V, O'Donohue M-F, et al. Ribosomal protein L5 and L11 mutations are associated with cleft palate and abnormal thumbs in Diamond-Blackfan anemia patients. Am J Hum Genet 2008; 83:769-780.

Gazda HT, Preti M, Sheen MR, O'Donohue M-F, Vlachos A, et al. Frameshift mutation in p53 regulator RPL26 is associated with multiple physical abnormalities and a specific pre-ribosomal RNA processing defect in Diamond-Blackfan anemia. Hum Mutat 2012; 33:103710-44.

Geiss-Friedlander R, Melchior F. Concepts in sumoylation: a decade on. Nat Rev Mol Cell Biol 2007; 8:947-956.

Gong WJ, Golic KG. Ends-out, or replacement, gene targeting in *Drosophila*. Proc Natl Acad Sci USA 2003; 100:2556-2561.

Gu SQ, Peske F, Wieden HJ, Rodnina MV, Wintermeyer W. The signal recognition particle binds to protein L23 at the peptide exit tunnel of *Escherichia coli* ribosome. Mol Cell 2003; 9:566-573.

Harrison P, Gerstein M: Studying genomes through the aeons: protein families, pseudogenes and proteome evolution. J Mol Biol 2002, 318:1155-1174.

Hennig W. Chromosomal proteins in the spermatogenesis of Drosophila. Chromosoma 2003; 111:489-494.

Hime GR, Brill JA, Fuller MT. Assembly of ring canals in the male germ line from structural components of the contractile ring. J Cell Sci 1996; 109:2779-2788.

Houmani JL, Davis CI, Ruf, IK. Growth-Promoting Properties of Epstein-Barr Virus EBER-1 RNA Correlate with Ribosomal Protein L22 Binding. J Virol 2009; 83:9844-9853.

Houmani JL, Ruf IK. Clusters of basic amino acids contribute to RNA binding and nucleolar localization of ribosomal protein L22. PLoS One 2009; 4:e5306.

Hrdlicka L, Gibson M, Kiger A, Micchelli C, Schober M, Schöck F, Perrimon N. Analysis of twenty-four Gal4 lines in *Drosophila melanogaster*. Genesis 2002; 34:51-57.

Huh WK, Falvo JV, Gerke LC, Carroll AS, Howson RW, Weissman JS, O'Shea EK. Global analysis of protein localization in budding yeast. Nature 2003; 425:686-691.

Hummel M, Cordewener JH, de Groot JC, Smeekens S, America AH, Hanson J. Dynamic protein composition of *Arabidopsis thaliana* cytosolic ribosomes in response to sucrose feeding as revealed by label free MSE proteomics. Proteomics 2012; 12:1024-1038.

Huang J, Zhou W, Watson AM, Jan YN, Hong Y. Efficient ends-out gene targeting in *Drosophila*. Genetics 2008; 180:703-707.

Hwang S, Gou Z, Kuznetsov IB. DP-Bind: a web server for sequence-based prediction of DNA-binding residues in DNA-binding proteins. Bioinformatics 2007; 23:634-636.

Ivankova N, Tretyakova I, Lyozin GT, Avanesyan E, Zolotukhin A, Zatsepina OG, Evgen'ev MB, Mamon LA. Alternative transcripts expressed by small bristles, the *Drosophila melanogaster nxf1* gene. Gene 2010; 458:11-19.

Jang CY, Shin HS, Kim HD, Kim JW, Choi SY, Kim J. Ribosomal protein S3 is stabilized by SUMOylation. Biochem Biophys Res Commun 2011; 414:523-527.

Jang CY, Kim HD, Zhang X, Chang JS, Kim J. Ribosomal protein S3 localizes on the mitotic spindle and functions as a microtubule associated protein in mitosis. Biochem Biophys Res Commun 2012; 429:57-62.

Jiang J, White-Cooper H. Transcriptional activation in *Drosophila* spermatogenesis involves the mutually dependent function of *aly* and a novel meiotic arrest gene *cookie monster*. Development 2003; 130:563-573.

Jin A, Itahana K, O'Keefe K, Zhang Y. Inhibition of HDM2 and activation of p53 by ribosomal protein L23. Mol Cell Biol 2004; 24:7669-7680.

Kai, T, Williams, D, Spradling, AC. The expression profile of purified *Drosophila* germline stem cells. Dev Biol 2005; 283:486-502
.
Kalmykova AI, Shevelyov YY, Polesskaya OO, Dobritsa AA, Evstafieva AG, Boldyreff B, Issinger OG, Gvozdev VA. CK2(beta)tes gene encodes a testis-specific isoform of the

regulatory subunit of casein kinase 2 in Drosophila melanogaster. Eur J Biochem 2002; 269:1418-1427.

Kamath RS, Fraser AG, Dong Y, Poulin G, Durbin R, Gotta M, Kanapin A, Le Bot N, Moreno S, Sohrmann M, et al. Systematic functional analysis of the *Caenorhabditis elegans* genome using RNAi. Nature 2003; 421:231-237.

Kaplan Y, Gibbs-Bar L, Kalifa Y, Feinstein-Rotkopf Y, Arama E. Gradients of a ubiquitin E3 ligase inhibitor and a caspase inhibitor determine differentiation or death in spermatids. Dev Cell 2010; 19:160-173.

Kearse MG, Chen AS, Ware VC. Expression of ribosomal protein L22e family members in *Drosophila melanogaster*: rpL22-like is differentially expressed and alternatively spliced. Nucleic Acids Res 2011; 39:2701-2716.

Kemphues KJ, Raff RA, Kaufman TC, Raff EC. Mutation in a structural gene for a beta-tubulin specific to testis in *Drosophila melanogaster*. Proc Natl Acad Sci USA 1979; 76:3991-3995.

Keren H, Lev-Maor G, Ast G. Alternative splicing and evolution: diversification, exon definition and function. Nat Rev Genet 2010; 11:345-355.

Kressler D, Hurt E, Bassler J. Driving ribosome assembly. Biochim Biophys Acta 2010; 1803:6723-683.

Kim HD, Lee JY, Kim J. Erk phosphorylates threonine 42 residue of ribosomal protein S3. Biochem Biophys Res Commun 2005; 333:110-115.

Kim TS, Kim HD, Shin HS, Kim J. Phosphorylation status of nuclear ribosomal protein S3 is reciprocally regulated by protein kinase C{delta} and protein phosphatase 2A. J Biol Chem 2009; 284:21201-21208.

Kim TY, Ha CW, Huh WK. Differential subcellular localization of ribosomal protein L7 paralogs in *Saccharomyces cerevisiae*. Mol Cells 2009; 27:539-546.

Kirthi N, Roy-Chaudhuri B, Kelley T, Culver GM. A novel single amino acid change in small subunit ribosomal protein S5 has profound effects on translational fidelity. RNA 2006; 12:2080-2091.

Koc EC, Koc H. Regulation of mammalian mitochondrial translation by post-translational modifications. Biochim Biophys Acta 2012; 1819:1055-1066.

Komili S, Farny NG, Roth FP, Silver PA. Functional specificity among ribosomal proteins regulates gene expression. Cell 2007; 131:557-571.

Kondrashov N, Pusic A, Stumpf CR, Shimizu K, Hsieh AC, Xue S, Ishijima J, Shiroishi T, Barna M. Ribosome-mediated specificity in Hox mRNA translation and vertebrate tissue patterning. Cell 2011; 145:383-397.

Koushika SP, Soller M, DeSimone SM, Daub DM, White K. Differential and inefficient splicing of a broadly expressed *Drosophila erect wing* transcript results in tissue-specific enrichment of the vital EWG protein isoform. Mol Cell Biol 1999; 19:3998-34007.

Koyama Y, Katagiri S, Hanai S, Uchida K, Miwa M. Poly(ADP-ribose) polymerase interacts with novel *Drosophila* ribosomal proteins, L22 and L23a, with unique histone-like amino-terminal extensions. Gene 1999; 226:339-345.

Kuznetsov IB, Gou Z, Li R, Hwang S. Using evolutionary and structural information to predict DNA-binding sites on DNA-binding proteins. Proteins 2006; 64:19-27.

Lai K, Amsterdam A, Farrington S, Bronson RT, Hopkins N, Lees JA. Many ribosomal protein mutations are associated with growth impairment and tumor predisposition in zebrafish. Dev Dyn 2009; 238:76-85.

Lam YW, Lamond AI, Mann M, Andersen JS. Analysis of nucleolar protein dynamics reveals the nuclear degradation of ribosomal proteins. Curr Biol 2007; 17:749-760.

Lambertsson A. The minute genes in *Drosophila* and their molecular functions. Adv Genet 1998; 38:69-134.

Lane DP. p53, guardian of the genome. Nature 1992; 358:15-16.

Lareau LF, Green RE, Bhatnagar RS, Brenner SE. The evolving roles of alternative splicing. Curr Opin Struct Biol 2004; 14:273-282.

Lavergne JP, Conquet F, Reboud JP, Reboud AM. Role of acidic phosphoproteins in the partial reconstitution of the active 60 S ribosomal subunit. FEBS Lett 1987; 216:83-88.

Le S, Sternglanz R, Greider CW. dentification of two RNA-binding proteins associated with human telomerase RNA. Mol Biol Cell 2000; 11:999-1010.

Lee SW, Berger SJ, Martinović S, Pasa-Tolić L, Anderson GA, Shen Y, Zhao R, Smith RD. Direct mass spectrometric analysis of intact proteins of the yeast large ribosomal subunit using capillary LC/FTICR. Proc Natl Acad Sci USA 2002; 99:5942-5947.

Leopardi R, Roizman B. Functional interaction and colocalization of the herpes simplex virus 1 major regulatory protein ICP4 with EAP, a nucleolar-ribosomal protein. Proc Natl Acad Sci USA 1996; 93:4572-4576.

Leopardi R, Ward PL, Ogle WO, Roizman B. Association of herpes simplex virus regulatory protein ICP22 with transcriptional complexes containing EAP, ICP4, RNA polymerase II, and viral DNA requires posttranslational modification by the U(L)13 protein kinase. J Virol 1997; 71:1133-1139.

Levine AJ and Oren M. The first 30 years of p53: growing ever more complex. Nat Rev Cancer 2009; 9:749-758.

Lin TY, Viswanathan S, Wood C, Wilson PG, Wolf N, Fuller MT. Coordinate developmental control of the meiotic cell cycle and spermatid differentiation in *Drosophila* males. Development 1996; 122:1331-1341.

Lindstrom MS. Emerging functions of ribosomal proteins in gene specific transcription and translation. Biochem Biophys Res Commun 2009; 379:167-170.

Liu JM, Ellis SR. Ribosomes and marrow failure: coincidental association or molecular paradigm? Blood 2006; 107:4583-4588.

Lohrum MA, Ludwig RL, Kubbutat MH, Hanlon M, Vousden KH. Regulation of HDM2 activity by the ribosomal protein L11. Cancer Cell 2003; 3:577-587.

Lomelí H, Vázquez M. Emerging roles of the SUMO pathway in development. Cell Mol Life Sci 2011; 68:4045-4064.

Lopes AM, Miguel RN, Sargent CA, Ellis PJ, Amorim A, Affara NA. The human RPS4 paralogue on Yq11.223 encodes a structurally conserved ribosomal protein and is preferentially expressed during spermatogenesis. BMC Mol Biol 2010; 11:33.

Luft F. The rise of a ribosomopathy and increased cancer risk. J Mol Med (Berl) 2010; 88:1-3.

Ma X, Zhang K, Li X. Evolution of *Drosophila* ribosomal protein gene core promoters. Gene 2009; 432:54-59.

MacInnes AW, Amsterdam A, Whittaker CA, Hopkins N, Lees JA. Loss of p53 synthesis in zebrafish tumors with ribosomal protein gene mutations. Proc Natl Acad Sci USA 2008; 105:10408-10413.

Maeder ML, Thibodeau-Beganny S, Osiak A, Wright DA, Anthony RM, Eichtinger M, et al. Rapid "open-source" engineering of customized zinc-finger nucleases for highly efficient gene modification. Mol Cell 2008; 31:294-301.

Mahajan R, Delphin C, Guan T, Gerace L, Melchior F. A small ubiquitin-related polypeptide involved in targeting RanGAP1 to nuclear pore complex protein RanBP2. Cell 1997; 88:97-107.

Margoliash E. Homology: a definition. Science 1969; 163:127.

Margoliash E, Fitch WM, Dickerson RE. Molecular expression of evolutinary phenomena in the primary and tertiary structures of cytochrome c. Brookhaven Symp Biol 1968; 21:259-305.

Marygold SJ, Roote J, Reuter G, Lambertsson A, Ashburner M, Millburn GH, Harrison PM, Yu Z, Kenmochi N, Kaufman TC, Leevers SJ, Cook KR. The ribosomal protein genes and Minute loci of *Drosophila melanogaster*. Genome Biol 2007; 8:R216

Matic I, Schimmel J, Hendriks IA, van Santen MA, van de Rijke F, van Dam H, Gnad F, Mann M, Vertegaal AC. Site-specific identification of SUMO-2 targets in cells reveals an inverted SUMOylation motif and a hydrophobic cluster SUMOylation motif. Mol Cell 2010; 39:641-652.

Matafora V, D'Amato A, Mori S, Blasi F, Bachi A. Proteomics analysis of nucleolar SUMO-1 target proteins upon proteasome inhibition. Mol Cell Proteomics 2009; 8:2243-2255.

Mattox W, Baker BS. Autoregulation of the splicing of transcripts from the *transformer-2* gene of *Drosophila*. Genes Dev 1991; 5:786-796.

Matunis MJ, Coutavas E, Blobel G. A novel ubiquitin-like modification modulates the partitioning of the Ran-GTPase-activating protein RanGAP1 between the cytosol and the nuclear pore complex. J Cell Biol 1996; 135:1457-1470.

Mauri F, McNamee LM, Lunardi A, Chiacchiera F, Del Sal G, Brodsky MH, Collavin L. Modification of *Drosophila* p53 by SUMO modulates its transactivation and pro-apoptotic functions. J Biol Chem 2008; 283:20848-20856.

Mauro VP, Edelman GM. The ribosome filter hypothesis. Proc Natl Acad Sci USA 2002; 99:12031-12036.

Mauro VP, Edelman GM. The ribosome filter redux. Cell Cycle 2007; 6:2246-2251.

Malygin AA, Parakhnevitch NM, Ivanov AV, Eperon IC, Karpova GG. Human ribosomal protein S13 regulates expression of its own gene at the splicing step by a feedback mechanism. Nucleic Acids Res 2007; 35:6414-6423.

McIntosh KB, Bonham-Smith PC. Ribosomal protein gene regulation: what about plants? Can J Bot 2006; 84:342-362.

Metzendorf C, Lind MI. Drosophila mitoferrin is essential for male fertility: evidence for a role of mitochondrial iron metabolism during spermatogenesis. BMC Dev Biol 2010; 10:68.

Meyuhas O. Synthesis of the translational apparatus is regulated at the translational level. Eur J Biochem 2000; 267:6321-6330.

Michot B, Hassouna N, Bachellerie JP. Secondary structure of mouse 28S rRNA and general model for the folding of the large rRNA in eukaryotes. Nucleic Acids Res 1984; 12:4259-4279.

Mikhaylova LM, Nguyen K, Nurminsky DI. Analysis of the Drosophila melanogaster testes transcriptome reveals coordinate regulation of paralogous genes. Genetics 2008; 179:305-315.

Montanaro L, Treré D, Derenzini M. Nucleolus, ribosomes, and cancer. Am J Pathol 2008; 173:301-310.

Mount SM, Burks C, Hertz G, Stormo GD, White O, Fields C. Splicing signals in *Drosophila*: intron size, information content, and consensus sequences. Nucleic Acids Res 1992; 20:4255-4262.

Nagarajan N, Bertrand D, Hillmer AM, Zang ZJ, Yao F, Jacques PE. Whole-genome reconstruction and mutational signatures in gastric cancer. Genome Biol 2012; 13:R115

Nakao A, Yoshihama M, Kenmochi N. RPG: the Ribosomal Protein Gene database. Nucleic Acids Res 2004; 32:D168-170.

Narla A, Ebert BL. Ribosomopathies: human disorders of ribosome dysfunction. Blood 2010; 115:3196-3205.

Ni JQ, Liu LP, Hess D, Rietdorf J, Sun FL. *Drosophila* ribosomal proteins are associated with linker histone H1 and suppress gene transcription. Genes Dev 2006; 20:1959-1973.

Nie M, Xie Y, Loo JA, Courey AJ. Genetic and proteomic evidence for roles of Drosophila SUMO in cell cycle control, Ras signaling, and early pattern formation. PLoS One 2009; 4:e5905.

Novetsky AP, Zighelboim I, Thompson DM Jr, Powell MA, Mutch DG, Goodfellow PJ. Frequent mutations in the RPL22 gene and its clinical and functional implications. Gynecol Oncol 2013; 128:470-474.

Ørom UA, Nielsen FC, Lund AH. MicroRNA-10a binds the 5'UTR of ribosomal protein mRNAs and enhances their translation. Mol Cell 2008; 30:460-471.

Panasenko OO, Collart MA. Presence of Not5 and ubiquitinated Rps7A in polysome fractions depends upon the Not4 E3 ligase. Mol Microbiol 2012; 83:640-653.

Parenteau J, Durand M, Morin G, Gagnon J, Lucier JF, Wellinger RJ, Chabot B, Elela SA. Introns within ribosomal protein genes regulate the production and function of yeast ribosomes. Cell 2011; 147:320-331.

Parks AL, Cook KR, Belvin M, Dompe NA, Fawcett R, et al. Systematic generation of high-resolution deletion coverage of the *Drosophila melanogaster* genome. Nat Genet 2004; 36: 288-292.

Pederson T. Ribosomal protein mutations in Diamond-Blackfan anemia: might they operate upstream from protein synthesis? FASEB J 2007; 21:3442-3445.

Pei A, Nossa CW, Chokshi P, Blaser MJ, Yang L, Rosmarin DM, Pei Z. Diversity of 23S rRNA genes within individual prokaryotic genomes. PLoS One 2009; 4:e5437.

Pelczar P, Filipowicz W. The host gene from intronic U17 small nucleolar RNAs in mammals has no protein-coding potential and is a member of the 5′-terminal oligopyrimidine gene family. Mol Cell Biol 1998; 18:4509-4518.

Peltz SW, Hammell AB, Cui Y, Yasenchak J, Puljanowski L, Dinman JD. Ribosomal protein L3 mutants alter translational fidelity and promote rapid loss of the yeast killer virus. Mol Cell Biol 1999; 19:384-391.

Perry RP. Balanced production of ribosomal proteins. Gene 2007; 401:1-3.

Pourquie O. Hox Genes (San Diego: Academic Press) 2009.

Qin X, Ahn S, Speed TP, Rubin GM. Global analyses of mRNA translational control during early *Drosophila* embryogenesis. Genome Biol 2007; 8:R63

Ramagopal S. Induction of cell-specific ribosomal proteins in aggregation-competent nonmorphogenetic *Dictyostelium discoideum*. Biochem Cell Biol 1990; 68:1281-1287.

Ramagopa S, Ennis HL. Regulation of synthesis of cell-specific ribosomal proteins during differentiation of *Dictyostelium discoideum*. Proc Natl Acad Sci USA 1981; 78:3083-3087.

Rao S, Lee SY, Gutierrez A, Perrigoue J, Thapa RJ, Tu Z, et al. Inactivation of ribosomal protein L22 promotes transformation by induction of the stemness factor, Lin28B. Blood 2012; 120:3764-73.

Rathke C, Baarends WM, Jayaramaiah-Raja S, Bartkuhn M, Renkawitz R, Renkawitz-Pohl R. Transition from a nucleosome-based to a protamine-based chromatin configuration during spermiogenesis in *Drosophila*. J Cell Sci 2007; 120:1689-1700.

Ren J, Wang Y, Liang Y, Zhang Y, Bao S, Xu Z. Methylation of ribosomal protein S10 by protein-arginine methyltransferase 5 regulates ribosome biogenesis. J Biol Chem 2010; 285:12695-12705.

Reo E, Seum C, Spierer P, Bontron S. SUMOylation of *Drosophila* SU(VAR)3-7 is required for its heterochromatic function. Nucleic Acids Res 2010; 38:4254-4262.

Rosby R, Cui Z, Rogers E, deLivron MA, Robinson VL, DiMario PJ. Knockdown of the *Drosophila* GTPase nucleostemin 1 impairs large ribosomal subunit biogenesis, cell growth, and midgut precursor cell maintenance. Mol Biol Cell 2009; 20:4424-4434.

Rotenberg MO, Moritz M, Woolford JL Jr. Depletion of *Saccharomyces cerevisiae* ribosomal protein L16 causes a decrease in 60S ribosomal subunits and formation of half-mer polyribosomes. Genes Dev 1988; 2:160-172.

Rudolph JE, Kimble M, Hoyle HD, Subler MA, Raff EC. Three *Drosophila* beta-tubulin sequences: a developmentally regulated isoform (beta 3), the testis-specific isoform (beta 2), and an assembly-defective mutation of the testis-specific isoform (B2t8) reveal both an ancient divergence in metazoan isotypes and structural constraints for beta-tubulin function. Mol Cell Biol 1987; 7:2231-2242.

Ruvinsky I, Sharon N, Lerer T, Cohen H, Stolovich-Rain M, Nir T, Dor Y, Zisman P, Meyuhas O. Ribosomal protein S6 phosphorylation is a determinant of cell size and glucose homeostasis. Genes Dev 2005; 19:2199-211.

Saenz-Robles MT, Remacha M, Vilella MD, Zinker S, Ballesta JP. The acidic ribosomal proteins as regulators of the eukaryotic ribosomal activity. Biochim Biophys Acta 1990; 1050:51-55.

Sakabe NJ, de Souza SJ. Sequence features responsible for intron retention in human. BMC Genomics 2007; 8:59.

Sambrook J, Fritsch EF, Maniatis T. Molecular Cloning: A Laboratory Manual. NY: Cold Spring Harbor Laboratory Press; 1989.

Samuels ME, Schedl P, Cline TW. The complex set of late transcripts from the *Drosophila* sex determination gene sex-lethal encodes multiple related polypeptides. Mol Cell Biol 1991; 11:3584-3602.

Sandigursky M, Yacoub A, Kelley MR, Xu Y, Franklin WA, Deutsch WA. The yeast 8-oxoguanine DNA glycosylase (Ogg1) contains a DNA deoxyribophosphodiesterase (dRpase) activity. Nucleic Acids Res 1997; 25:4557-4561.

Sano H, Nakamura A, Kobayashi S. Identification of a transcriptional regulatory region for germline-specific expression of vasa gene in *Drosophila melanogaster*. Mech Dev 2002; 112:129-139.

Santiago Y, Chan E, Liu PQ, Orlando S, Zhang L, Urnov FD, et al. Targeted gene knockout in mammalian cells by using engineered zinc-finger nucleases. Proc Natl Acad Sci USA 2008; 105:5809-5814.

Sanz E, Yang L, Su T, Morris DR, McKnight GS, Amieux PS. Cell-type-specific isolation of ribosome-associated mRNA from complex tissues. Proc Natl Acad Sci USA 2009; 106:13939-13944

Sartain CV, Cui J, Meisel RP, Wolfner MF. The poly(A) polymerase GLD2 is required for spermatogenesis in *Drosophila melanogaster*. Development 2011; 138:1619-1629.

Shcherbik N, Pestov DG. Ubiquitin and ubiquitin-like proteins in the nucleolus: multitasking tools for a ribosome factory. Genes Cancer 2010; 1:681-689.

Sheth N, Roca X, Hastings ML, Roeder T, Krainer AR, Sachidanandam R. Comprehensive splice-site analysis using comparative genomics. Nucleic Acids Res. 2006; 34:3955-3967.

Shigenobu S, Arita K, Kitadate Y, Noda C, Kobayashi S. Isolation of germline cells from *Drosophila* embryos by flow cytometry. Dev Growth Differ 2006a; 48:49-57.

Shigenobu S, Kitadate Y, Noda C, Kobayashi S. Molecular characterization of embryonic gonads by gene expression profiling in *Drosophila melanogaster*. Proc Natl Acad Sci USA 2006b; 103:13728-13733.

Smith M, Mallin DR, Simon JA, Courey AJ. Small ubiquitin-like modifier (SUMO) conjugation impedes transcriptional silencing by the polycomb group repressor Sex Comb on Midleg. J Biol Chem 2011; 286:11391-11400.

Spence J, Gali RR, Dittmar G, Sherman F, Karin M, Finley D. Cell cycle-regulated modification of the ribosome by a variant multiubiquitin chain. Cell 2000; 102:67-76.

Staley JP, Woolford JL Jr. Assembly of ribosomes and spliceosomes: complex ribonucleoprotein machines. Curr Opin Cell Biol 2009; 21:109-118.

Studier FW. Protein production by auto-induction in high density shaking cultures. Protein Expr Purif 2005; 41:207-234.

Sugihara Y, Honda H, Iida T, Morinaga T, Hino S, Okajima T, Matsuda T, Nadano D. Proteomic analysis of rodent ribosomes revealed heterogeneity including ribosomal proteins L10-like, L22-like 1, and L39-like. J Proteome Res 2010; 9:1351-1366.

Szick-Miranda K, Bailey-Serres J. Regulated heterogeneity in 12-kDa P-protein phosphorylation and composition of ribosomes in maize (*Zea mays* L.). J Biol Chem 2001; 276:10921-10928.

Takyar S, Hickerson RP, Noller HF. mRNA helicase activity of the ribosome. Cell 2005; 120:49-58.

Tazuke SI, Schulz C, Gilboa L, Fogarty M, Mahowald AP, Guichet A, Ephrussi A, Wood CG, Lehmann R, Fuller MT. A germline-specific gap junction protein required for survival of differentiating early germ cells. Development 2002; 129:2529-2539.

Theodosiou NA, Xu T. Use of FLP/FRT system to study Drosophila development. Methods 1998; 14:355-65.

Thorrez L, Van Deun K, Tranchevent LC, Van Lommel L, Engelen K, Marchal K, Moreau Y, Van Mechelen I, Schuit F. Using ribosomal protein genes as reference: a tale of caution. PLoS One 2008; 3:e1854.

Toczyski DP, Matera AG, Ward DC, Steitz JA. The Epstein-Barr virus (EBV) small RNA EBER1 binds and relocalizes ribosomal protein L22 in EBV-infected human B lymphocytes. Proc Natl Acad Sci USA 1994; 91:3463-3497.

Tonner P, Srinivasasainagendra V, Zhang S, Zhi D. Detecting transcription of ribosomal protein pseudogenes in diverse human tissues from RNA-seq data. BMC Genomics 2012; 13:412.

Uechi T, Nakajima Y, Nakao A, Torihara H, Chakraborty A, Inoue K, Kenmochi N. Ribosomal protein gene knockdown causes developmental defects in zebrafish. PLoS One 2006; 1:e37.

Ulrich HD. The fast-growing business of SUMO chains. Mol Cell 2008; 32:301-305.

Urnov FD, Rebar EJ, Holmes MC, Zhang HS, Gregory PD. Genome editing with engineered zinc finger nucleases. Nat Rev Genet 2010; 11:636-646.

van Spaendonk RM, Ramesar J, van Wigcheren A, Eling W, Beetsma AL, van Gemert GJ, Hooghof J, Janse CJ, Waters AP. Functional equivalence of structurally distinct ribosomes in the malaria parasite, *Plasmodium berghei*. J Biol Chem 2001; 276:22638-22647.

Venken KJ, He Y, Hoskins RA, Bellen HJ. P[acman]: a BAC transgenic platform for targeted insertion of large DNA fragments in D. melanogaster. Science 2006; 314:1747-1751.

Warner JR, McIntosh KB. How common are extraribosomal functions of ribosomal proteins? Mol Cell 2009; 34:3-11.

Wapinski I, Pfiffner J, French C, Socha A, Thompson DA, Regev A. Gene duplication and the evolution of ribosomal protein gene regulation in yeast. Proc Natl Acad Sci USA 2010; 107:5505-5510.

Webb KJ, Zurita-Lopez CI, Al-Hadid Q, Laganowsky A, Young BD, Lipson RS, Souda P, Faull KF, Whitelegge JP, Clarke SG. A novel 3-methylhistidine modification of yeast ribosomal protein Rpl3 is dependent upon the YIL110W methyltransferase. J Biol Chem 2010; 285:37598-37606.

Wellik DM. Hox genes and vertebrate axial pattern. Curr Top Dev Biol 2009; 88: 257-278.

Wilson D, Charoensawan V, Kummerfeld SK, Teichmann SA. DBD – taxonomically broad transcription factor predictions: new content and functionality. Nucleic Acids Res 2008; 36:D88-D92.

White-Cooper H. Studying how flies make sperm--investigating gene function in *Drosophila* testes. Mol Cell Endocrinol 2009; 306:66-74.

White-Cooper H. Molecular mechanisms of gene regulation during *Drosophila* spermatogenesis. Reproduction 2010; 139:11-21.

White-Cooper H. Tissue, cell type and stage-specific ectopic gene expression and RNAi induction in the *Drosophila* testis. Spermatogenesis 2012; 2:11-22.

Whittle CA, Krochko JE. Transcript Profiling Provides Evidence of Functional Divergence and Expression Networks among Ribosomal Protein Gene Paralogs in *Brassica napus*. Plant Cell 2009; 21:2203-2219.

Xie HB, Golic KG. Gene deletions by ends-in targeting in *Drosophila melanogaster*. Genetics 2004; 168:1477-1489.

Xue S, Barna M. Specialized ribosomes: a new frontier in gene regulation and organismal biology. Nat Rev Mol Cell Biol 2012; 13:355-369.

Yacoub A, Augeri L, Kelley MR, Doetsch PW, Deutsch WA. A *Drosophila* ribosomal protein contains 8-oxoguanine and abasic site DNA repair activities. EMBO J 1996; 15:22306-12.

Yeo G, Burge CB. Maximum entropy modeling of-PB sequence motifs with applications to RNA splicing signals. J Comput Biol 2004; 11:377-394.

Young BD, Weiss DI, Zurita-Lopez CI, Webb KJ, Clarke SG, McBride AE. Identification of methylated proteins in the yeast small ribosomal subunit: a role for SPOUT methyltransferases in protein arginine methylation. Biochemistry 2012; 51:5091-5104.

Yu J, Pacifico S, Liu G, Finley RL Jr. DroID: the Drosophila Interactions Database, a comprehensive resource for annotated gene and protein interactions. BMC Genomics 2008; 9:461.

Yu Z, Morais D, Ivanga M, Harrison PM. Analysis of the role of retrotransposition in gene evolution in vertebrates. BMC Bioinformatics 2007; 8:308.

Zachar Z, Chou TB, Bingham PM. Evidence that a regulatory gene autoregulates splicing of its transcript. EMBO J 1987; 6:4105-4111.

Zhao W, Bidwai AP, Glover CV. Interaction of casein kinase II with ribosomal protein L22 of *Drosophila melanogaster*. Biochem Biophys Res Commun 2002; 298:60-66.

Zhang Y, Duc AC, Rao S, Sun XL, Bilbee AN, Rhodes M, Li Q, Kappes DJ, Rhodes J, Wiest DL. Control of hematopoietic stem cell emergence by antagonistic functions of ribosomal protein paralogs. Dev Cell 2013; 24:411-425.

Zhang Y, Wolf GW, Bhat K, Jin A, Allio T, Burkhart WA, Xiong Y. Ribosomal protein L11 negatively regulates oncoprotein MDM2 and mediates a p53-dependent ribosomal-stress checkpoint pathway. Mol Cell Biol 2003; 23:8902-8912.

Zhang Z, Harrison P, Gerstein M. Identification and analysis of over 2000 ribosomal protein pseudogenes in the human genome. Genome Res 2002, 12:1466-1482.

Zheng Q, Wang Y, Vargas E, DiNardo S. *magu* is required for germline stem cell self-renewal through BMP signaling in the *Drosophila* testis. Dev Biol 2011; 357:202-210.

Zhong S, Müller S, Ronchetti S, Freemont PS, Dejean A, Pandolfi PP. Role of SUMO-1-modified PML in nuclear body formation. Blood 2000; 95:2748-2752.

Michael G. Kearse

Lehigh University
Department of Biological Sciences
111 Research Drive, B-217
Bethlehem, PA 18015

610-390-7806
mgk207@lehigh.edu

Education:

Ph.D. Candidate, Cell and Molecular Biology
Lehigh University, Bethlehem, PA
Advisor: Vassie C. Ware, Ph.D.
Expected Graduation: May 2013

B.S. with *Distinction*, Biotechnology (major) and Microbiology (minor), 2007
The Pennsylvania State University, University Park, PA

Experience:

Research and Teaching Assistant
Lehigh University, Bethlehem, PA
Department of Biological Sciences
August 2007 – Present

Cooperative Education Research Assistant
GlaxoSmithKline, King of Prussia, PA
Cardiovascular and Urogenital Center of Excellence in Drug Discovery
Vascular Biology and Thrombosis Department
Advisor: Douglas G. Johns, Ph.D. (now Director at Merck Research Laboratories)
January 2007 – June 2007
Drug discovery for novel targets of hypertension, atherosclerosis and thrombosis.

Cooperative Education Research Assistant
McNeil Consumer and Specialty Pharmaceuticals, Fort Washington, PA
Department of Research and Development
Advisor: Shun Por Li, Ph.D.
June 2005 – January 2006
Analytical material science of tablet coatings for drug delivery.

Research Assistant
The Pennsylvania State University – Berks Campus, Reading, PA
Department of Biology
Advisor: Tami Mysliwiec, Ph.D.
August 2003 – May 2004
Fetal alcohol syndrome using chicks as a model.

Honors and Fellowships:

Lehigh University
Marjorie Nemes Fellowship, Summer 2012
Marjorie Nemes Fellowship, Fall 2011
Lehigh University's Nominee for 2011 Lindau Nobel Laureate Meeting
Marjorie Nemes Fellowship, Fall 2010
College of Arts & Sciences Summer Research Fellowship, 2009

The Pennsylvania State University
Degree with *Distinction*, 2007
Eberly College of Science Cooperative Education Student of the Year Nominee, 2007
Eisenhower Memorial Award Scholarship, 2006-2007
Kappa Theta Epsilon Honor Society, 2005-2007
Golden Key International Honor Society, 2004-2007
The President's Freshman Award, 2003
Eberly College of Science Academic Achievement Award, 2002-2007

Undergraduate Mentoring, Lehigh University:

Sukhdip (Kammy) U. Kaur ('10) – now at Penn State School of Medicine

Jill A. Ireland ('11) – Honors student; now at University of Central Florida College of Medicine; co-author of Kearse *et al*. (2013) *In revision*

Alex S. Chen ('12) – Eckardt Scholar; now research associate (postbac IRTA) at NICHD-NIH; co-author of Kearse *et al*. (2011); co-author of Kearse *et al*. (2013) *In revision*

Smrithi M. Prem ('12) – now at University of Medicine and Dentistry of New Jersey, Robert Wood Johnson Medical School; co-author of Kearse *et al*. (2013) *In revision*

Professional Societies:

American Association for the Advancement of Science
American Society for Cell Biology
RNA Society
Sigma Xi

Grants:

National Academy of Science Grant-In-Aid of Research (GIAR) administrated by Sigma Xi -"Exploring Roles of Paralogous Genes in *Drosophila melanogaster*: *In vivo* Knockdown of the L22e Ribosomal Protein Family in the Male Germline"
Grant ID: G20100315152292, $805
Funded: April 19, 2010

GenBank Submissions:

Accession Number JN660814 – Mycobacterium phage Dreamboat, complete sequence
Accession Number JF704091 – Mycobacterium phage ABU, complete sequence
Accession Number JN153086 – Mycobacterium phage Euphoria, complete genome
Accession Number GU339467 – Mycobacteriophage RedRock, complete genome
Accession Number HM756190 – *Drosophila melanogaster* RpL22-like-PB isoform mRNA, complete coding sequence, alternatively spliced
Accession Number HQ190956 – Drosophila melanogaster ribosomal protein L22-like protein mRNA, complete coding sequence

Publications:

Gatto GJ Jr, Ao Z, **Kearse MG**, Zhou M, Morales CR, Daniels E, Bradley BT, Goserud MT, Goodman KB, Douglas SA, Harpel MR, Johns DG. (2013). NADPH oxidase-dependent and -independent mechanisms of reported inhibitors of reactive oxygen generation. *J Enzyme Inhib Med Chem*, 28: 95-104. [Epub, 2011 Dec 3]

Kearse MG, Chen AS, Ware VC. (2011). Expression of ribosomal protein L22e family members in *Drosophila melanogaster*: *rpL22-like* is differentially expressed and alternatively spliced. *Nucleic Acids Res*, 39: 2701-2716. [Epub 2010 Dec 7]

In revision:
Kearse MG, Ireland JA, Prem SM, Chen AS, Ware VC. RpL22e, but not RpL22e-like-PA, is SUMOlylated and localizes to the nucleoplasm of *Drosophila* meiotic spermatocytes. *Nucleus*

In review:
Fischl MJ, Weimann SR, **Kearse MG**, Burger RM. Slowly emerging glycinergic transmission enhances inhibition in the sound localization pathway of the avian auditory system. *J Neurosci*

In preparation:
Kearse MG, Ware VC. Male germline-specific RpL22e-like is non-essential in spermatogenesis or fertility in Drosophila melanogaster.

Conference Abstracts:

Matthew J. Fischl, Sonia R. Weimann, **Michael G. Kearse**, R. Michael Burger. Glycine receptors expressed in "timing" neurons of the avian auditory brainstem modulate GABAergic inhibition. *The Association of Research in Otolaryngology Annual Meeting*. February 2013. Baltimore, MD, USA.

Matthew J. Fischl, Sonia R. Weimann, **Michael G. Kearse**, R. Michael Burger. Glycine occludes GABAergic inhibition in the avian sound localization pathway. *Society for Neuroscience Annual Meeting*. October 2012. New Orleans, LA, USA.

Michael G. Kearse and Vassie C. Ware. Functional Diversification within the *Drosophila melanogaster* Ribosomal Protein L22e Family: Differential Post-Translational Modification and Subcellular Localization of L22e Paralogues within the Male Germline. *9th International Conference on Ribosome Synthesis*. August 2012. Banff, Alberta, Canada.

Michael G. Kearse, Jill A. Ireland, Vassie C. Ware. Investigating Duplicated Ribosomal Proteins Reveals Differential Post-Translational Modification of the RpL22e Family in the Male Germline: Evidence for SUMOylation of RpL22. 5*3rd Annual Drosophila Research Conference*. March 2012. Chicago, IL, USA.

Michael G. Kearse and Vassie C. Ware. Investigation of Functional Diversity within the Ribosomal Protein L22e family in *Drosophila melanogaster*: Evidence for SUMOlyation of RpL22. *51st Annual Meeting of the American Society for Cell Biology*. December 2011. Denver, CO, USA.

Michael G. Kearse, Alex S. Chen, Vassie C. Ware. Differential Expression and Localization of Eukaryotic-Specific Ribosomal Protein L22e Paralogues in *Drosophila melanogaster*. *50th Annual Meeting of the American Society for Cell Biology*. December 2010. Philadelphia, PA, USA.

Michael G. Kearse and Vassie C. Ware. Differential Expression and Localization of Ribosomal Protein L22e Family Paralogues in *Drosophila melanogaster*. *15th Annual Meeting of the RNA Society*. June 2010. Seattle, WA, USA.

Michael G. Kearse and Vassie C. Ware. Tissue-specific Expression of the Putative Ribosomal Protein L22-like in *Drosophila melanogaster*: A Mechanism for Generating Ribosome Diversity? *8th International Conference on Ribosome Synthesis*. August 2009. Regensburg, Bavaria, Germany.

Gregory J. Gatto, Jr., Zhaohui Ao, **Michael G. Kearse**, Mei Zhou, Cyndi R. Morales, Erin Daniels, Benjamin T. Bradley, Matthew T. Goserud, Krista B. Goodman, Stephen A. Douglas, Mark R. Harpel, Douglas G. Johns. Pharmacological Inhibitors of NADPH

Oxidase: Characterization of Newly-Described Tools. *2009 Basic Cardiovascular Sciences Annual Conference of the American Heart Association*. July 2009. Las Vegas, NV, USA.

Michael G. Kearse and Vassie C. Ware. Novel Splicing Generates Unique mRNA Isoforms from Ribosomal Protein L22-like Gene in *Drosophila melanogaster*. *14th Annual Meeting of the RNA Society*. May 2009. Madison, WI, USA.

Vassie C. Ware and **Michael G. Kearse**. Analysis of Yeast Chimeric rRNAs Harboring *Drosophila* D7a Expansion Segments within the Binding Site for Ribosomal Protein L25. *48th Annual Meeting of the American Society for Cell Biology*. December 2008. San Francisco, CA, USA.

Diane Husic, Michael Kuchka, Yi Li, **Michael Kearse**. The D-Lactate Dehydrogenase in C*hlamydomonas reinhardtii*: a Bioinformatics and Gene Expression Study. *2008 Annual Meeting of the American Society of Plant Biologists*. June 2008. Mérida, Yucatán, Mexico.

Daniel Garcia*, **Michael Kearse***, Tami Mysliwiec, Ike Shibley. Analysis of the Expression of Acetaldehyde Dehydrogenase in Normal and Chronic Ethanol Exposed Chicken Embryos. *80th Annual Meeting of the Pennsylvania Academy of Science*. March 2004. Monroeville, PA, USA.

*Denotes equal contribution to work